AMMRC CTR 77-21

MACHINE CASTING OF HIGH TEMPERATURE ALLOYS FOR TURBINE ENGINE COMPONENTS

SEPTEMBER 1977

L. F. SCHULMEISTER, J. D. HOSTETLER, and C. C. LAW
United Technologies Corporation
Pratt & Whitney Aircraft Group
Government Products Division
West Palm Beach, Florida 33402

Final Report

Contract Number DAAG46-76-C-0029

Sponsored by: Defense Advanced Research Projects Agency, ARPA Order No. 2267
Program Code No. 4D10
Effective Date of Contract: 17 February 1976
Contract Expiration Date: 18 May 1977
Amount of Contract: $154,796.00
Contract Period Covered by Report: 1 March 1976-30 May 1977

Prepared for

ARMY MATERIALS AND MECHANICS RESEARCH CENTER
Watertown, Massachusetts 02172

UNCLASSIFIED

SECURITY CLASSIFICATION OF THIS PAGE (When Data Entered)

18 19

REPORT DOCUMENTATION PAGE

READ INSTRUCTIONS BEFORE COMPLETING FORM

1. REPORT NUMBER AMMRC CTR-77-21	2. GOVT ACCESSION NO.
3. RECIPIENT'S CATALOG NUMBER	
6 4. TITLE (and Subtitle) Machine Casting of High Temperature Alloys for Turbine Engine Components	9 5. TYPE OF REPORT & PERIOD COVERED Final Report, 1 Mar[redacted]76 - 30 Apr[redacted]77
	14 6. PERFORMING ORG. REPORT NUMBER FR-8984
10 7. AUTHOR(s) L. F. Schulmeister, C. C. Law J. D. Hostetler	15 8. CONTRACT OR GRANT NUMBER(s) DAAG 46-76-C-0029, ARPA Order-2267
9. PERFORMING ORGANIZATION NAME AND ADDRESS United Technologies Corporation Pratt & Whitney Aircraft Group Government Products Division West Palm Beach, Florida 33402	10. PROGRAM ELEMENT, PROJECT, TASK AREA & WORK UNIT NUMBERS D/A Project: ARPA Order No. 2267 AMCMS Code: 6410 Agency Accession: DA OE4735
11. CONTROLLING OFFICE NAME AND ADDRESS Army Materials and Mechanics Research Center Watertown, Massachusetts 02172	11 12. REPORT DATE Sep[redacted]77
	13. NUMBER OF PAGES ~~77~~ 12 82 p.
14. MONITORING AGENCY NAME & ADDRESS (if different from Controlling Office)	15. SECURITY CLASS. (of this report) Unclassified
	15a. DECLASSIFICATION/DOWNGRADING SCHEDULE

16. DISTRIBUTION STATEMENT (of this Report)

Approved for public release; distribution unlimited

DDC RECEIVED MAR 2 1978 F

17. DISTRIBUTION STATEMENT (of the abstract entered in Block 20, if different from Report)

18. SUPPLEMENTARY NOTES

Sponsored by: Defense Advanced Research Projects Agency, ARPA Order No. 2267
Program Code No. 4D10 — Effective Date of Contract: 17 February 1976
Contract Expiration Date: 18 May 1977 — Amount of Contract: 154,796.00
Contract Period Covered by Report: 1 March 1976 – 30 May 1977

19. KEY WORDS (Continue on reverse side if necessary and identify by block number)

Die casting	Compressor parts
Solidification	Turbine parts
Heat resistant alloys	Quality assurance
Iron alloys	

20. ABSTRACT (Continue on reverse side if necessary and identify by block number)

A program has been initiated to evaluate the capability of machine casting for fabricating components for gas turbine engines such as compressor airfoils. The goal is to evaluate the capability of the process to produce an end product of high quality on an economic basis.

During this contract, machine casting activity consisted of equipment modification to an existing machine casting unit which included mechanization of the process. Concurrently, statistical assessment of process parameter effects using Rheocast Haynes Alloy 31 (cobalt-base alloy) as a vehicle was performed. Machine casting preforms containing

DD FORM 1 JAN 73 1473 EDITION OF 1 NOV 65 IS OBSOLETE

UNCLASSIFIED

SECURITY CLASSIFICATION OF THIS PAGE (When Data Entered)

392 887

varying volume fractions of solid were inspected at different die temperatures and injection speeds and were evaluated both non-destructively and metallographically. Results indicated that quality of high volume fraction parts was improved using high injection speeds and low die temperatures. An alternate die design was also evaluated.

Heat treatment response studies were also performed on machine cast specimens. Results indicated that long term anneals followed by aging yielded microstructures similar to cast and heat treated Haynes 31.

Mechanical property evaluation consisted of room temperature, 1000°F and 1450°F tensile testing, 1450°F stress rupture and room temperature high cycle fatigue (HCF) testing. Tensile data indicated that tensile design goals could be achieved. Stress rupture and HCF goals were achieved through the use of hot isostatic capacition to reduce internal porosity in the machine cast specimens.

An economic analysis was performed which indicated that machine casting has the potential for competing with foreign for gas turbine components, however there appeared to be no significant cost advantage when compared to investment casting.

FOREWORD

This report covers work done during the period 1 March 1976 through 30 April 1977 under the general title "Machine Casting of High Temperature Alloys for Turbine Engine Components". The work was administered through the Pratt & Whitney Aircraft Group, Government Products Division, West Palm Beach, Florida, with the work being performed at the Pratt & Whitney Aircraft Group, Commercial Products Division, East Hartford, Connecticut by the principal investigators, J. D. Hosteller, C. C. Law, and L. F. Schulmeister. The work was sponsored by the Defense Advanced Research Projects Agency under DARPA Order No. 2267 (Amendment No. 6 - Code 4D10) and Contract No. DAAG46-76-C-0029 at the Army Material and Mechanics Research Center, Watertown, MA 02172.

The authors are grateful to W. H. Rand and J. S. Erickson for their active participation in the early phase of this program. We would also like to express our appreciation to C. W. Steinke for his technical assistance, C. P. Sullivan and A. F. Giamei for their interest in and helpful discussions on this work and Prof. R. Mehrabian, University of Illinois, for his timely assistance during the entire course of this effort.

TABLE OF CONTENTS

LIST OF ILLUSTRATIONS

LIST OF ILLUSTRATIONS (Cont'd.)

LIST OF ILLUSTRATIONS (Cont'd.)

LIST OF ILLUSTRATIONS (Cont'd.)

LIST OF ILLUSTRATIONS (Cont'd.)

LIST OF TABLES

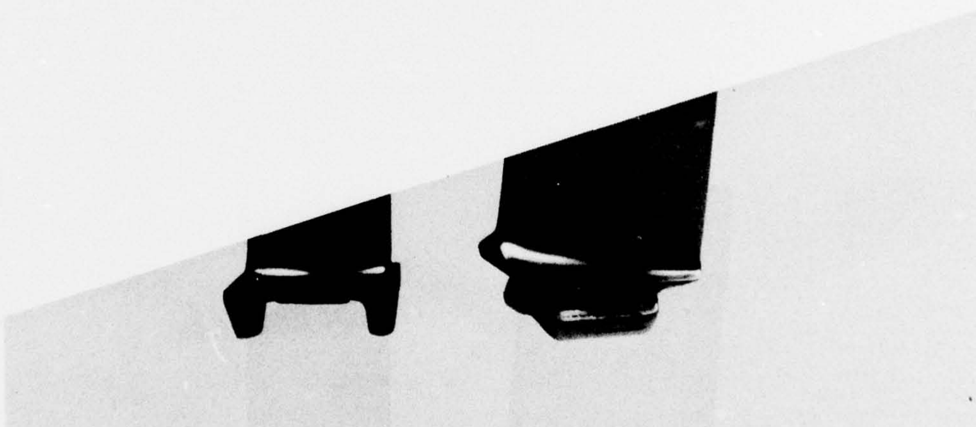

Figure 1 *Die Cast Ferrous Alloy Compressor Vane (left) and Compressor Blade (right) Approximately 1.5X)*

High-cycle-fatigue testing of the die cast ferrous airfoils indicated that the presence of internal voids adversely affected the fatigue strength of the material. Fatigue strengths for the die cast AM 355 blades were about 60 percent of the fatigue strength levels normally achieved

in forged AM 355 blades. Reduction of porosity through hot isotatic pressing (HIP) improved attainable stress levels to 80 percent of normal fatigue strength, indicating the potential for the die casting of critical components for gas turbine engines provided that internal casting soundness could be achieved.

More recently the Defense Advanced Research Projects Agency (DARPA) has initiated programs directed toward the "Machine Casting of Ferrous Alloys".[1-6] One of the innovative approaches being pursued involves forming high temperature alloys in the thixotropic state in order to obtain improved product quality.[7-10] The anticipated quality improvement results from the fact that a thixotropic alloy is injected in the machine casting system in the slurry (partially solid) state, thereby improving die fill characteristics. In addition, since the metal is partially solid at the time of injection, less shrinkage porosity results and the castings spend a shorter time in the die before they are completely solid. The lower temperatures associated with the thixotropic input material as contrasted to current die casting practice should provide for improved die life by reducing the thermal shock experienced at the die face.

Pratt & Whitney Aircraft Group has recently joined the DARPA Machine Casting Activity. The program described in the following section is the Pratt & Whitney Aircraft part of the overall DARPA effort and involves applying the machine casting processes to the fabrication of gas turbine components in order to see if this approach has the potential to significantly improve casting quality.

II. PROGRAM AND FACILITY DESCRIPTION

A. PROGRAM OUTLINE

During the course of the program, thixotropic processing of ferrous and superalloy materials into gas turbine components was evaluated. A general outline of the program is presented in Figure 2.

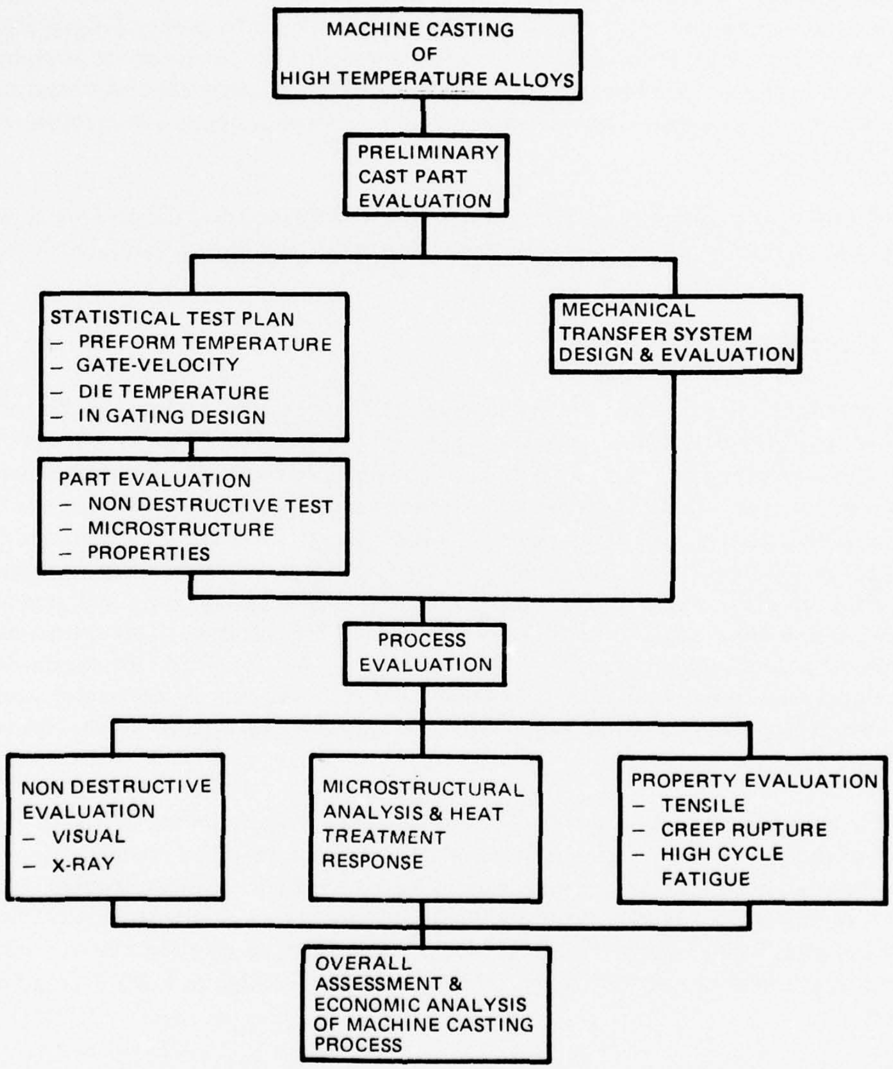

Figure 2 General Outline for DARPA - P&WAG Machine Casting Program

A continuing effort to improve the machine-casting system was conducted throughout the program. This included both equipment modifications and mechanization of various steps in the process. Concurrent with this effort was a series of planned experiments designed to determine the influence of critical process parameters, such as rheocast preform temperature, gate velocity conditions, die temperature, gating configurations, and rheocast preform quality on cast part quality.

A comprehensive metallurgical characterization was performed, including microstructural analysis and alloy heat treatment response. Mechanical property evaluation, including high temperature tensile and creep rupture testing as well as high frequency fatigue testing, was also conducted. This information was used to determine the feasibility of applying machine casting concepts to the fabrication of critical gas turbine components. An assessment of overall part quality, using standard nondestructive testing methods was incorporated into this feasibility analysis.

In addition to the metallurgical characterization of machine cast components, a preliminary economic analysis of the process comparing it with existing fabrication techniques was performed.

B. MACHINE CASTING UNIT

Pratt & Whitney Aircraft has, under independent funding, modified an injection-molding press for use in their machine casting projects. This equipment (Figures 3 and 4) was used throughout this machine casting contract as a method of producing high temperature alloy gas turbine shapes. The press is a converted transfer press originally used for the forming of thermosetting plastic parts and consists of a press frame, die assembly, hydraulic die clamping system, and hydraulic injection system. These details are depicted in Figures 5 and 6. Clamping force on the die assembly is maintained at approximately 25 tons, and injection force is limited to 6000 pounds to prevent die separation. The addition of an accumulator system (Figure 6) allowed the attainment of ram velocities up to 30 in./sec. An instrumentation recording system, shown in Figure 7, automatically recorded process parameter data such as ram velocity, pressure, and ram position. An example of the type of data recorded is shown in Figure 8.

The die assembly, used for a majority of the injection trials, is shown in Figure 9. In the interest of promoting uniform front filling with this particular die, a relatively large gate (0.062 in.^{2}) with a constant cross section was used. The die, preform loading cradle, and liner were made from H-11 tool steel. The die assembly, which was thermally insulated from the press frame, was heated by means of cartridge-type resistance heaters placed in cavities machined into the die halves. Die temperatures as high as 1100°F could be maintained.

Work performed at the University of Illinois [11] indicated, however, that the die design of Figure 9 could lead to poor filling behavior and internal porosity. A modified die (shown in Figures 10 and 11), using design data generated at University of Illinois, was constructed and used in the latter stages of the program. Results of the use of this die design will be found in Section III - E .

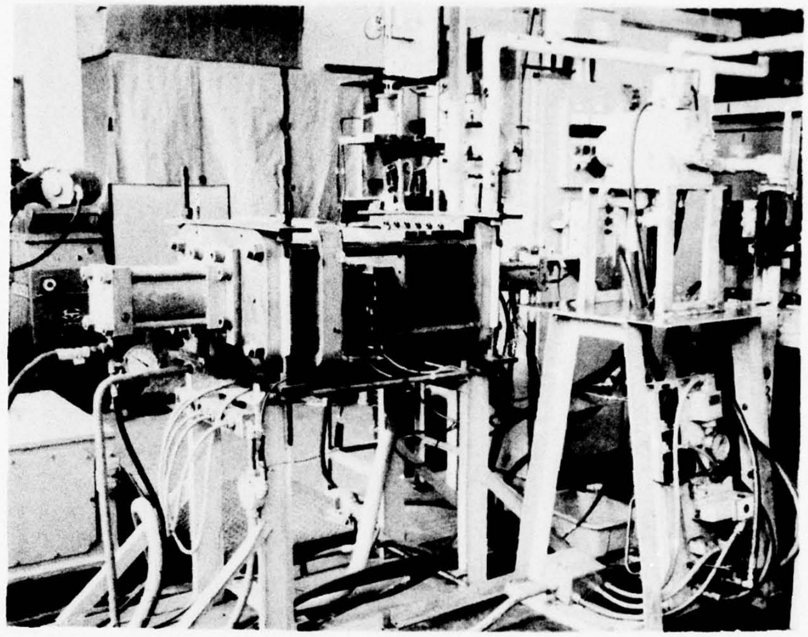

Figure 3 Machine Casting Unit

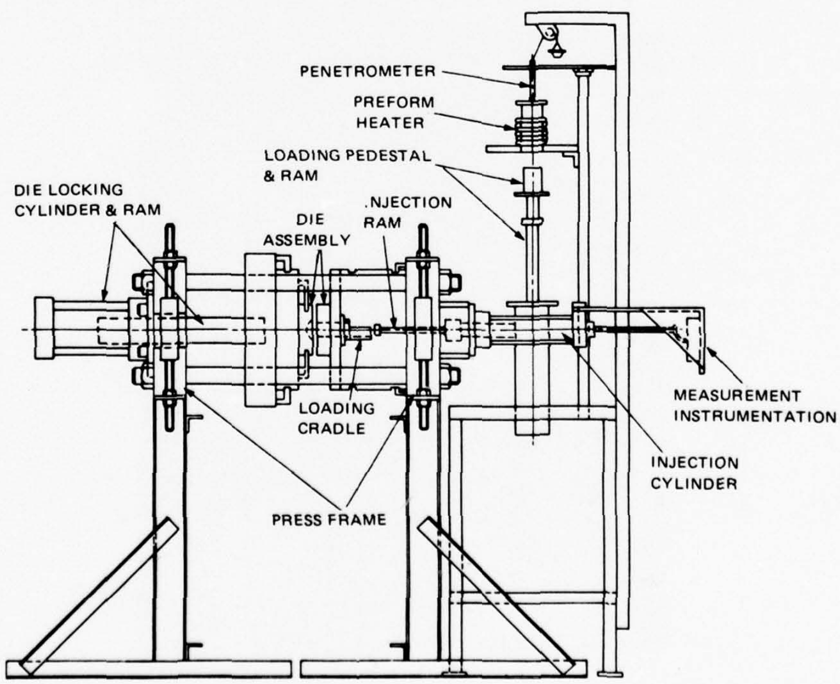

Figure 4 Schematic of Machine Casting Unit

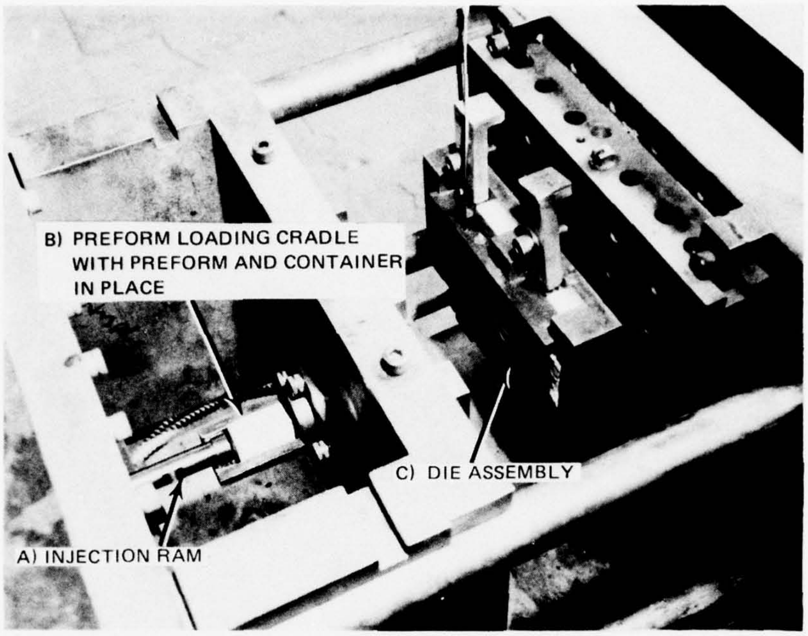

Figure 5 *Machine Casting Unit Showing A) Injection Ram, B) Preform Loading Cradle with Preform and Container in Place and C) Die Assembly*

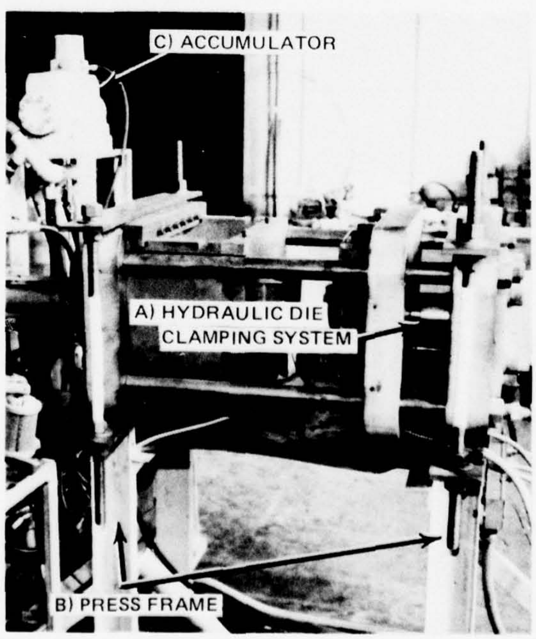

Figure 6 *Machine Casting Unit Showing A) Hydraulic Die Clamping System, B) Press Frame and C) Accumulator*

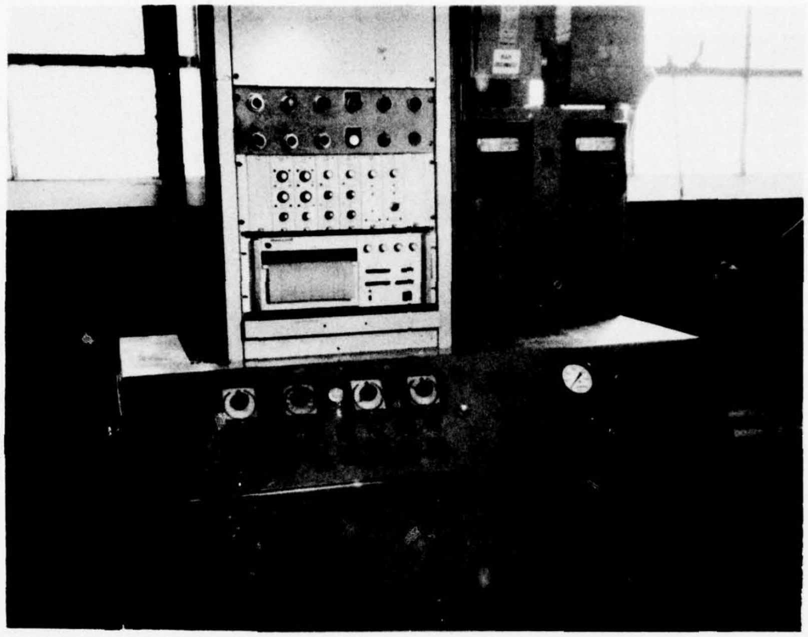

Figure 7 *Instrumentation Monitor Console for Measuring and Recording Machine Casting Unit Process Parameters*

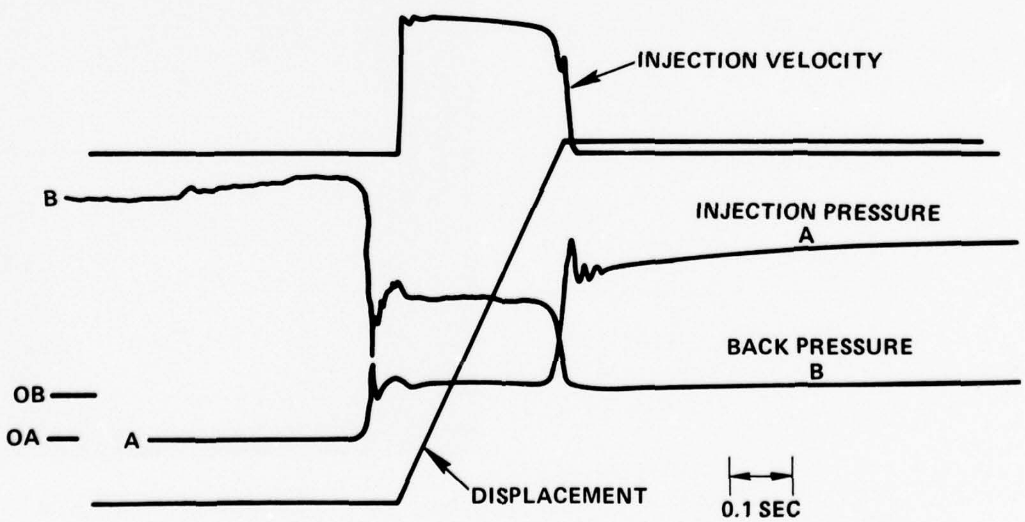

Figure 8 *Sample of Data Automatically Recorded During Machine Casting Trials*

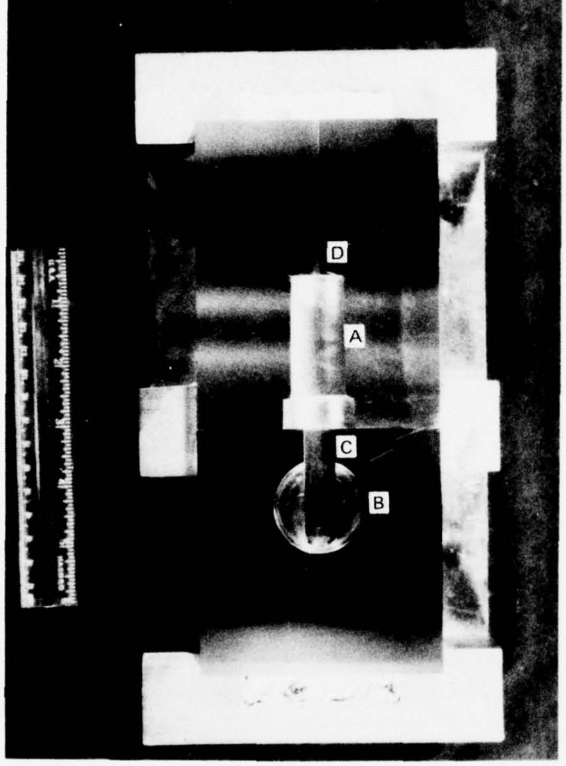

Figure 9 *Machine Casting Unit Die Assembly Showing A) Die Cavity, B) Entry Port, C) Gate and D) Vent*

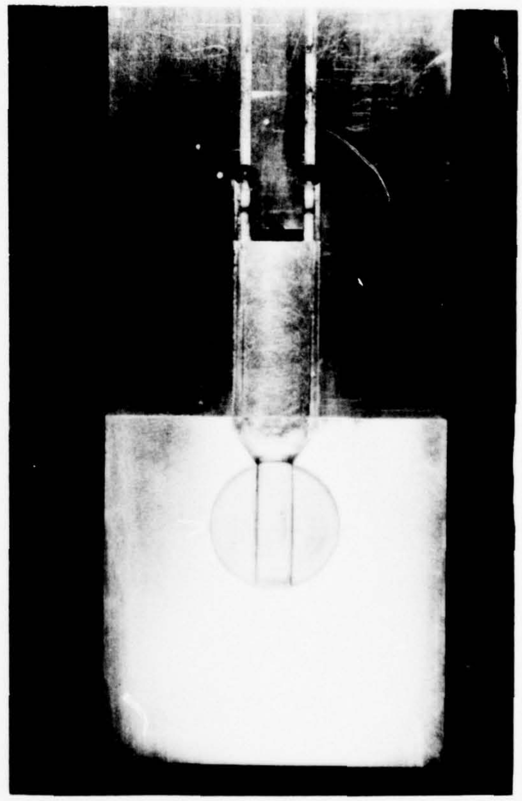

Figure 10 *Photograph of Modified Die*

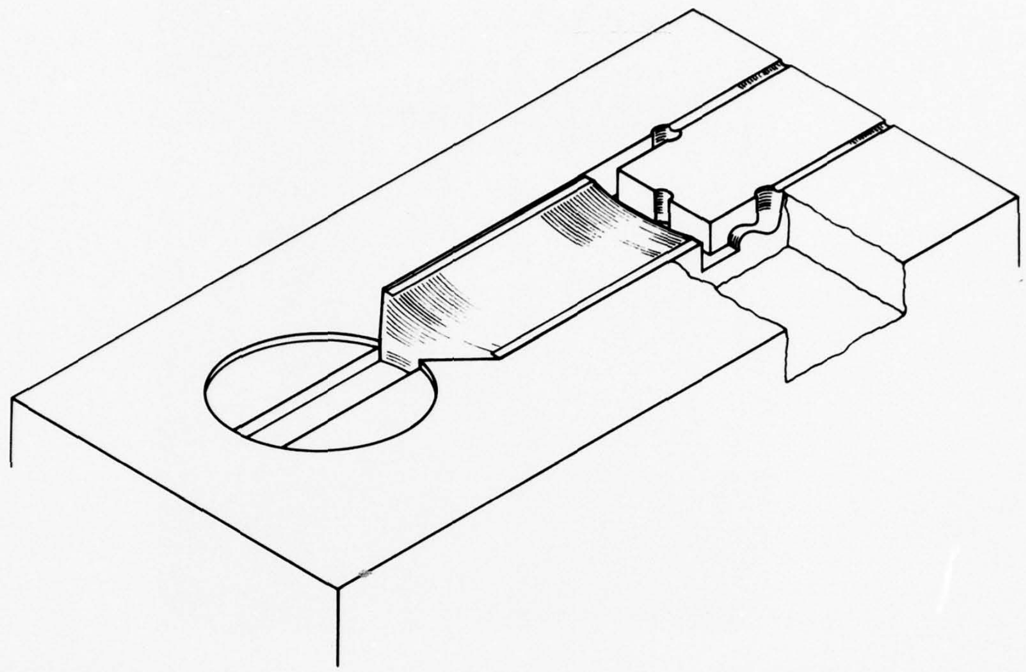

Figure 11 Sketch of Modified Die

The thixotropic alloy preform, usually of cylindrical shape, is preheated to the desired processsing temperature in a directly coupled, inductively heated furnace, as shown in Figure 12. The induction coil is powered by a high frequency Pilar power supply. The preform is placed in a ceramic container which is positioned on a pedestal attached to a hydraulically activated cylinder. The preform and containor is then raised into the furnace. The proper volume fraction solid in the heated preform is monitored through the use of a variable-load penetrometer. After the penetrometer stylus penetrates the preform, indicating that a given fluidity (and, therefore, volume fraction solid) has been achieved, the preform is removed from the furnace by lowering the platform and is manually transferred to the machine casting unit, placed in the preform loading cradle, and injected into the die.

C. PROCESS AUTOMATION/MECHANIZATION

Machine casting processes are dependent on a variety of factors, including starting material costs, die life, ability to cast multiple parts, etc. However, a major factor in achieving high part quality is process reproducibility. Parametric studies can point toward the proper processing conditions to achieve high quality parts; however, part reproducibility is also a function of the consistency of the machine casting equipment operation. In order to achieve operational reproducibility, it is necessary to automate/mechanize wherever possible to insure minimal variations in the processing procedures.

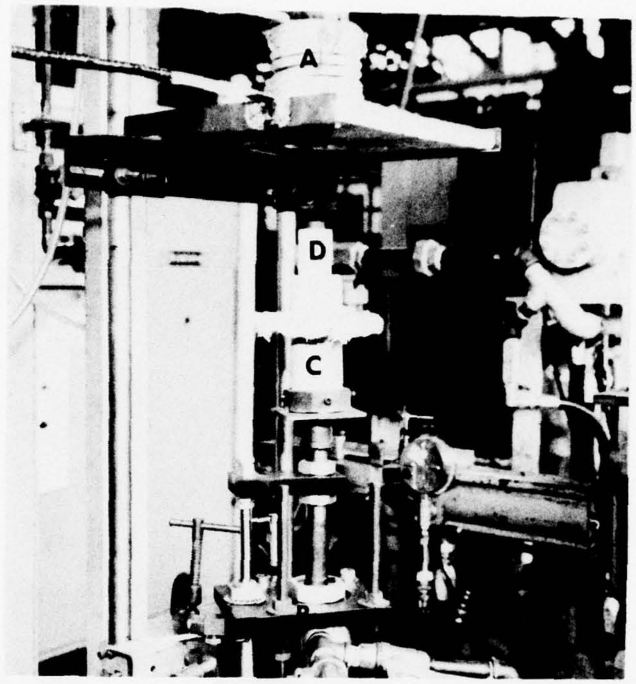

Figure 12 Preform Heater Showing A) Induction Furnace, B) Loading Cylinder, C) Pedestal and D) Preform and Container

A description of the manual operating mode for the machine casting unit appeared in the prior section (II-B). The critical operations, preform unloading, transfer, and injection, are keyed to the skill of the operator and can normally occupy a combined interval of from 3.5 to 4.5 seconds under ideal conditions. Excessive length and variability of transfer time might adversely affect the quality of the machine cast part because of variable preform heat losses. These can readily be compensated for through the use of automated control of the process.

An assessment of automated transfer of the rheocast specimen machine casting unit was made a part of this program. A simple means of process control is shown in Figure 13 and Figure 14 and basically consists of limit-switch control in the heating, transfer, and injection steps of the process. The preform heater is located directly above the loading area of the machine casting unit. The preform and container are placed on a hollow pedestal attached to a loading ram and located in the heater. When the part reaches the proper volume fraction solid, the penetrometer pierces the preform. The downward movement of the penetrometer triggers a limit switch which activates the loading ram. The platform which holds the pedestal is both ported and hinged and has a cam follower wheel attached. As the platform is lowered, the wheel will follow the cam surface, shown in Figure 14. The cam surface translates the preform and container from its initial vertical position to a horizontal position directly into the preform cradle. When the preform reaches its final position, another limit switch is tripped which in turn activates the injection ram. The ram travels through the platform "port" and the hollow pedestal, and then through the preform container injecting the preform into the die. This transfer and injection can occur in less than three seconds with variations of as little as ±0.1 second. Cylinder dampers, alignment rods, cover shields, etc. were also added to insure consistent alignment and operation. Operational details will be discussed in Section III - E.

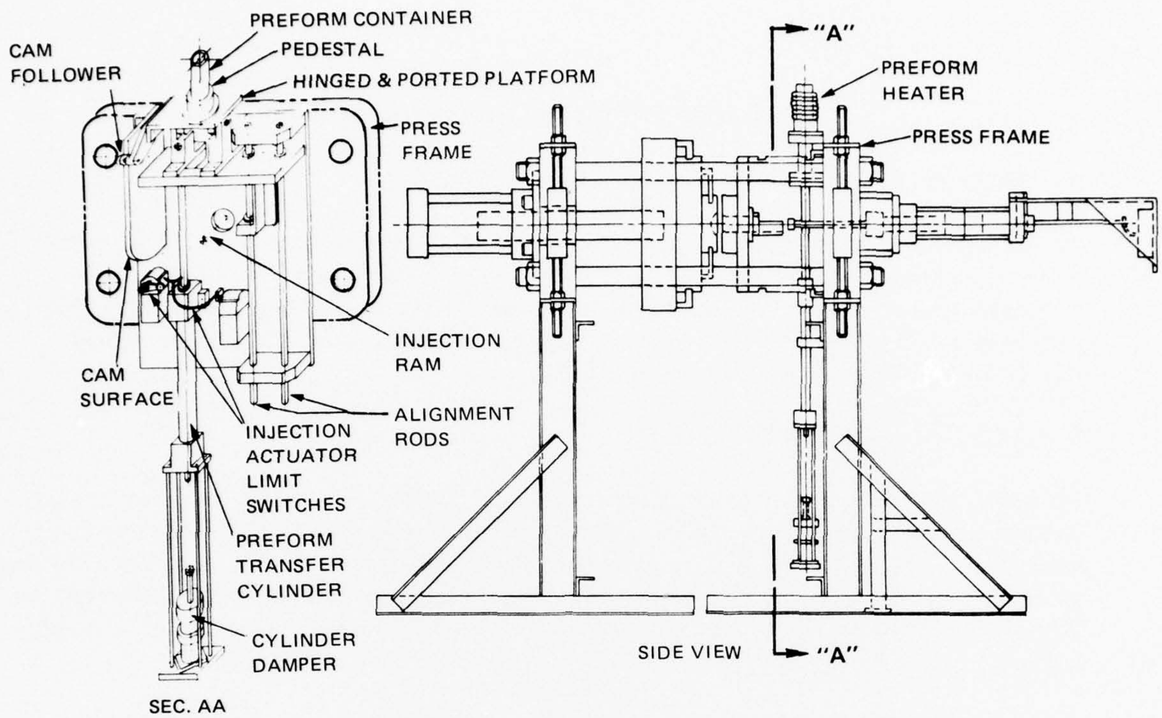

Figure 13 Schematic of Automatic Transfer System for Use With The Machine Casting Unit

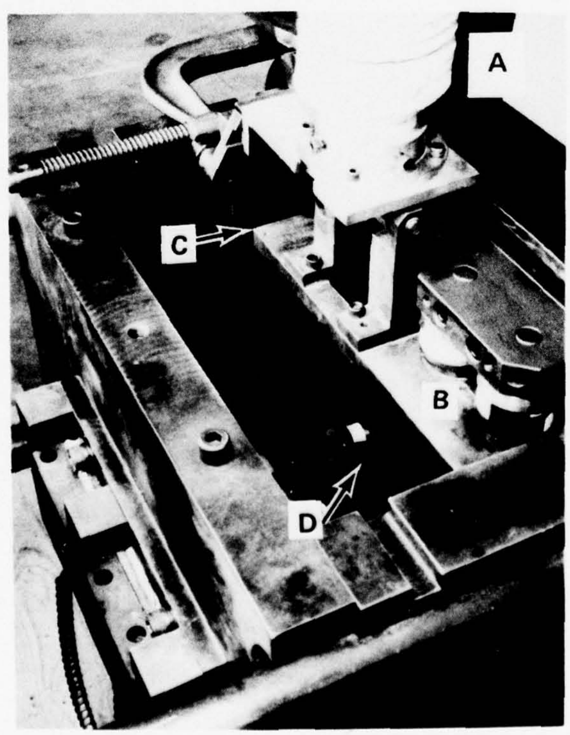

Figure 14 Mechanical Transfer System Showing A) Preform Heater B) Preform Platform C) Cam Follower & Surface and D) Injection Ram

III. MACHINE CASTING INJECTION TRIALS

A. INTRODUCTION

Several series of machine-casting trials were performed to evaluate both the machine-casting unit and casting parametric behavior. These series included the assessment of the machine-casting unit for operational modifications evaluation of machine casting parameters, and operation of a mechanical transfer system installed on the casting unit. The details of these various series of evaluation are discussed below.

B. SERIES I - INJECTION TRIALS

The initial series of injection trials (approximately 25 shots was conducted to determine the operating characteristics of the machine casting system. Haynes 31 (Alloy X-40),* an air-melted cobalt-based superalloy, was selected for the injection trials, as it represented a reasonable balance between availability (in the rheocast form) and applicability. It was supplied to MIT as investment cast bars which were rheocast in their continuous casting unit.[4] A typical quenched microstructure of the MIT rheocast product is shown in Figure 15.

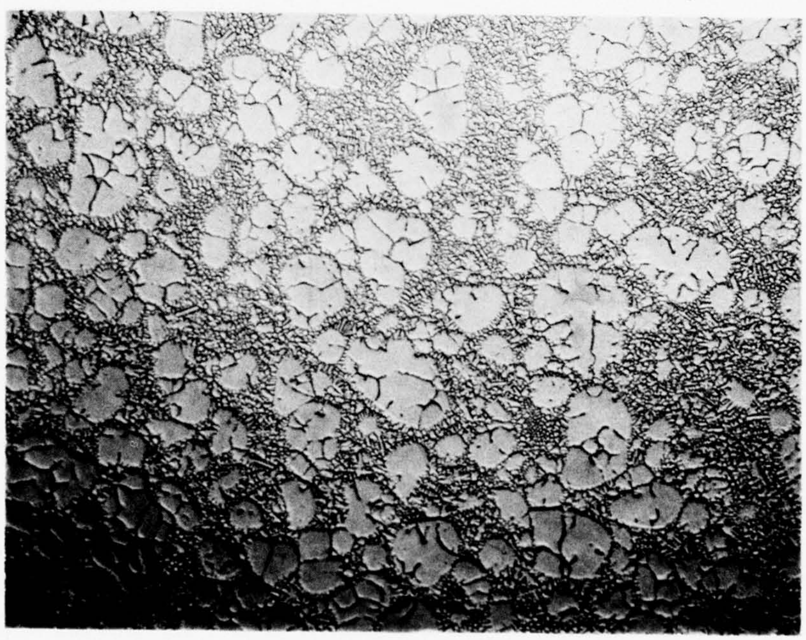

Figure 15 Haynes 31 Quenched Specimen Taken Form Continuous Rheocast Run Preformed at MIT (50X)

*Nominal Composition – Co-25.5% Cr - 10.5% Ni - 7.5% w - 0.5% C

Preform volume fraction solid was varied by changing penetrometer loads, and die temperature was varied in this particular series of trials. It was found that with this system die fill was inadequate because of excessive ingate length. Long preform transfer times (5-7 seconds) also contributed to the observed problems. Modifications, including the die design shown previously in Figure 9, were made to the unit to relieve these conditions. Sufficient quantities of test material were obtained, however, to machine specimens for some preliminary testing. The results of this testing are reported in Section IV-C.

One additional complicating factor observed in this initial injection series was that the Fiberfrax container system used to hold the rheocast preform tended to adhere to the preform surface and fragments of Fiberfrax ended up as inclusions in the injected casting. In addition, transfer of the preform from the heater to the machine casting unit was impeded by the lack of rigidity of the Fiberfrax container at the preheat temperature. This resulted in the periodic loss of the entire test specimen through leakage of the alloy from the container. To alleviate this problem, mullite and shell molded Al_2O_3-SiO_2 tubes, both with Fiberfrax bottoms, were evaluated. The three types of containers are shown in Figure 16. The preform containers are cut to about two inch lengths and Fiberfrax discs, soaked in colloidal SiO_2, are then positioned in one end of the tubes and the assembly is baked to bond the Fiberfrax in place. A preform is loaded in the container, heated in the furnace (vertical position), and manually transferred to the loading cradle (horizontal position). The injection ram then punches out the Fiberfrax bottom while injecting the preform material into the die. Because of the smaller size of the ram relative to the preform container inner diameter, neither the Fiberfrax bottom nor the container cylinder fragment to the point where additional inclusions are injected into the part forming portion of the die. The injection sequence is shown schematically in Figure 17. As a result of the ease of handling provided by the tube rigidity, the use of this type of container design reduced transfer time to about 3.5-4.5 seconds. Furthermore, it was found that the Al_2O_3-SiO_2 shell material provided additional shock resistance as compared with the high density mullite and it, therefore, was adopted for use throughout the remainder of the program.

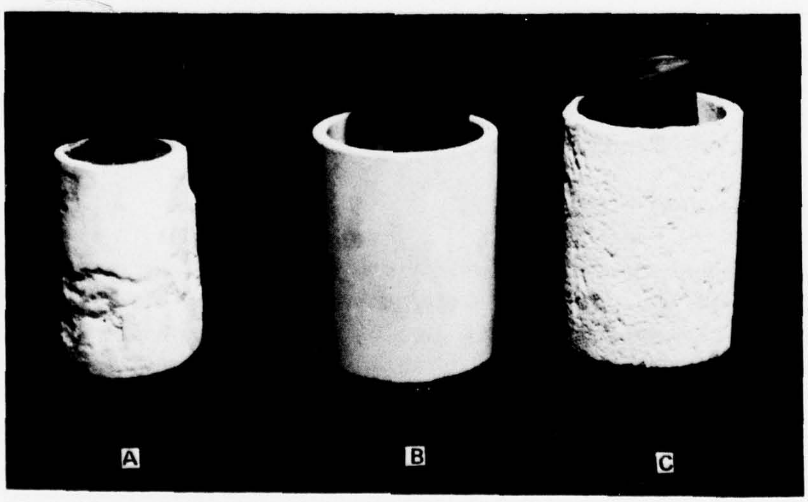

Figure 16 Preform Container – A) Formed Fiberfrax Container, B) Mullite Tube With Fiberfrax Bottom and C) Al_2O_3 - SiO_2 Shell Container With Fiberfrax Bottom

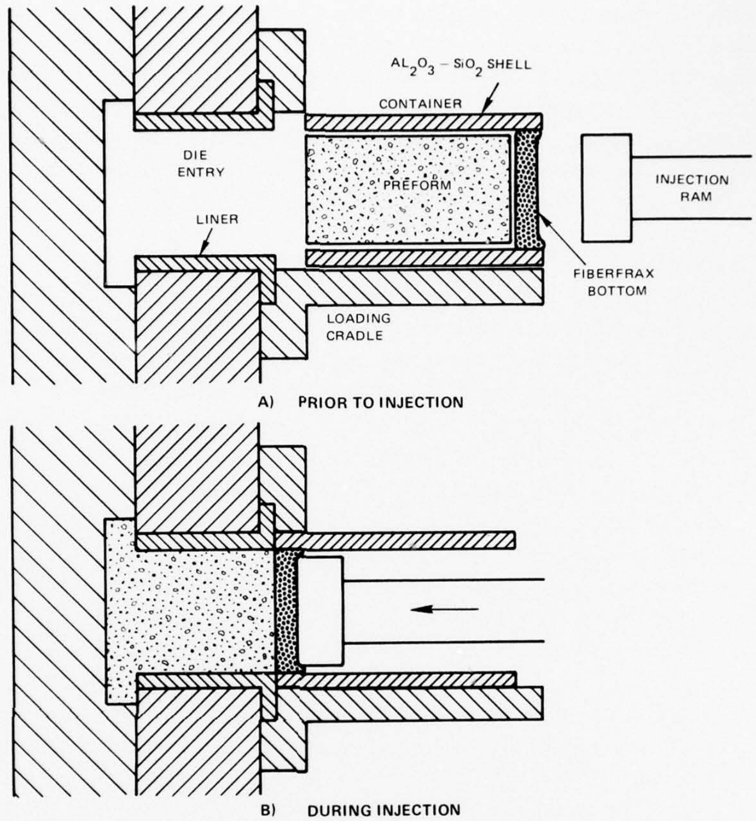

Figure 17 Schematic Representation of Injection Process Using Al_2O_3-SiO_2 Shell Containers With Fiberfrax Bottom

One other significant modification made to the machine casting unit following the Series I trials was to change the preform heater from a susceptor-coupled induction system to a directly coupled induction system using an induction coil designed to minimize axial temperature variations. Direct coupling resulted in reducing preform heat-up time from about 20 minutes to less than four minutes.

C. SERIES II - INJECTION TRIALS

After the aforementioned modifications were made to the machine casting system, a second series of castings (approximately 35 shots) was made. The first trials in this series indicated that the die fill characteristics of the system had been significantly improved. Examples of simulated airfoil castings so produced are shown in Figure 18 and a comparison with a gas turbine engine compressor vane is shown in Figure 19. To gain further assessment of the influence of injection parameters on blade quality, both preform volume fraction solid and die temperatures were varied as before in the Series I trials. Since preform volume fraction solid was monitored by means of a penetrometer, the solid content of the specimen could be adjusted by varying the penetrometer weight. The penetrometer stylus used was 0.150 inch in diameter and the two weights employed were 50 g and 25 g. The heavier weight typically

yielded higher volume fractions of solid in the cast part, indicating that higher penetrometer weights normally correspond to lower preform temperatures.

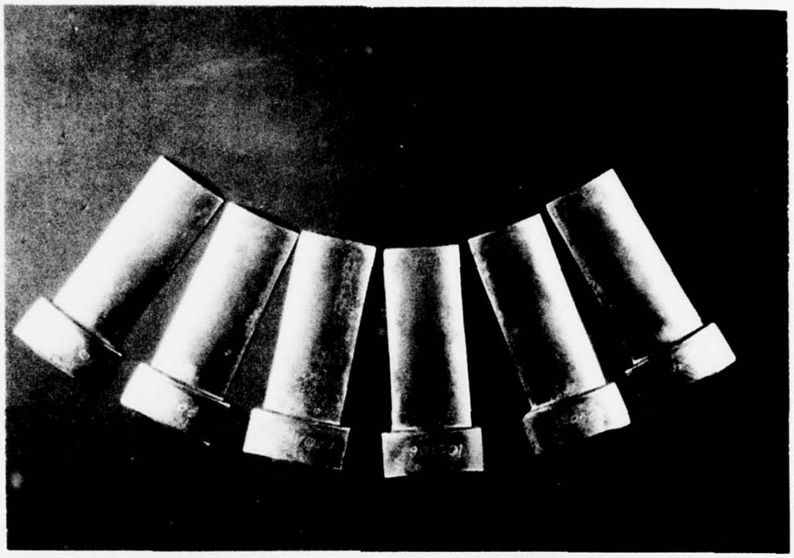

A – CONVEX SURFACE

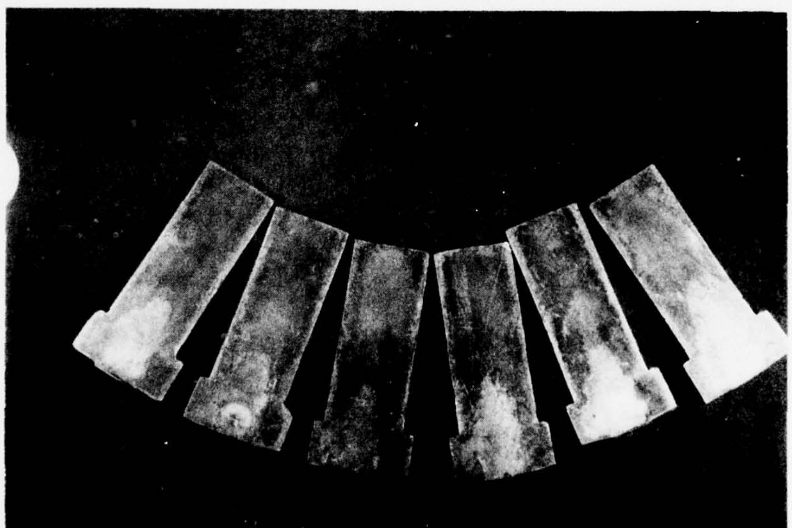

B – BACK OR FLAT SURFACE

Figure 18 *Machine Cast (Thixocast) Simulated Airfoil Cast Into Modified Die Assembly Showing A) Convex Surface and B) Back Or Flat Surface*

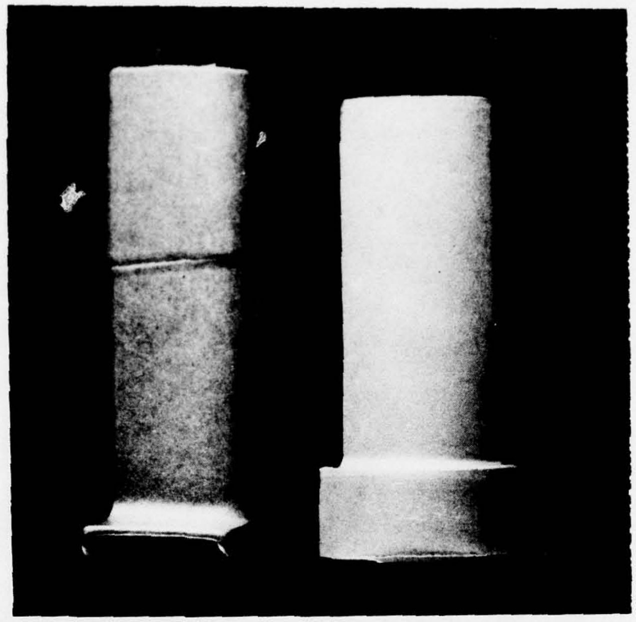

A) COMPRESSOR VANE CONVENTIONALLY FORGED

B) SIMULATED AIRFOIL MACHINE CAST

Figure 19 Comparison of A) Conventional Forged Compressor Vane With B) Machine Cast Simulated Airfoil

Die temperature was varied between 600°F and 1000°F to gain an initial insight as to its influence on part quality. It was possible to control the die temperatures to within about ±20°F of the desired set point temperature. It was noted, however, that at a 1000°F die temperatures there was evidence of accelerating die wear.

Basic machine settings controlling injection speed were held constant (8 in./sec.) for all castings made in this test series. As mentioned previously in Section II-A, a relatively large (0.062 in.^{2}) gate was employed to promote plane front filling with the viscous alloy slurry. Under these conditions, the die cavity fill time was calculated to be about 0.032 sec.

D. SERIES II - INJECTION TRIAL EVALUATION

The castings made with the above mentioned variations in preform and die temperatures and reduced length of die ingate were examined both metallographically and nondestructively (radiography and visual examinations). The metallographic evaluation indicated that at the low penetrometer load (25 g) the resultant castings were generally 60% liquid as shown in Figure 20A. The higher penetrometer load (50 g) normally resulted in a higher volume fraction solid (50%), more typical of the values commonly used in the earlier MIT work (see Figure 20B.)

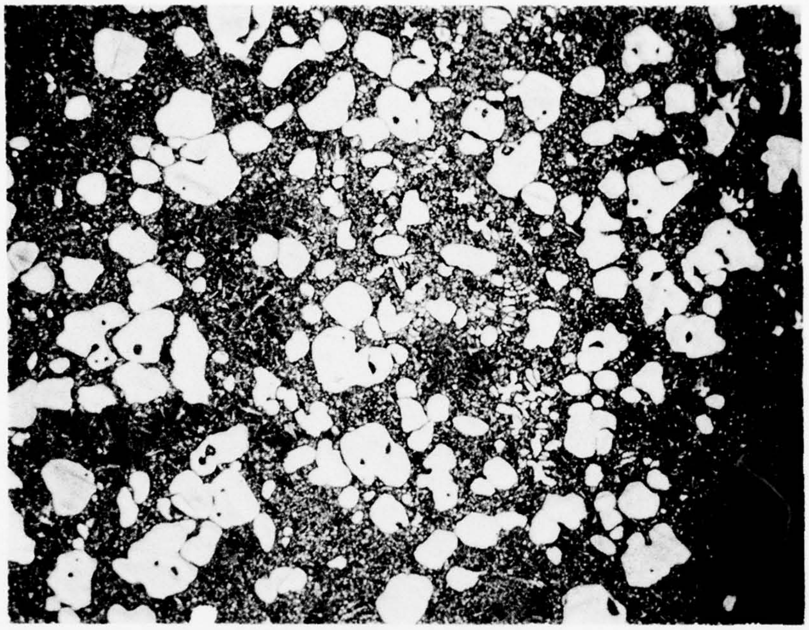

A) LOW V/O SOLID

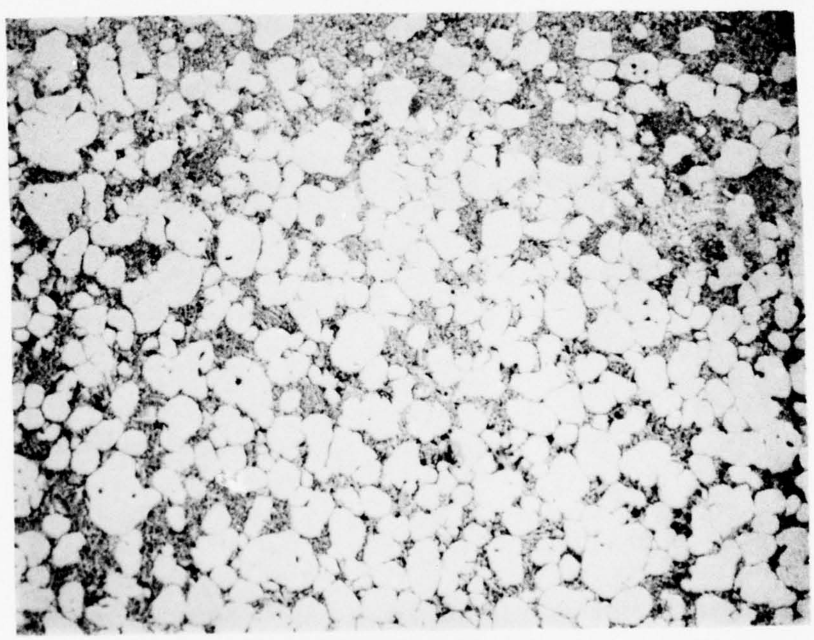

B) HIGH V/O SOLID

Figure 20 Machine Cast Simulated Airfoil Showing Resultant Microstructure From A) Part Using 25g Penetrometer Load (Low V/O Solid) and B) Part Using 50g Penetrometer Load (High V/O Solid) (50X)

The microstructure that existed at the remelting temperature was found to be preserved by the rapid cooling of the slurry in the die. During such solidification, the surfaces of the primary solid particles provided nucleation sites for dendrites, Figure 21. Furthermore, the growth of these dendrites was more rapid at particular locations on the surface of the primary solid particles. The apparent orthogonality of these preferred growth regions suggests $< 100 >$-type orientation. Since the primary solid particles are oriented randomly in the slurry, this results in a corresponding random mix of dendrites in the prior liquid regions. The implication of this observation on mechanical properties will be discussed later, in Section IV.

(A)

(B)

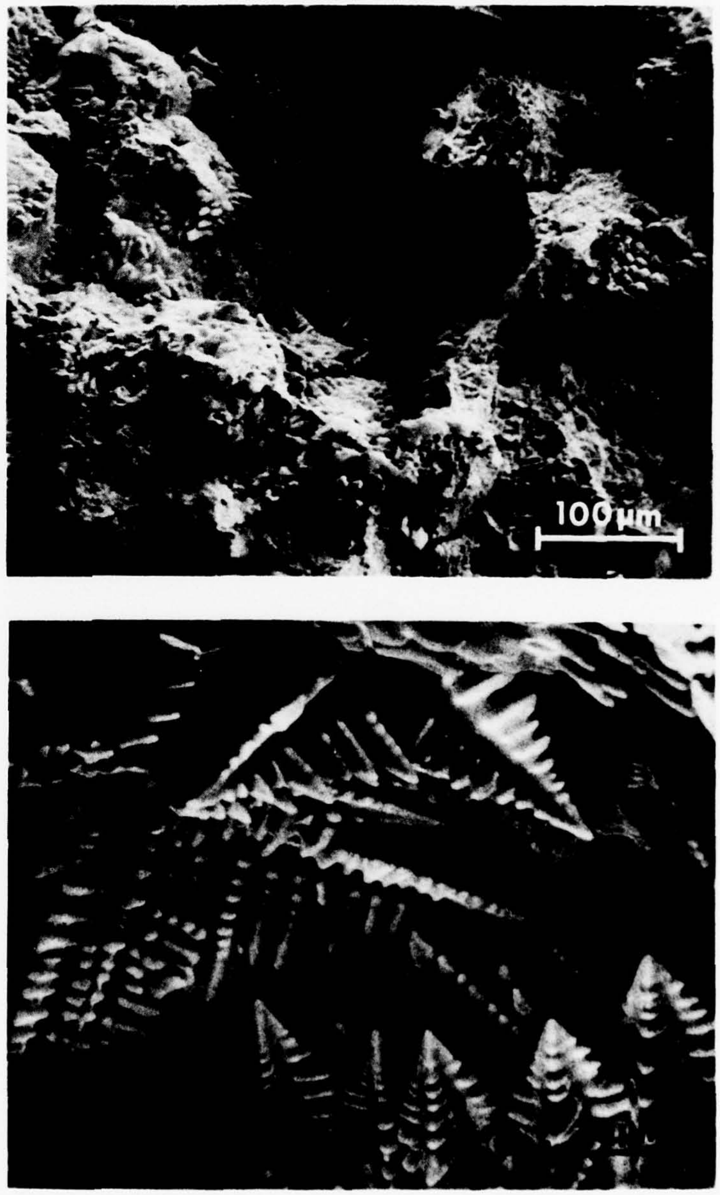

Figure 21 Scanning Electron Micrograph of Haynes 31 Showing A) Nucleation of Dendrites On Surface of Primary Solid Particles During Machine Thixocasting and B) The Random Dentrite Structure In the Prior Liquid Region

Another microstructural feature of a "typical" machine thixocast simulated airfoil section, shown in Figure 22, is the presence of a prior 100 percent liquid layer at the surface. The section contained less than 40% prior solid particles. This layer became much thinner and less distinct in injection trials containing higher prior solid contents, as shown in Figure 23, where in this case, the injected part contained ~60% prior solid. This indicates that this layering phenomenon is due to the slurry flow characteristics and not to variations in preform heating characteristics. Further examination of the injected part shown in Figure 23, however, showed that there was a gradation of prior solid particles varying from 45-50% at or near the surface to about 60-65% near the center. It could be surmised from these observations that any potential effects of liquid layering could be negated by insuring that machine cast parts contain high volume fractions of solid.

Radiographic analysis indicated a significant difference in quality between castings initially containing low volume fraction solid and those containing high volume fraction solid. Examination of radiographs, shown in Figure 24, revealed that the degree of shrinkage type defects was higher in the low volume fraction solid materials than in the high volume fraction solid materials. These data are consistent with the propensity for shrinkage type defects associated with die casting of liquid alloys.

Visual examination of cast parts showed a difference in surface texture between those parts cast using a die temperature of 600°F and a die temperature of 1000°F. A smoother surface existed at the higher die temperature, as shown in Figure 25. This effect was more thoroughly studied and documented in the next task of this program. There appeared to be no surface smoothness differences resulting from variations in preform temperature.

E. SERIES III - INJECTION TRIALS - STATISTICAL EVALUATION

The overall quality of machine cast components can be affected by several process variables, including preform temperature, gate velocity, die temperature, transfer time, and gating configuration. To assess these parametric effects, a statistical test plan, described in Appendix "A", was prepared. The test matrix from this plan is shown in Figure 26. The parameters selected are as follows:

Die Temperature:	100°F, 400°F, and 800°F
Injection Velocity:	15 in./sec, 20 in./sec and 30 in./sec
Penetrometer Weight:	25 g, 40 g, and 55 g

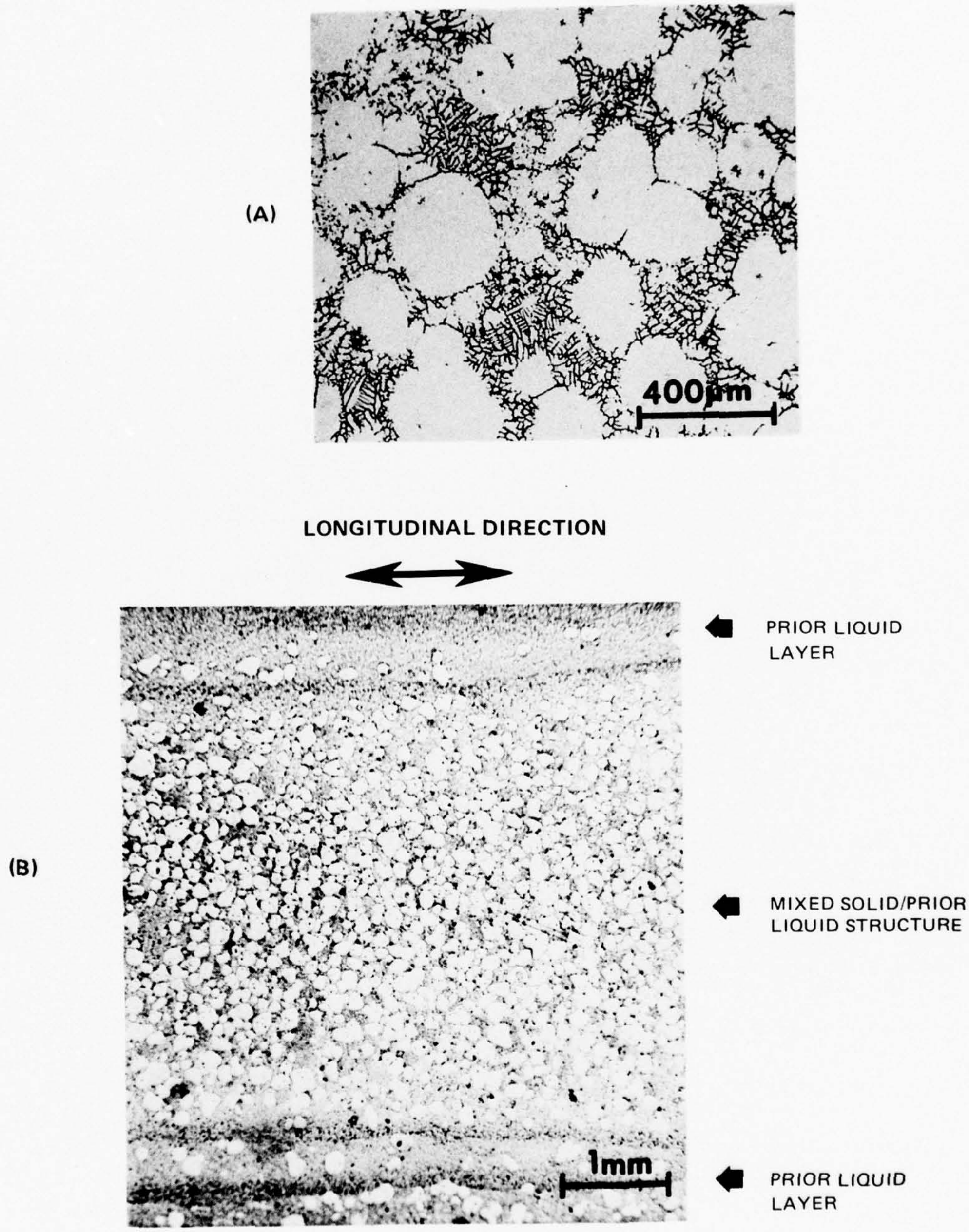

Figure 22 Microstructure of Machine Thixocast Haynes 31 Simulated Airfoil Section From Preliminary Runs: A) General View and B) Detailed Microstructure Near Center of the Airfoil Section Showing the Quenched Rheocast Microstructure Showing the Solid/Prior-Liquid Mixture at The Center of the Airfoil and The Prior Liquid Layer at the Surface.

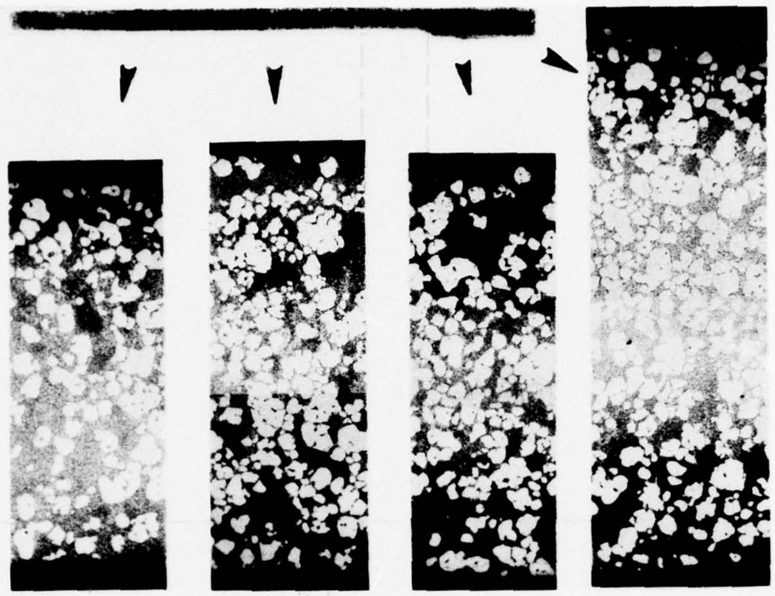

Figure 23 *Microstructural Variation Along The Length of a Series II Machine Cast Simulated Airfoil*

A) LOW V/O SOLID

B) HIGH V/O SOLID

Figure 24 *Radiograph of Machine Cast Blades Showing A) High Levels of Porosity Associated With High Preheat Temperature (Low V/O Solid – <20 V/O) and B) Low Levels of Porosity Associated With Lower Preheat Temperature (High V/O Solid – ~50 V/O)*

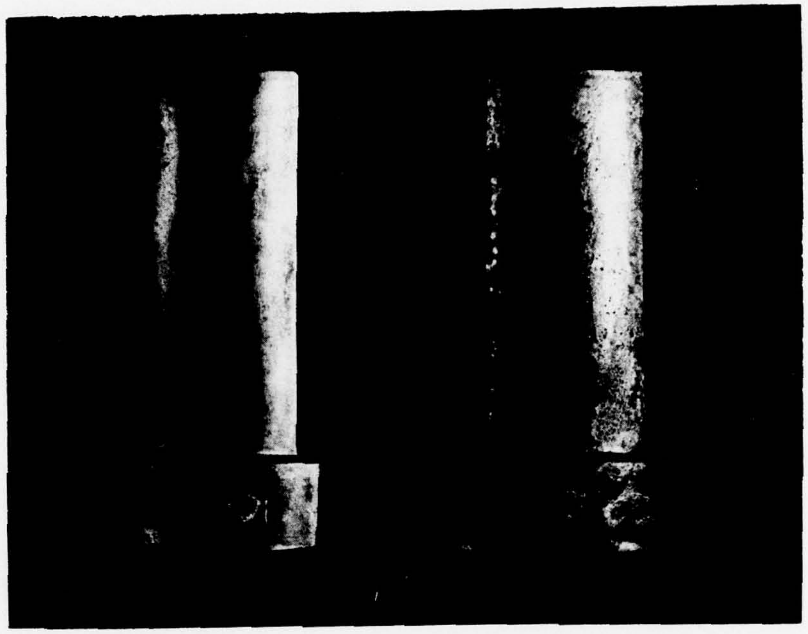

A) 1000°F DIE TEMP

B) 600°F DIE TEMP

Figure 25 Comparison of Machine Cast Simulated Airfoil From Trials Employing A) 1000°F Die Temperature and B) 600°F Die Temperature

TEXT MATRIX

% SOLID	T1 V1	T1 V3	T2 V2	T3 V1	T3 V3
S1	X	X		X	X
S2			X		
S3	X	X		X	X

DIE TEMPERATURE (T1, T2, T3); GATE VELOCITY (V1, V2, V3)

X = TEST POINT

Figure 26 Statistical Test Matrix for Evaluation of Machine Casting Parameters

Die temperatures were selected to give as wide a range as possible for variable evaluation. A maximum temperature of 800°F was selected because of potential thermal effects on the H-11 die as mentioned previously in Section III-C. Injection velocity was varied from the maximum rate (30 in./sec) to one-half the maximum rate (15 in./sec). Using the die shown in Figure 9, these rates correspond to gate velocities of 380 and 190 in./sec., respectively. Penetrometer weights were varied within a fairly narrow range, corresponding to experience with the injection capabilities of the machine casting unit. Significantly higher penetrometer loads led to a high incidence of die-filling problems. It should be noted that both injection and die clamping pressures are well below those normally used in conventional die casting. In addition the transfer time for each injection trial was recorded. The measured effects of these parametric studies were volume fraction solid (metallographic evaluation), internal quality (radiographic evaluation), and surface quality (visual examination).

Volume fraction solid was measured by point count (50 points per examination) techniques. Radiographic evaluations were based on the criteria shown in Figure 27. Visual examinations were based on the criteria listed in Table I. The injection series was performed according to the matrix plan and each part was analyzed as described above. The parametric conditions and analysis of results are listed in Table II.

It should be noted that there was some variation in volume fraction solid with penetrometer loading. It is suspected that the specific penetrometer system used with the machine casting unit had not operated with consistency, thus causing variations in the volume fraction solid in the finished part. It was noted that there was significant variation in the rate at which the penetrometer stylus penetrated the specimen, but no correlation could be made between this penetration rate and resultant volume fraction solid. This variation ranged from a minimum of about one second upwards to 15 sec for a 0.3 inch penetration. It is also possible that unmonitored thermal fluctuations in the heating system caused inconsistent heat-up in the starting preform.

Since there was a variation of volume fraction solid as a function of penetrometer loading, it was decided to use the volume fraction solid as the controlled variable rather than penetrometer load in the statistical analysis. Three ranges of volume fraction solid were employed below 41 percent, 42 to 60 percent, and above 60 percent. Examples are shown in Figure 28.

The initial statistical analysis was run to determine first-order (noninteractive) effects of injection speed, die temperature, and volume fraction solid on surface and radiographic quality. It was found that for both internal quality there was no direct correlation with the processing variables when the latter were treated as noninteractive variables. There appeared to be some effect of volume fraction solid on surface quality.

Interactive effects were next measured between die temperature and injection speed, die temperature and volume fraction solid, and injection speed and volume fraction solid. All three interactions showed effects internal quality. For low volume fractions solid (below 41%), maximum die temperature and injection speeds produced the best internal quality. This is generally consistent with liquid die casting experience. A similar effect was noted for moderate volume fraction solid (42 to 60%). Finally, at high volume fraction solid (above 60%), low speeds and die temperatures produced improved internal quality.

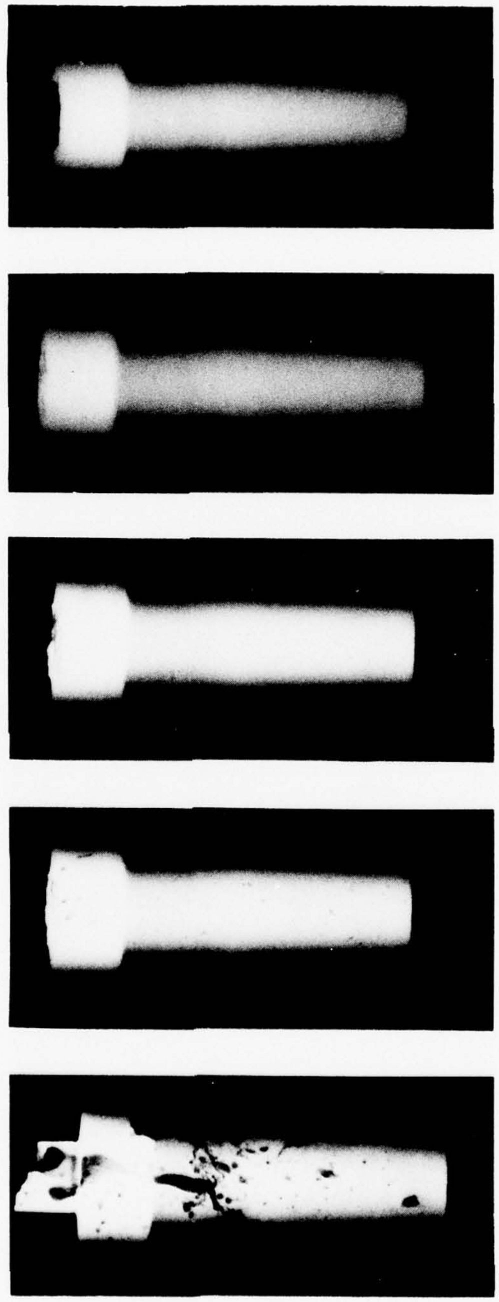

X4686-9
021506

X4592-7
021004

X4592-15
021406

X4592-14
021405

X4592-13
021404

Figure 27 *Examples of X-Radiographs Illustrating the X-Ray Quality Ranking Criteria*

TABLE I – SURFACE GRADING CRITERIA

GRADE	DESCRIPTION
1	Smooth surface, free of laps, cracks, flowlines.
2	Grainy or pebbly surface. No flowlines or laps.
3	Light flowlines and laps (probably not an acceptable casting for service).
4	Deep flowlines, some cracks.
5	Very deep flowlines, longitudinal cracks, grainy surface-connected porosity.

The relation of die temperature and injection speed showed somewhat improved internal and external quality with lower speeds at high die temperatures and the opposite injection speed trend at low die temperatures. This apparently was caused by the wide variations of volume fraction solid noted previously.

One last effect measured was transfer time which varied from 3.2 to 6.2 seconds. There was no measurable correlation of transfer time with any of the above mentioned variables, which implies that within this range of times, preform heat losses are minimal because of the insulation provided by the ceramix container.

In summary, interactive effects control the internal and external quality of machine cast parts, implying a rather complex behavior of reheated rheocast material during injection and solidification. Detailed analysis beyond the scope of this program would be required to define the specific parametric behaviors necessary to consistently machine cast high quality gas turbine components. The results of this evaluation are tabulated in Appendix "A".

TABLE II

MACHINE CASTING DATA SUMMARY

Test Number	Dia. Temperature °F	Penetrometer Weight Grams	Injection Velocity in/sec	V/O Solid %	Total Transfer Time Sec	X-Ray Quality	Surface Quality
020701	100°	Std	30	52	3.4	3	5
020702	100°	Std	30	34	3.6	4	3
020703	100°	-10	30	52	4.1	3	3
020704	100°	-10	30	67	3.5	2	2
020705	100°	-20	30	73	4.1	2	3
020706	100°	-20	30	54	3.7	3	2
020707	100°	-30	30	60	3.2	3	5
020708	100°	-30	30	–	5.5	–	–
020709	100°	-30	30	37	3.2	5	4
020901	100°	Std	20	75	4.7	4	1
020902	100°	Std	20	65	–	3	1
020903	100°	Std	20	73	–	3	5
021001	100°	Std	30	56	3.6	3	4
021002	100°	Std	30	75	3.4	3	2
021003	100°	Std	30	63	3.5	3	2
021004	100°	-30	30	53	3.3	2	2
021005	100°	-30	30	71	3.5	2	2
021006	100°	-30	30	–	–	–	–
021007	100°	-30	30	56	3.5	3	2
021401	100°	-30	20	50	4.3	4	4
021402	100°	-30	20	27	4.3	4	5
021403	100°	-30	20	69	4.3	4	2
021404	400°	-15	15	–	–	5	–
021405	400°	-15	15	29	5.6	4	4
021406	400°	-15	15	65	6.2	3	1
021407	400°	-15	15	–	–	–	–
021408	400°	-15	15	75	6.1	3	5
021501	800°	Std	20	63	4.7	2	4
021502	800°	Std	20	46	4.6	4	3
021503	800°	Std	20	65	4.4	3	3
021504	800°	Std	20	–	4.5	–	–
021505	800°	Std	20	56	4.5	3	3
021506	800°	Std	20	63	4.3	2	3
021507	800°	Std	30	67	3.4	5	3
021508	800°	Std	30	60	3.3	2	4
021509	800°	Std	30	29	3.4	4	3
021601	800°	-30	30	23	3.8	3	4
021602	800°	-30	20	79	4.1	3	3
021701	800°	-30	30	58	3.6	4	5
021702	800°	-30	20	73	4.4	3	5
021703	800°	-30	20	63	4.4	2	5
021704	800°	-30	20	65	6.0	2	2

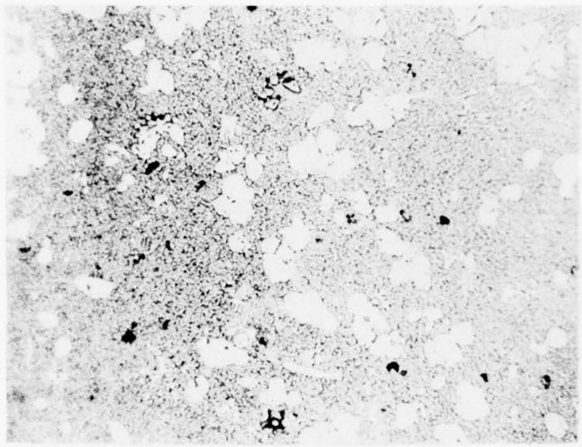

021601 50X
BELOW 41% SOLID

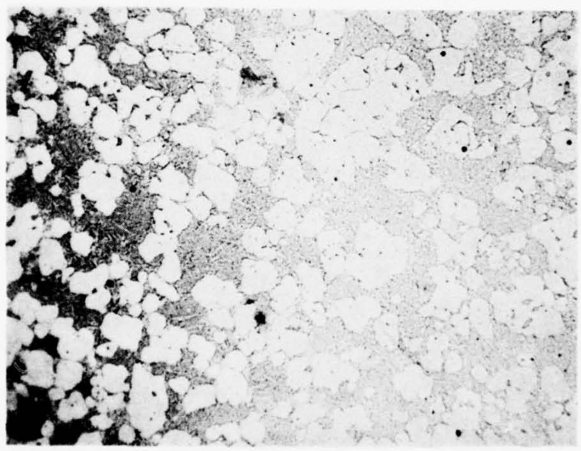

020708 NECK 50X
42 TO 60% SOLID

020704 NECK 50X
ABOUT 60% SOLID

Figure 28 Examples of Low, Medium, and High Volume-Fraction-Solid Microstructure

F. SERIES IV INJECTION TRIALS – DIE MODIFICATION, PREFORM PREPARATION, AND MECHANICAL TRANSFER SYSTEM

1. Advanced Simulated Vane Die

The gating for the advanced simulated die, shown in Figure 10, was suggested by gating studies using high-speed cinematography of a die cavity similar to that used in the earlier stages of the program. Figure 29 shows a selection of parts made in this die. Additional complexities in the form of a platform and root tangs were added to the simulated vane to more closely approximate an actual compressor vane configuration; an advanced simulated vane and an actual vane is shown in Figure 30. Because injection trials with this die were conducted late in the program, no mechanical property specimens were machined from the parts.

Figure 29 Sample Castings Made in the Advanced Simulated Airfoil Die Cavity

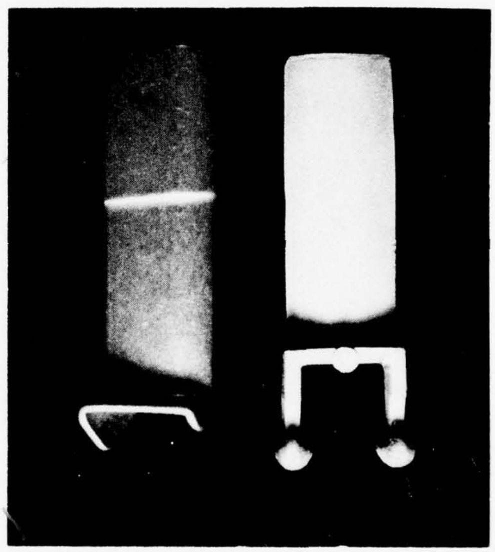

Figure 30 Advanced Simulated Airfoil Compared With an Actual Compressor Vane Configuration

With this advanced die, the incoming metal tended to separate even at reduced injection speeds, producing partial shots that consisted of the two ends of the casting, but no central portion. This malfunction was correlated with a partially blocked gate entrance which increased the metal stream velocity through the remaining unblocked gate area above that expected from calculations. Radiography showed improvements in internal quality as compared to castings with the original die when clear gate conditions were maintained.

2. Preform Preparation

Standard practices throughout the program were to prepare rheocast preforms by sandbladting to remove the surface oxide layer present on the as-received rheocast bars and to maintain a flowing argon atmosphere in the reheating chamber during heat-up in preparation for machine casting.

Analysis of failure origins in early mechanical property specimens suggested that an improvement in properties could be expected if nonmetallic inclusions could be eliminated from the microstructure.

An end view of an as-received rheocast bar is presented in Figure 31a, showing the distribution of inclusions near the surface of the bar. A longitudinal section through a casting made from such a preform is shown in Figure 31b. Figure 31c shows a cross section of a preform from which 0.1 inch of the surface layer had been removed, and a longitudinal section through a casting made from a preform prepared in this manner is shown in Figure 31d. Clearly, removal of a majority of incoming inclusions had significantly improved the cleanliness of the casting. Such surface removal techniques are well-established in the processing of melt stock for investment casting.

On the theory that some of the porosity of the final casting might be caused by preexisting pores, a number of preforms from which the surface had been removed were subjected to a hot isostatic pressing cycle to reduce the porosity of the starting material. However, no reduction in porosity was noted in castings produced from these preforms. It is concluded, therefore, that turbulence and shrinkage are the primary sources of porosity, not the porosity of the rheocast preform.

3. Mechanical Transfer System

The system for mechanically transferring the heated specimen from the induction coil to the injection position (Figure 14) was constructed and operated. With this system, transfer time (measured from start of specimen motion to start of injection) was reduced from the 3.5–4.5-second range to a consistent 2.5 seconds. The path traversed by the specimen is shown by the multiple-exposure photograph in Figure 32.

The reduced and consistent transfer time appeared to improve microstructural consistency from shot to shot, although some variations persisted because of irregularities in penetrometer operation.

G. INJECTION TRIALS/SUMMARY

The machine casting characteristics were evaluated through the performance of four series of injection trials. The results of these trials are:

1. The machine casting unit, as modified, was effective in producing simulated airfoils out of Haynes 31 cobalt-base superalloy.

2. Die designs used in these studies were not useful for fabricating parts with uniform quality.

3. Parametric analysis of process variables indicate that high volume fraction solids in the preform, relatively slow injection speeds, and low die temperatures would lead to improved nondestructive quality.

4. The porosity in the cast parts appears to be primarily a function of injection and die design and not the porosity in the preform.

5. Removal of surface nonmetallic inclusions from the preform improves the internal quality of the machine-cast parts.

6. Mechanization of the machine casting system reduces processing time and can produce incremental improvements of part quality.

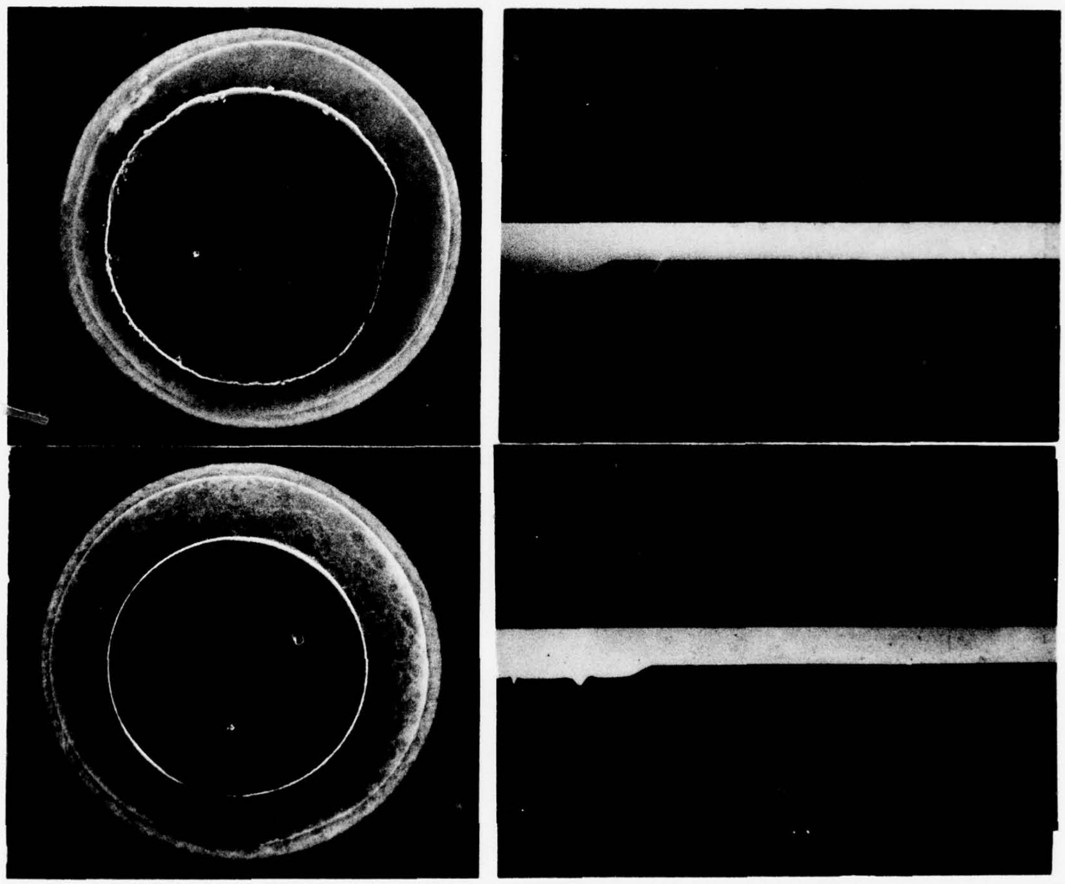

Figure 31 *Effects of Surface Skin Removal on Cleanliness of Machine Cast Simulated Die – A. Cross Section of As-Received Rheocast Starting Material; B. Longitudinal Section Through Machine Cast Simulated Airfoil Made From Starting Material Shown in "A"; C. Cross Section of Starting Stock With 0.100 Inch Removed From Original Surface Skin; D. Longitudinal Section Through a Machine Cast Simulated Airfoil Made From Starting Material Shown in "C".*

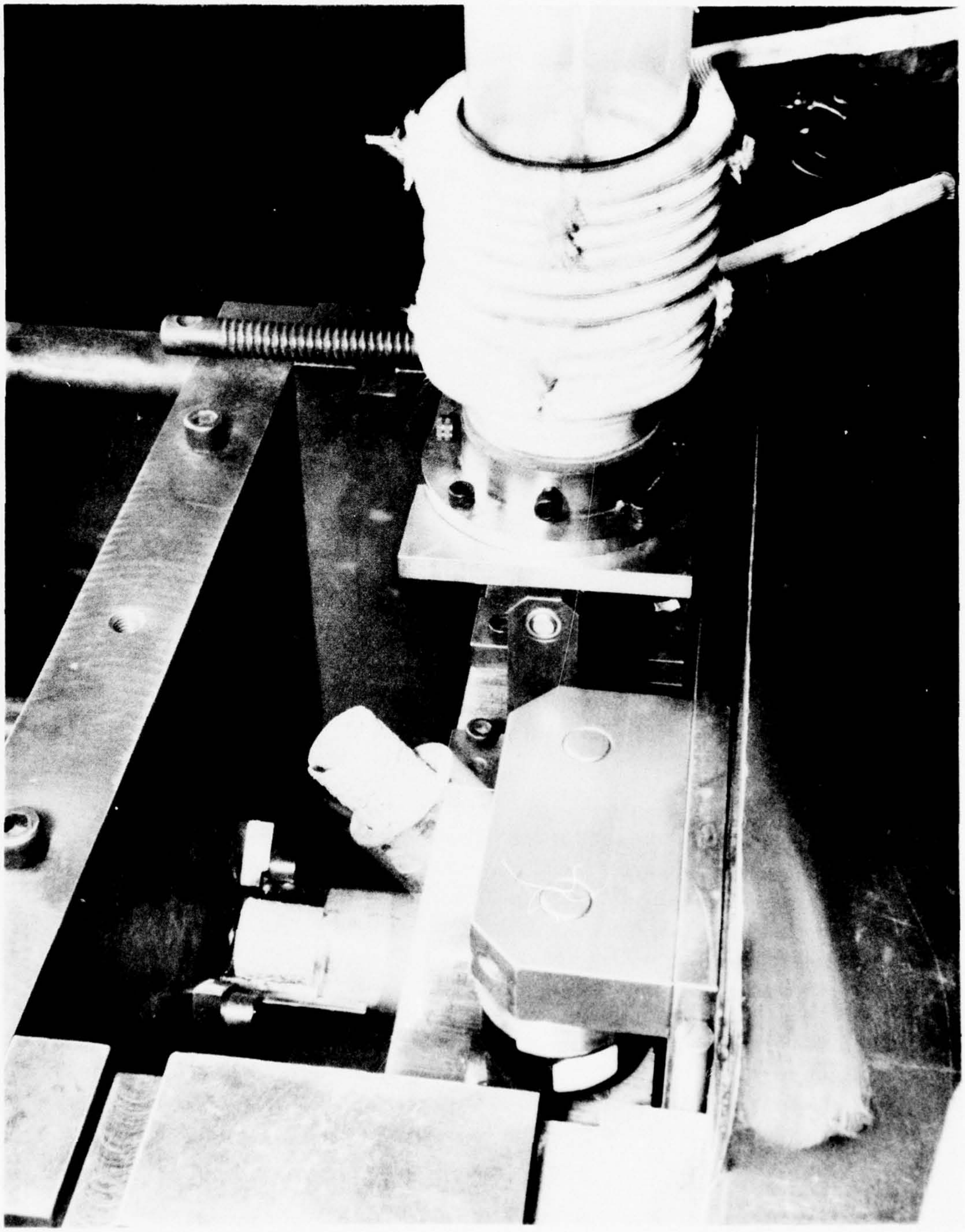

Figure 32 Multiple Exposure Photograph Showing Path Traversed By Specimen With Automatic Transfer Mechanism

IV. MECHANICAL PROPERTY EVALUATION

A. INTRODUCTION

The mechanical properties of machine-cast specimens were evaluated throughout the various development stages of the thixocasting process. The evaluation was conducted while the experimental setup and casting procedures were undergoing evolutionary modifications and refinements. Briefly during the initial casting trials (Series I), incomplete die-fill was experienced, but changes in the design of the die eliminated this problem. Subsequent cast trials, using the revised die (Series II, III, and IV), involved variations of the casting procedures.

Cast parts were chosen for mechanical property evaluation on the basis of their relative x-radiographic quality and surface appearance, and not on process parameters. Tensile, stress-rupture, and high-cycle-fatigue (HCF) properties were obtained from Series II and III cast parts. Only tensile tests were performed on the Series I parts. A limited number of stress-rupture and HCF tests were performed using Series IV cast parts.

Although complete die-fill was achieved with the die used for the Series II, III, and IV trials, die and gating designs were not optimized. During injection, turbulent flow of the semisolid slurry occurred in the die, resulting in a considerable quantity of trapped porosity which adversely affected the tensile, stress rupture, and HCF properties. This deficiency was largely negated by hot isostatic pressing (HIP) of the cast parts. The HIP conditions used, however, did not significantly change the thixocast microstructure and, therefore, some of the observations from this material presented below should be representative of Haynes 31 parts fabricated by the machine thixocasting process.

B. EXPERIMENTAL CONDITIONS

1. Specimen Fabrication and Test

Cylindrical tensile specimens (Figure 33a) were machined from machine thixocast parts resulting from Series I trials. Sheet-type of specimens – more compatible with the geometry of the simulated airfoil produced in Series II, III and IV trials – were used for tensile, stress rupture, and HCF tests. The same specimen design (Figure 33b) was used for both tensile tests and stress rupture tests. A miniature version of the specimen (mini-Krause, Figure 33c) was used for HCF tests. These specimens were tested as-thixocast, as-thixocast plus HIP or as-thixocast plus HIP plus heat treated.

Heat treatments were performed on selected thixocast simulated airfoils prior to machining into specimens. All the specimens were oriented with their longitudinal axis parallel to the thixocast simulated airfoils. Except for two noted tensile specimens, all the specimens were from the same batch of rheocast material.

Tensile tests were performed at room temperature, 1000°F, and 1450°. Room temperature elastic modulus was also obtained in the tensile tests from the strain-gage and stress measurements. Stress rupture tests were performed at 1450°F with a stress of 30 ksi. High-cycle-fatigue tests in fully reversed bending mode were performed at room temperature, using a limited alternating stress range of 40 ksi to 60 ksi and a frequency of 450 cycles per minute. All specimen surfaces were tested in their as-machined condition.

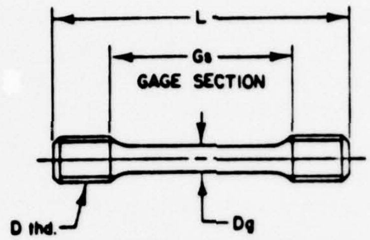

L	Gs	Dg	Dthd
1.500	.700	.100	10-32

a

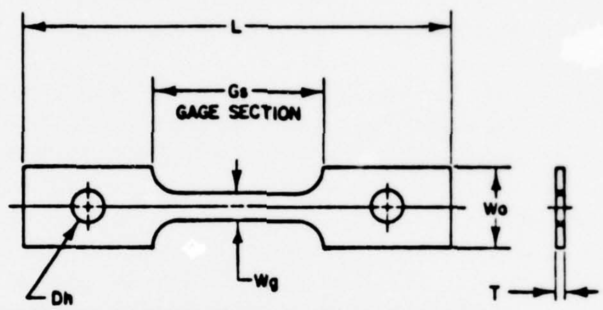

L	Gs	Wo	Wg	Dh	T
2.250	.500	.625	.140	.250	.060

b

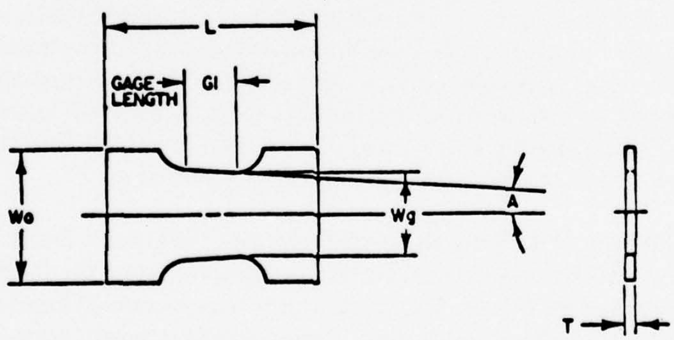

L	Gl	Wo	Wg	A	T
2.000	.510-.515	.740-.750	.495-.505	2°52'	.050-.060

c

Figure 33 *Dimensions in Inches of a) a Cylindrical Tensile/Stress-Rupture Specimen, b) a Sheet Type Tensile/Stress Rupture Specimen, and c) a Mini-Krause HCF Specimen Used in the Testing of Rheocast Material*

To determine if test results are affected by specimen geometry, stress-rupture, and HCF tests were conducted on conventional cast Haynes 31 using the specimen designs shown in Figure 33. To determine the effect of microstructure, tensile and stress-rupture tests were also conducted on the rheocast material, the starting material used for the thixocasting process. These specimens were taken from the interior regions of rheocast bars. The machined specimen blanks were then hot isostatically pressed for three hours at 2250°F and 15 ksi. The specimen geometry for the tensile and stress-rupture tests is shown in Figure 33b.

2. Heat Treatment Procedures

Preliminary heat-treatment studies were performed on the rheocast material to determine the aging response and the variation of amounts of solid at temperatures between solid and liquid. All heat treatments were performed in an argon atmosphere.

For solution and aging treatments, a muffle furnace was used which had a temperature control of better than ±10°F. The quenching experiments from which the volume fractions of solid were determined at various temperatures were carried out in a vertical, platinum-wound, tube furnace. A specimen with dimensions about 0.2 x 0.2 x 0.5 inch was suspended in the furnace with an alumina crucible. After the desired thermal exposure, the specimen was dropped into the quench bath. The time of flight for the specimen was less than 0.1 second. The quenched microstructure was, therefore, assumed to be the same as that existing at the high temperature (i.e., coarsening of the primary solid particles during cooling was assumed to be negligible).

3. Metallographic and Fractographic Techniques

Metallographic samples of the conventional cast, the rheocast, and the thixocast Haynes 31 were all prepared alike. The samples were mechanically polished using standard metallographic techniques. The polished specimens were then electrolytically teched at two volts for two seconds, using a Pt cathode at room temperature in Michigan B (47 mil sulfuric acid, 41 mil nitric acid, 12 mil phosphoric acid, and 5g nickelous chloride). Unless otherwise noted, longitudinal sections of the samples were mounted for examination.

Lineal analysis was used to determine the average size and the volume fraction of the primary solid particles in the thixocast specimens. To obtain information on the fracture processes in tensile, stress-rupture, and HCF tests, fracture surfaces were examined using a scanning electron microscope (SEM). The SEM results are supplemented by metallographic observations on longitudinal sections through the fractures. In the case of the HCF fractures which (as shown below) were all surface initiated, the crack nucleation sites were determined by polishing away the machining marks. A surface layer of approximately 0.003 inch was removed by this procedure.

C. RESULTS AND DISCUSSION

1. Microstructures

The microstructures of Haynes 31 produced by conventional casting, rheocasting, and thixocasting are illustrated respectively in Figures 34a, 34b, and 34c. The conventional cast material consists of dendrites which are delineated by the interdendritic MC-type carbide. By contrast, the dendritic structure is not present in the rheocast microstructure, which consists of equiaxed grains surrounded by a network of primary carbide. The equiaxed grains evolved from the spheroidal primary solid particles by coarsening during cooling through the solidus-liquidus temperature range.

The basic difference between the machine thixocast and rheocast microstructures is that the prior liquid solidifies much more rapidly during thixocast and results in formation of dendrites. Note the finest of these dendrites compared with that of conventional cast material.

The shape of the machine thixocast simulated airfoil is shown in Figure 35a. The simulated airfoil is 2.5 inches long, 1.0 inch wide, and has a flat and a convex surface. The maximum thickness is 0.1 inch and the edges are 0.025 inch thick.

2. Effect of Thixocasting Processing Conditions on Microstructures

In general, the principal effect of reheating temperatures and holding time can be expected to be in the volume fraction of primary solid. Higher reheat temperatures and longer times favor lower volume of solid and smaller primary solid particle size. The upper limit of the solid particle size is determined by the initial rheocast microstructure.

Depending on the thermal insulation around the preheated slug at temperature, coarsening and coalescence of the primary solid particles occur during the transfer from the preheat chamber of the die. Over the range of transfer times observed in this program (three to six seconds), no significant effect on microstructure was observed. The primary solid particle sizes ranged from 0.003 to 0.005 inch for most of the specimens tested.

Although injection speed and die geometry affect the flow of the slurry into the die cavity, these parameters had no effect on microstructure over the range studied. Other parameters being constant, the die temperature determines the rate of solidification. Because of the thickness of the simulated airfoil (maximum thickness 0.1 inch), solidification occurs very rapidly even for the highest die temperature used (1000°F). The effects of die temperature can be observed from the dendrite structure in the prior liquid region. With the die at room temperature, the dendrites (Figure 36a) are short and nucleate randomly. By contrast, at higher die temperatures the dendrites are larger and nucleate at the surfaces of the primary solid particles as well as in the prior liquid (Figure 36b and Figure 37). This resulted in a scalloped primary solid-prior liquid interface, compared with the rather smooth interference when a room-temperature die was used. The effect of this interface morphology will be discussed later.

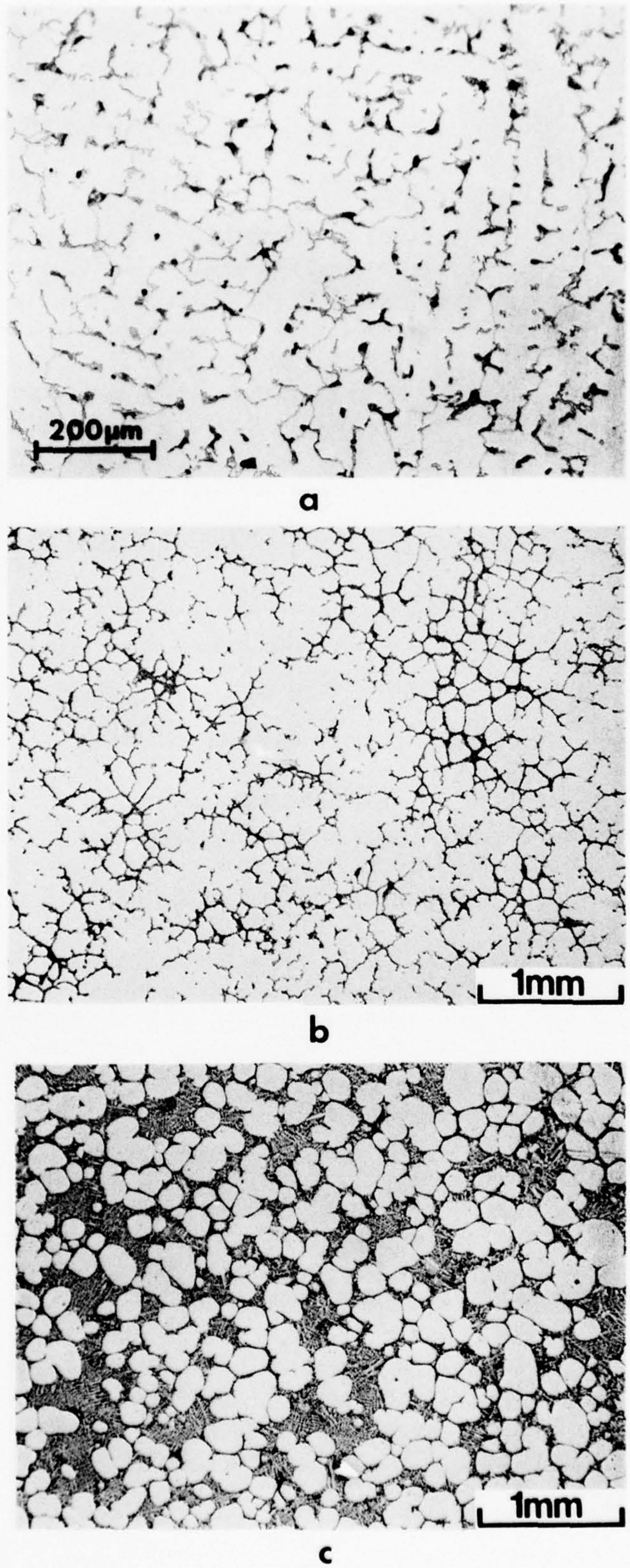

Figure 34 Typical Microstructures of Haynes 31 – a) Conventional Cast; b) Rheocast; c) Thixocast

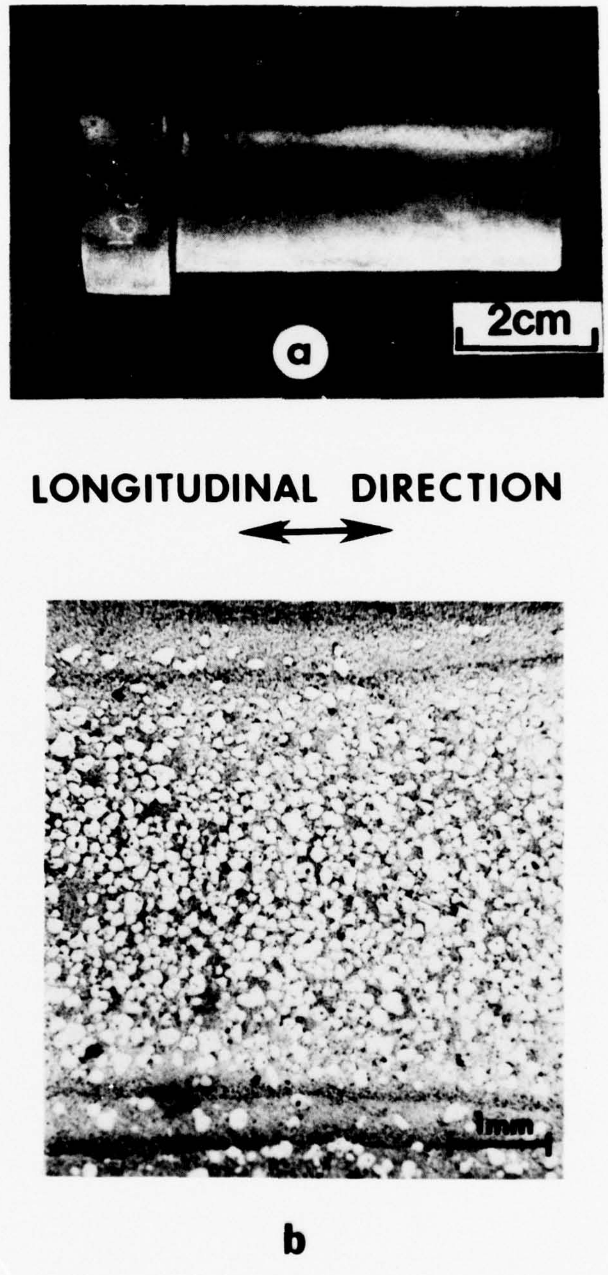

Figure 35 (a) Shape of the Simulated Airfoil and (b) Longitudinal Microstructure of a Machine Thixocast Simulated Airfoil

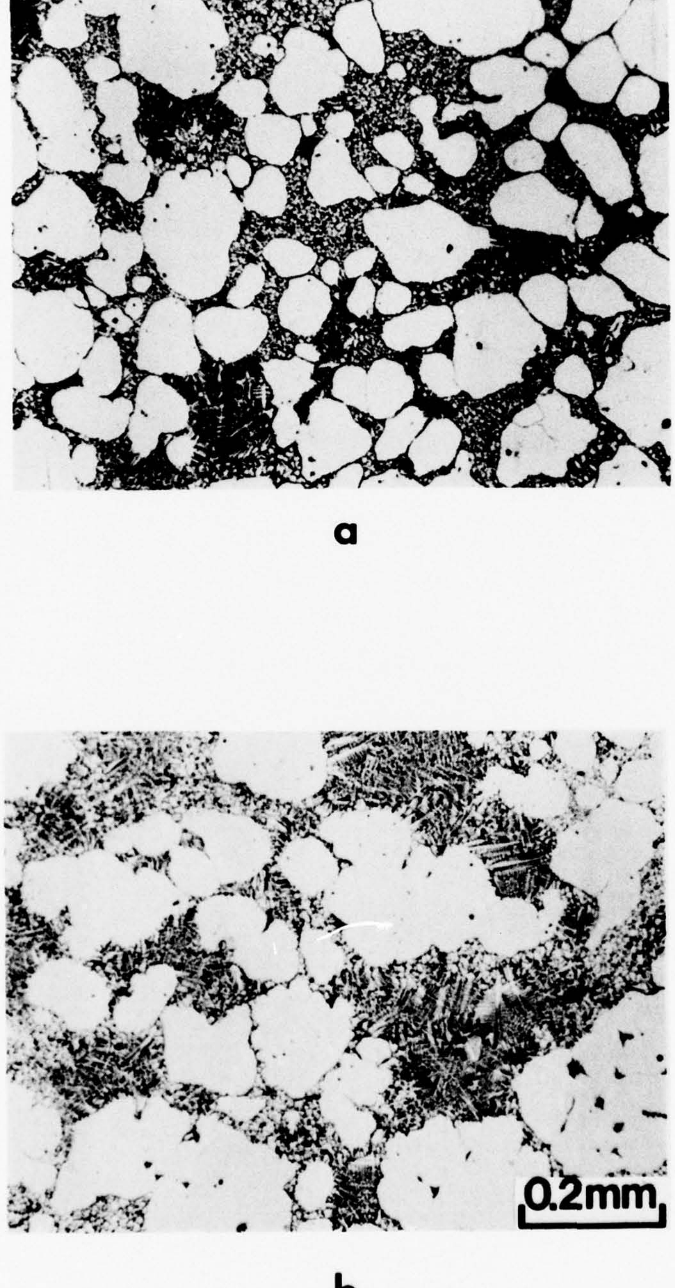

Figure 36 *Thixocast Microstructure Resulting From a Die Temperature of (a) 70°F and (b) 800°F*

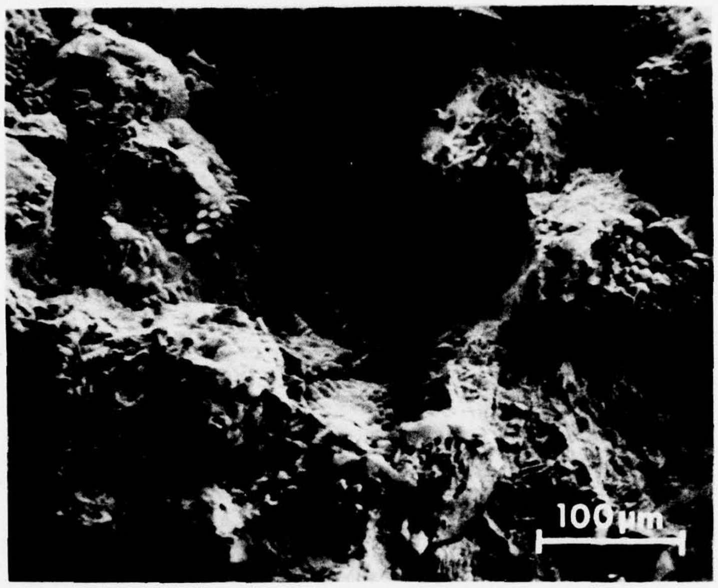

Figure 37   Nucleation of Dendrites From Surfaces of Primary Solid Particles During Thixocasting

3. Heat Treatment Response

Fraction of Solid at Various Preheat Temperatures

When rheocast material is overheated to temperatures within the solidus and liquidus preferential, remelting occurs at the primary carbides located at the prior liquid regions. The equilibrium amount of primary solid present during reheating depends on temperature, as depicted in Figure 38. The microstructures obtained after one-hour thermal exposure followed by water-quenching are illustrated in Figure 39.

Aging Response of Rheocast Haynes 31

The microstructures of the rheocast Haynes 31 after solutioning at 2250°F and aging at various temperatures are shown in Figure 40. The solution treatment results in partial dissolution of the primary carbide and coarsening by coalescence of the primary carbide (Figure 40a). Preferential precipitation of $M_{23}C_6$ type of carbide at subgrain boundaries and grain boundary regions can barely be observed after aging at 1350°F for 24 hours (Figure 40b). Much heavier precipitation of $M_{23}C_6$ can be observed when the aging was at 1500°F.

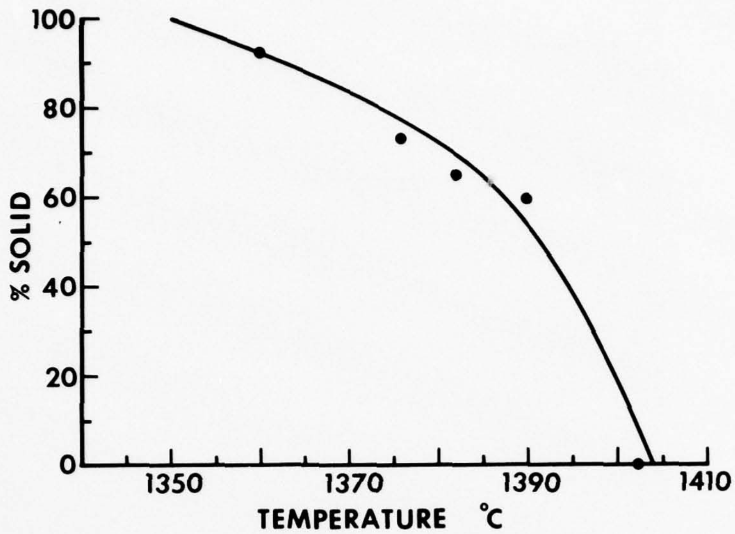

Figure 38 Volume Fraction of Primary Solid After One Hour at Various Reheating Temperature

Discrete carbide particles are distributed rather uniformly, and those in the grain matrix tend to align along crystallographic directions (Figure 40c). Similar observations can be made of the aging at 1650°F except that the distribution of the carbide particles is less uniform and tend to cluster at grain boundary regions (Figure 40d). The observed relative quantities and distributions of the $M_{23}C_6$ carbides precipitated during aging at various temperatures are those expected from the C-shape temperature-time-transformation (TTT) precipitation kinetics of $M_{23}C_6$ carbides. In this report, the aging response of rheocast Haynes 31 may be considered as typical of those conventionally solidified.

The room-temperature Rockwell hardness corresponding to the microstructures in Figure 40 is illustrated graphically in Figure 41. The hardness after solution treatment at 2250°F is the same as the as-received rheocast material, R_c27, indicating very little additional solutioning of carbon during the heat treatment (for comparison, the hardness of a conventionally cast Haynes 31 is R_c26). The hardness increases with aging temperature and reaches a maximum at about 1500°F which corresponds to copious precipitation of rather homogeneously distributed $M_{23}C_6$ carbide particles (Figure 39). Aging at temperatures above 1500°F resulted in heterogeneous precipitation and coarsening of $M_{23}C_6$ carbide particles, thus the observed decrease in hardness.

Effect of Solutioning on Machine Thixocast Haynes 31

The microstructures of machine thixocast Haynes 31 after HIP (2200°F, 4 hours, 15 ksi), HIP plus 2250°F for 8 hours, and HIP plus 2300°F for 10 hours are shown in Figures 42a, 42b, and 42c, respectively. HIP at a lower temperature of 2000°F for 4 hours, 15 ksi (microstructure not shown) resulted in no discernible change of the thixocast microstructure. HIP at 2200°F for 4 hours, 15 ksi produces spherodization of the interdendritic (primary) carbide, but otherwise the thixocast microstructure remained essentially unchanged.

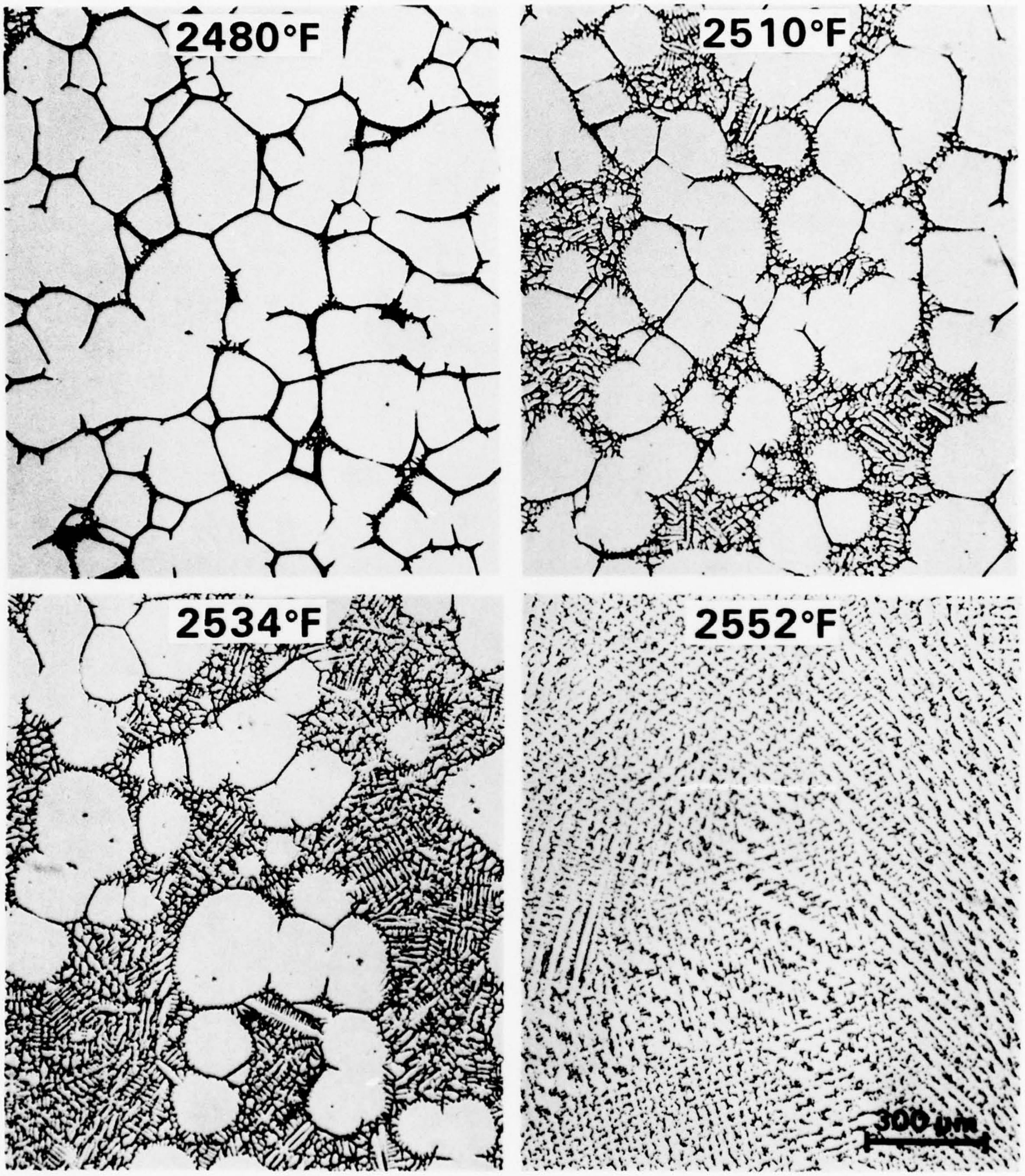

Figure 39 *The Quenched Rheocast Microstructures After One Hour at the Indicated Reheating Temperatures*

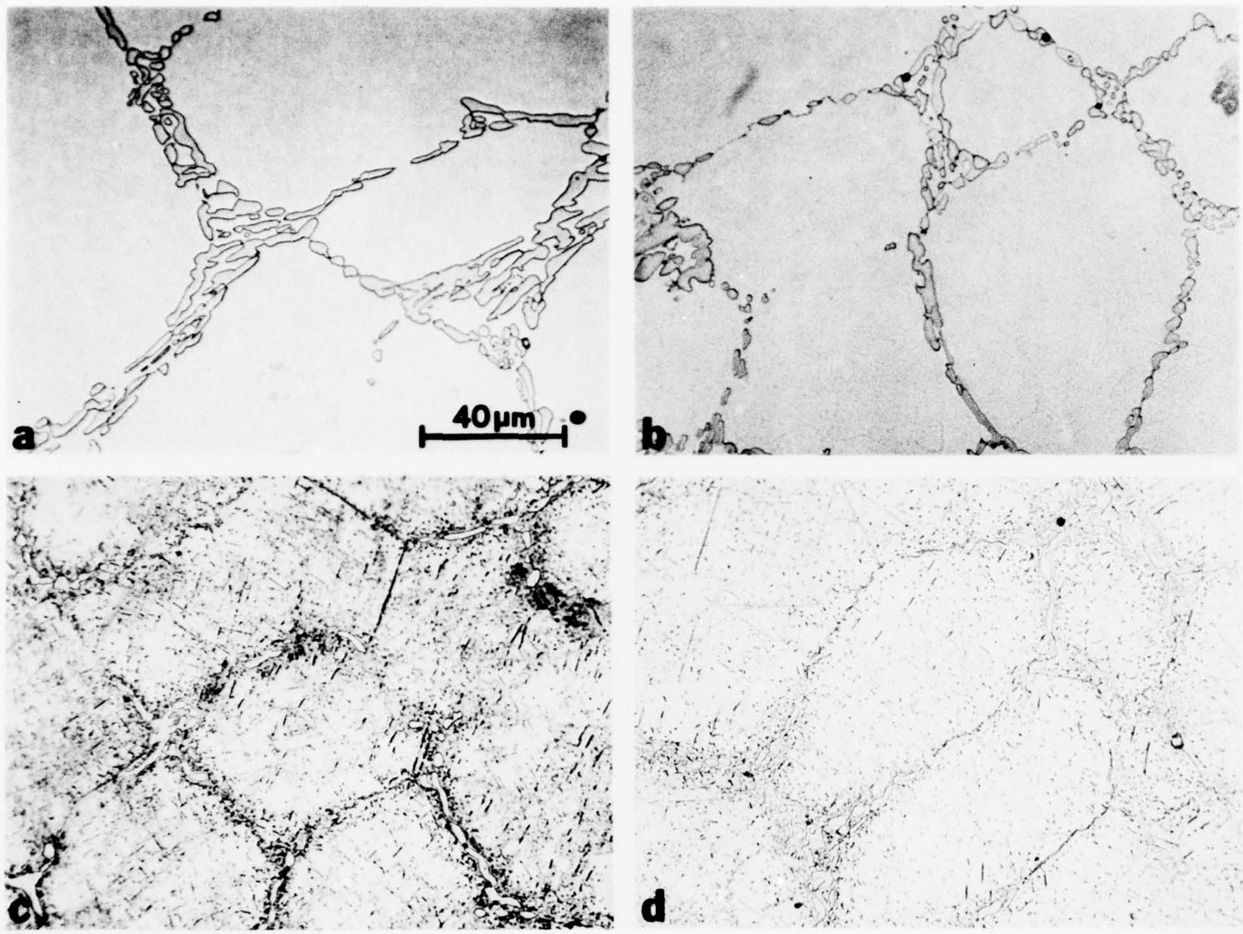

Figure 40 *Microstructure of Rheocast Haynes 31 After (a) Solution Treatment of 2250°F/8 Hr/ Rapid-Air-Cool, (b) Solution + 1350°F/24 Hr Age, (c) Solution + 1500°F/24 Hr Age, and (d) Solution + 1650°F/24 Hr Age*

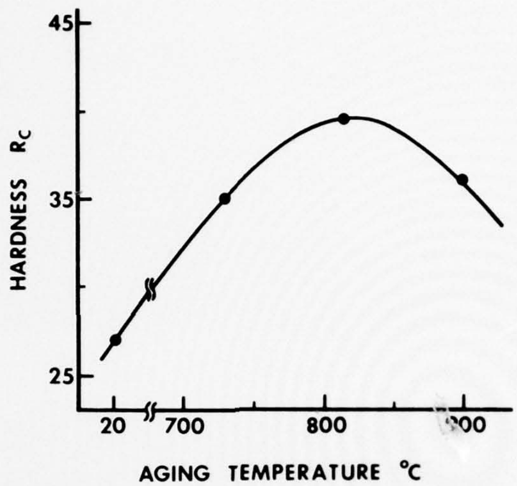

Figure 41 *Hardness of Rheocast Haynes 31 Versus Aging Temperature. The Heat Treatment Conditions and Their Resulting Microstructure are Those Given in Figure 40*

As shown in Figure 42b, a significant amount of primary carbide was solutioned after 2250°F for 8 hours. Spheroidization of the primary carbide and grain growth are also evident after the treatment. Solutioning at 2300°F for 10 hours resulted in coarsening of the primary carbides and incipient melting of the coarsened carbides (Figure 43). Compared with the 2250°F treatment, no significant grain growth was observed even at the incipient melting temperature.

Because of the unique thixocast microstructures and the high rate of solidification, the composition of the primary carbide is expected to be metastable and rather different from that of the conventional cast Haynes 31. Solution treatment after thixocasting would tend to restore the primary carbide composition to one more stable. These changes in the primary carbide composition can in fact be observed from the electron microprobe generated X-ray energy spectra, the results of which are summarized in Table III. The compositions of the primary carbides shown in Table III are characterized in terms of the ratios of the X-ray energy peaks of three principal metal elements present in the primary carbides: Cr, W, and Co.

Table III shows significant differences in Cr/Co and Cr/W ratios between the thixocast and conventional cast materials. These ratios increase with solution temperatures (i.e., the primary carbide becomes progressively more Cr-rich as the thixocast material is solutioned at higher temperatures). At the incipient melting temperature, the primary carbide composition should approach equilibrium. The Cr/Co and Cr/W ratios are 19.4 and 10.1, respectively. For thixocast material, the corresponding ratios for the conventional cast material are 18.9 and 5.7. This difference in the primary carbide composition may be responsible for the observed difference in the incipient melting temperatures which have been reported to be at least 70°F higher for conventional cast material than that observed for thixocast specimens.

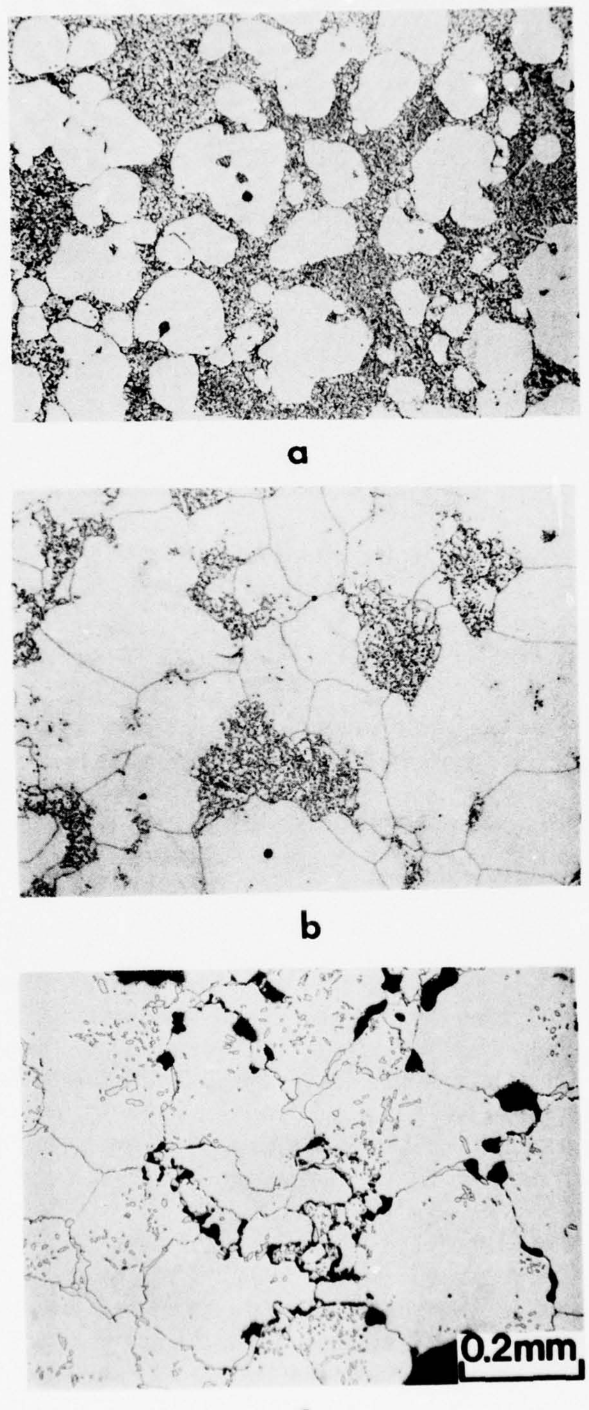

Figure 42 *The Microstructures of Haynes 31 After (a) HIP at 2250°F/15 ksi/4 Hr, (b) HIP + 2250°F/8 Hr, and (c) HIP + 2300°F/10 Hr*

TABLE III – EFFECT OF HEAT TREATMENT ON PRIMARY CARBIDE COMPOSITION OF THIXOCAST HAYNES 31

Heat Treatment	I_{Cr}/I_{Co}	I_{Cr}/I_W
None, As-Thixocast	3.2	2.1
HIP* + 2200°F/4 Hr	7.5	3.1
HIP* + 2250°F/8 Hr	13.3	6.6
HIP* + 2300°F/10 Hr	19.4	10.1
None, As-Conventional Cast	18.9	5.7

*HIP - 2200°F for 4 hours at 15 ksi

4. Tensile Tests

The tensile properties of Haynes 31 produced by conventional casting, rheocasting, and machine thixocasting are given in Table IV. The yield strengths of the thixocast material are 58, 65, and 79 percent higher than the conventional cast material at room temperature, at 1000°F, and at 1450°F, respectively. As shown in Table IV, the yield strengths cannot be correlated with the volume fractions of the primary solid particles. For example, a microstructure having no primary solid (S/N 46) has essentially the same yield strength as that having 15% primary solid (S/N 47). A qualitative correlation between the yield strength and the rate of solidification can, however, be observed.

The yield strengths increase in the same order as the rate of solidification: conventional cast, rheocast, and thixocast. Since Haynes 31 is a carbide strengthened alloy, the increase in yield strength is related to the finer dispersion of carbides associated with faster rate of solidification. For the same reason, the yield strengths of the Series I specimens are slightly lower than those from the Series II. This becomes evident by comparing the scale of the dendrites resulting from Series I trails shown in Figure 44a and from Series II trials shown in Figure 39. Figure 44 also illustrates the concomitant change in the morphology of the interface between the primary solid and the prior liquid with solidification rates, as described previously.

As shown in Table IV, hot isostatic pressing of the thixocast material at 2200°F for 4 hours has no effect in yield strength. As mentioned previously, this HIP condition results in spheroidization of the interdendritic carbide, but does not change the scale of the carbide dispersion.

The tensile ductility of the thixocast material is considerably lower than conventionally cast material because of porosity and inclusions in the specimens. Without such defects, tensile fracture would initiate at the interface between the primary solid and prior liquid and in the prior liquid region (see Figure 45a). For comparison, the modes of tensile fracture in the rheocast material and fully-liquid die-cast material (S/N 46) are also shown in Figures 45b and 45c, respectively.

TABLE IV – TENSILE PROPERTIES OF HAYNES 31

S/N	Microstructure	Thermomechanical Treatment	0.2% YS (ksi)	UTS (ksi)	El (%)	RA (%)	Comment
		75°F Tests					
MX01-01	Thixocast, 80% Solid	None	50.0	52.0	1.0	–	Series I, a
MX01-05	Thixocast, 60% Solid	None	71.0	82.0	2.9	4.0	Series I, a
7	Thixocast, 60% Solid	None	78.7	102.5	7.2	4.9	Series II, a
11	Thixocast, 78% Solid	None	88.3	119.2	5.0	5.0	Series II, a
48	Thixocast, 36% Solid	HIP*	78.3	91.0	2.0	–	Series II, b
34A	Rheocast	HIP	77.4	95.6	2.3	3.2	
38	Rheocast	HIP	74.6	104.2	3.7	2.5	
AMS5382	Conventional Cast Bar	None	50.0	83.0	4	7	
		1000°F Tests					
MX01-02	Thixocast, 50% Solid	None	43.0	59.0	6.1	10.9	Series I, a
MX01-06	Thixocast, 62% Solid	None	43.0	47.0	3.0	7.8	Series I, a
AMS5382	Conventional Cast Bar	None	26.0	65.0	10	8	
		1450°F Tests					
5	Thixocast, 35% Solid	None	41.0	54.5	6.0	5.0	Series II, a
8	Thixocast, 42% Solid	None	38.1	53.4	6.8	6.4	Series II, a
47	Thixocast, 15% Solid	HIP	44.3	75.6	11.8	13.0	Series II, c
46	Thixocast, 0% Solid	HIP	43.6	78.5	43.8	–	Series II
32A	Rheocast	HIP	37.1	59.7	6.2	8.0	
34	Rheocast	HIP	35.8	57.5	6.3	7.5	
AMS5382	Conventional Cast Bar	None	24.0	58.0	8	6	

*Hot isostatically pressed at 2200°F under a stress of 15 ksi for 4 hours.

a. Failure initiated at large pores.

b. Failure initiated at large inclusions.

c. Specimen contained surface-connected porosity.

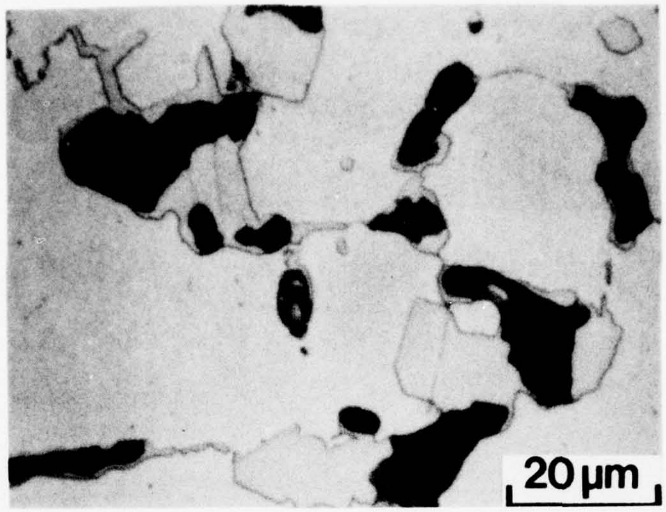

Figure 43 *Incipient Melting at the Carbide. The Microstructure and Heat Treatment Condition Are Those Given in Figure 42C*

a

b

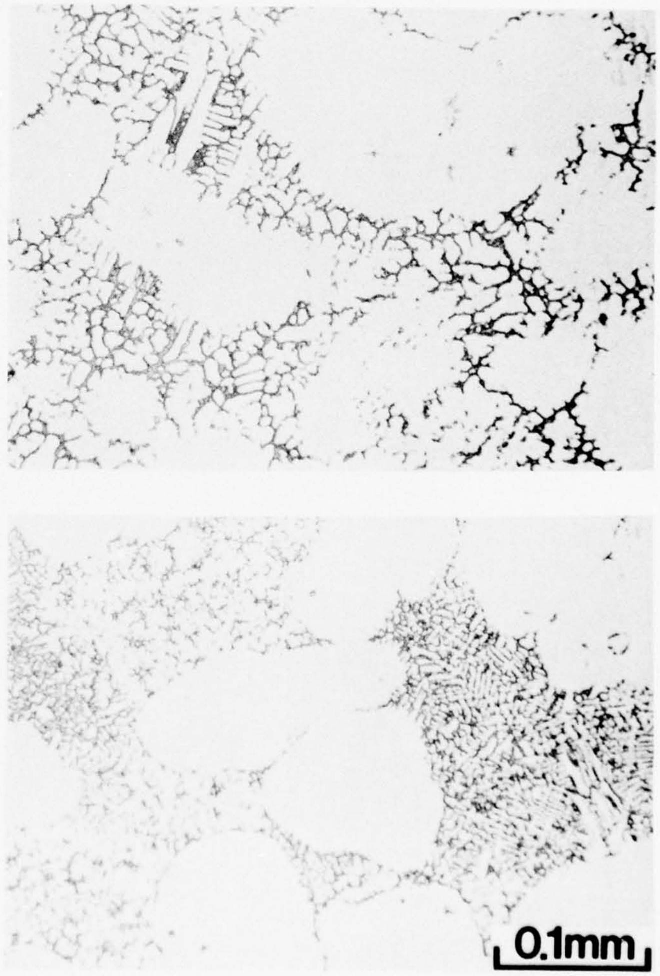

Figure 44 *Microstructures of Haynes 31 in (a) Thick Section and (b) Thin Section of a Casting*

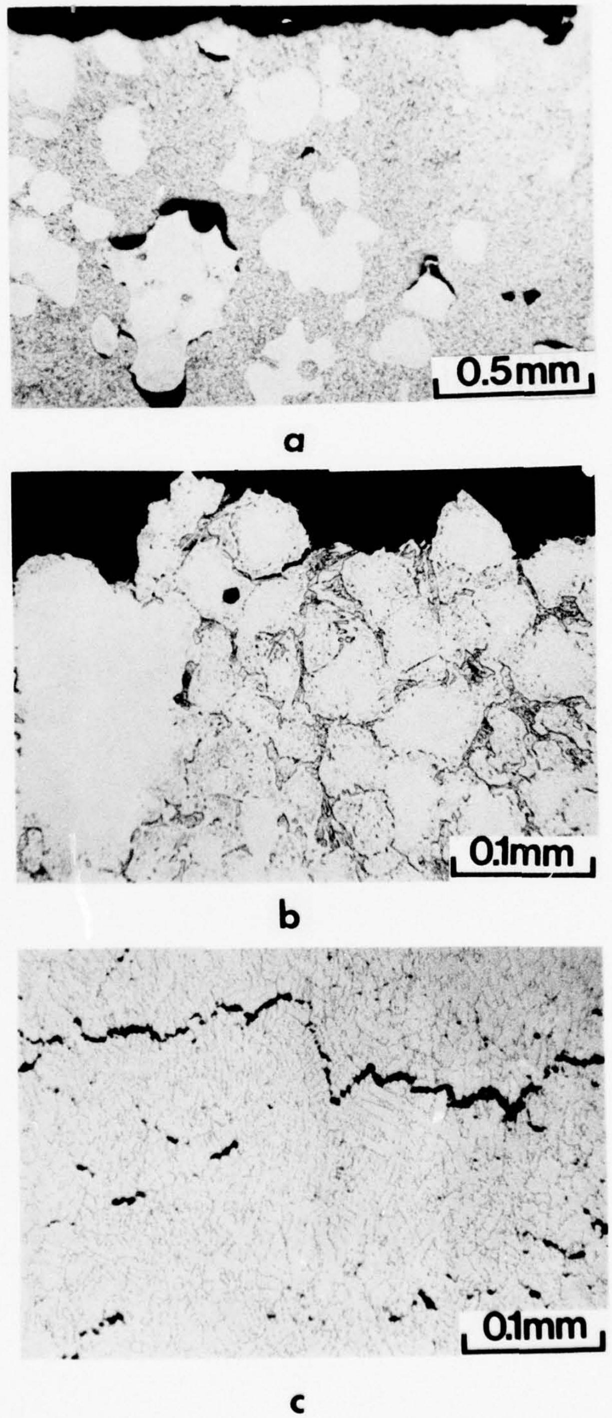

Figure 45 *Longitudinal Section Showing the Modes of Tensile Cracking in (a) Thixocast Microstructure, (b) Rheocast Microstructure and (c) Thixocast Microstructure With No Primary Solid*

The significance of the results from S/N 46 is that as a consequence of the high solidification rate, a large increase in tensile yield strength and ductility (43% elongation) are realized. These results suggest that the fine dendrite matrix of the thixocast material is inherently ductile. Therefore, the primary solid-prior liquid interface plays a key role in determining the tensile ductility of the thixocast material. One method of changing the interfacial strength is to modify the morphology of the interface. This can be achieved simply by varying the rate of solidification, as illustrated in Figure 44. A rough surface, or one where dendrites nucleate and grow, would produce a torturous crack path and, therefore, result in higher ductility. Direct, supportive evidence has not been obtained in the present work. However, different modes of tensile fracture resulting from differences in interfacial morphology have been observed.

Figure 46a shows a smooth interfacial separation in a rapidly solidified thixocasting. A rougher interfacial separation in a relatively less rapidly solidified thixocasting is illustrated in Figure 46b which also shows that in the case of dendrites growing on the primary solid. the fractures occur at the dendrite rather than at the interface. In view of the high tensile ductility of the dendritic structure resulting from the thixocasting, the latter interfacial microstructure is perhaps more desirable.

In summary, the tensile results show that thixocasting results in high yield strength which is independent of volume fraction solid, and somewhat lower ductility compared with conventionally cast material properties. Contributing factors for the observed low ductility are inclusions, entrapped porosity, and early primary solid-prior liquid interfacial separation. It is suggested that the interfacial strength can be increased simply by using a slower solidification rate which can be achieved by having lower fraction solid (higher preheat temperatures) and by heating the die to higher temperatures.

5. Stress Rupture Test Results

The results of the stress rupture tests at 1450°F and 30 ksi are presented in Table V. The thixocast material was tested in four different conditions: as cast, hot isostatically pressed at either 2000°F or 2200°F, and solution-and-aged following HIP. In the as-thixocast condition the stress rupture lives are less than 10 hours irrespective of volume fraction of primary solid present or the machine thixocast parameters. The reason for the low rupture lives is obvious from the fracture surfaces which invariably show casting pores.

Hot isostatic pressing can close the casting pores, provided the pores are not surface-connected. As shown in Table V, HIP substantially improves the rupture life of the thixocast material. After the 2200°F HIP, the stress rupture lives are about 30 to 40 hours, with no apparent correlation to the volume fraction of solid present. The latter observation implies – as in the case of tensile strength – that the fine dendrite matrix plays an important role in stress rupture properties. For comparison, the average rupture lives of the rheocast material and the conventional cast material are 59 hours and 155 hours, respectively. Therefore, it appears that stress-rupture life (unlike tensile strength) is inversely related to the rate of solidification which decreases in the order of machine thixocast, rheocast, and conventional cast. In terms of microstructure, this means that the coarser the microstructure the better the stress rupture properties. In this respect, coarsening of the thixocast microstructure by HIP at temperatures above the incipient melting temperature may improve the stress rupture capability. For conventional cast material this has been demonstrated to be the case[4].

TABLE V – 1450°F/30 KSI SMOOTH STRESS RUPTURE LIFE HAYNES 31

S/N	Microstructure	Thixocasting Parameters Die Temp. (°F)	Ram Speed (in./sec)	Thermomechanical Treatment	Life (hr)
3	Thixocast, 69% Solid	1000	8	None	3.8
10	Thixocast, 13% Solid	900	8	None	3.6
12	Thixocast, 44% Solid	75	8	None	5.5
27	Thixocast, 65% Solid	75	30	None	8.5
28	Thixocast, 62% Solid	75	30	None	4.7
65	Thixocast, 33% Solid	150	30	None	3.0
67	Thixocast, 63% Solid	800	20	None	0.5
21	Thixocast, 44% Solid	75	30	2200°F HIP(a)	35.7
23	Thixocast, 55% Solid	75	30	2200°F HIP	42.1
24	Thixocast, 55% Solid	75	30	2200°F HIP	28.7
20	Thixocast, 0% Solid	900	8	2200°F HIP	34.7
31	Rheocast	– –	– –	2200°F HIP	41.7
32	Rheocast	– –	– –	2200°F HIP	75.6
18	Thixocast, 4% Solid	900	8	2200°F HIP + SA(b)	0.5
19	Thixocast, 44% Solid	900	8	2200°F HIP + SA(b)	2.2
55	Thixocast, 58% Solid	75	30	2000°F HIP(a)	11.8
58	Thixocast, 66% Solid	75	30	2000°F HIP	18.0
51	Conventional Cast	– –	– –	None	53.1
52	Conventional Cast	– –	– –	None	256.9
AMS 5382	Conventional Cast	– –	– –	None	30

(a) Hot isostatically pressed at 15 ksi for 4 hours at indicated temperature.
(b) Solutioned at 2250°F for 8 hours, rapid aircool and aged at 1500°F for 20 hours, aircool.

The modes of fracture in the thixocast, rheocast, and conventional cast microstructures are illustrated in Figures 47a, 47b, and 47c, respectively. In the thixocast microstructure, cracking occurred at the prior liquid as well as at the interface between the primary solid and prior liquid regions. It may be possible to increase the rupture life by reducing the latter mode of cracking by changing the interface morphology as mentioned previously.

The general morphology of the fracture surface is illustrated in Figure 48a. The particulate appearance resulting from interfacial separation between the primary solid particles and the matrix is clearly evident. Cracking occurred in the rheocast microstructure at the carbide interface between the primary solid particles and at the grain boundaries. In case of the conventional microstructure, the cracks progressed along the interdendritic regions.

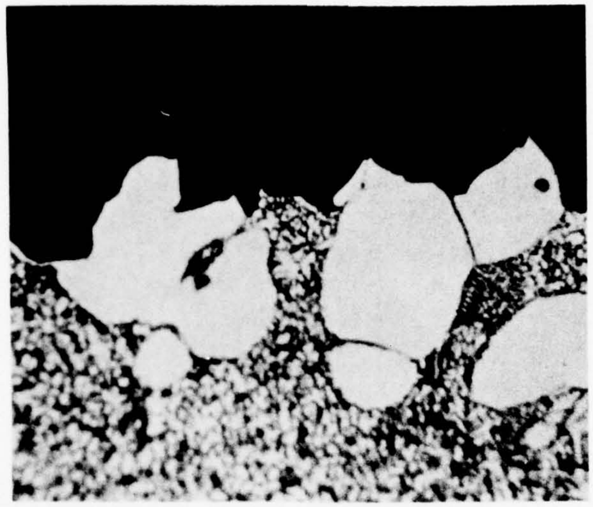

a

b

Figure 46 *Longitudinal Section Showing Effect of Primary Solid-Prior Liquid Interface Morphology on Appearance of the Interfacial Separation (a) a Smooth Separation and (b) an Irregular Separation*

As shown in Section IV-C-2, the microstructure of Haynes 31 is rather responsive to solution-and-age type of heat treatments. However, as indicated in Table V, a stress rupture debit resulted from one such treatment used in the present study. The microstructure after the heat treatment is shown in Figure 42b. The appearance of the fracture surface (Figure 48b) indicates that in this case the stress rupture failure was caused primarily by intergranular fracture. This may be a consequence of copious precipitation of grain boundary carbides upon aging.

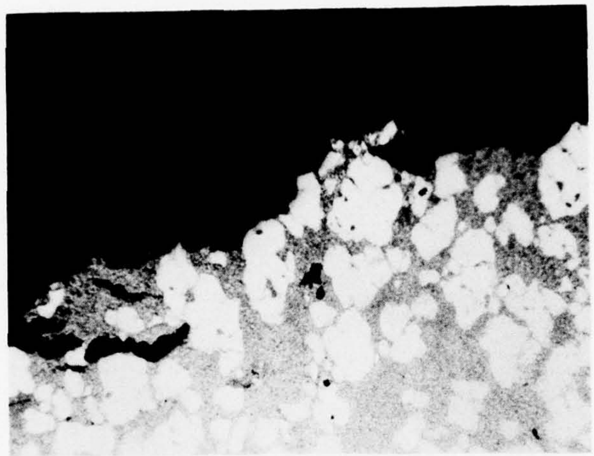

a

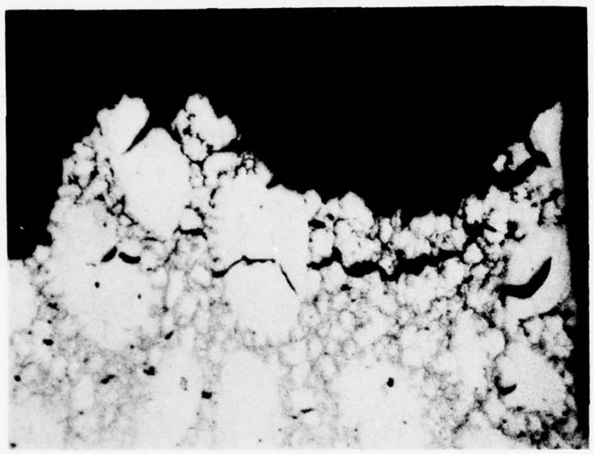

b

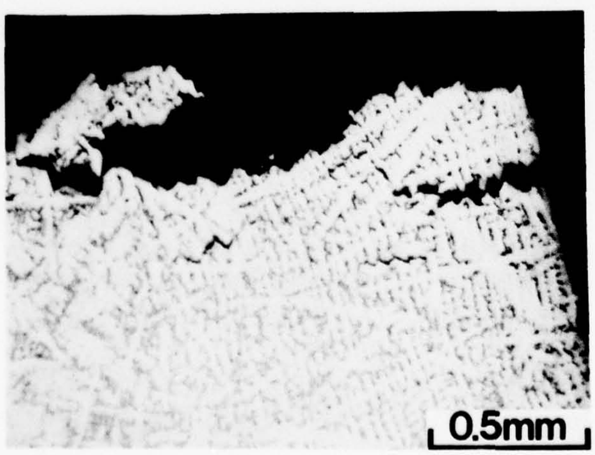

c

Figure 47 *Longitudinal Section Showing the Modes of Stress Rupture Cracking in (a) Thixocast, (b) Rheocast, and (c) Conventional Cast Microstructures*

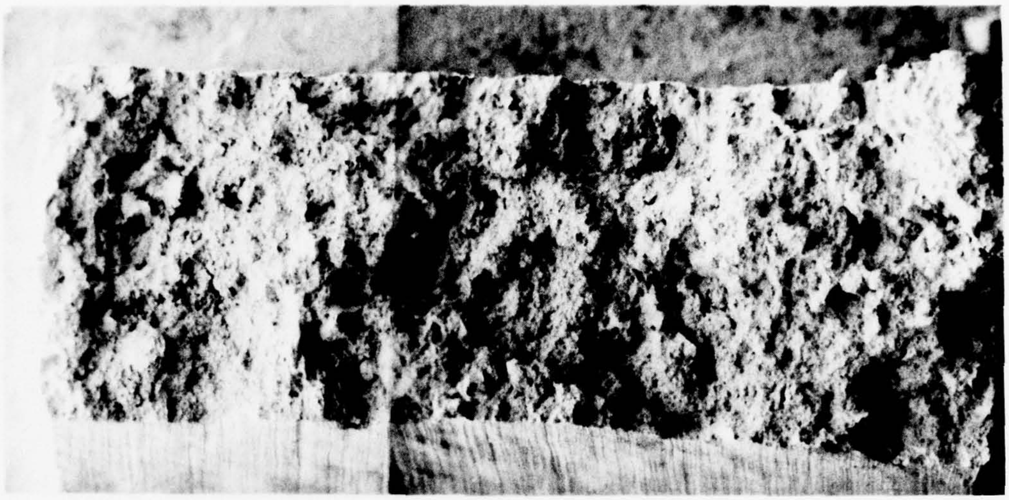

a

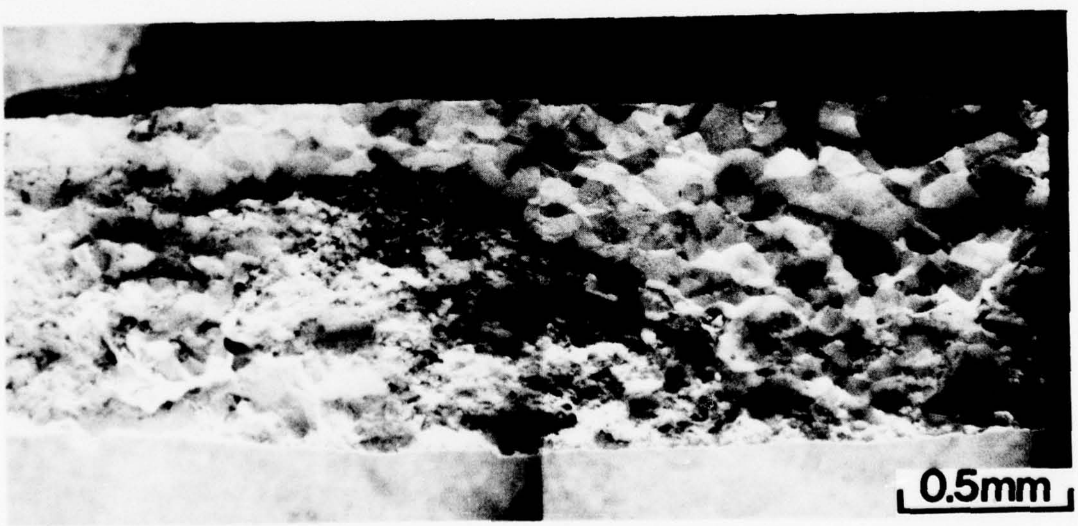

b

Figure 48 *Appearance of the Fracture Surface of Machine Thixocast Hyanes 31 in Stress Rupture After (a) HIP'ed at 2200°F/15 ksi/4Hr and (b) HIP + 2250°F/8 Hr/Rapid-Air-Cool Solution Followed by 1500°F/20 Hr/Air-Cool Age*

Hot isostatic pressing at 2000°F under 15 ksi also resulted in closure of casting porosity in the thixocast part. However, as shown in Table V, the gain in stress-rupture life is considerably less than at 2200°F.

The microstructure of a longitudinal section through the fracture is shown in Figure 49. As can be observed, in addition to the two modes of cracking at the 2000°F HIP (see Figure 48), intergranular cracking also occurred in the present case. The latter mode of cracking may be responsible for the lower rupture life.

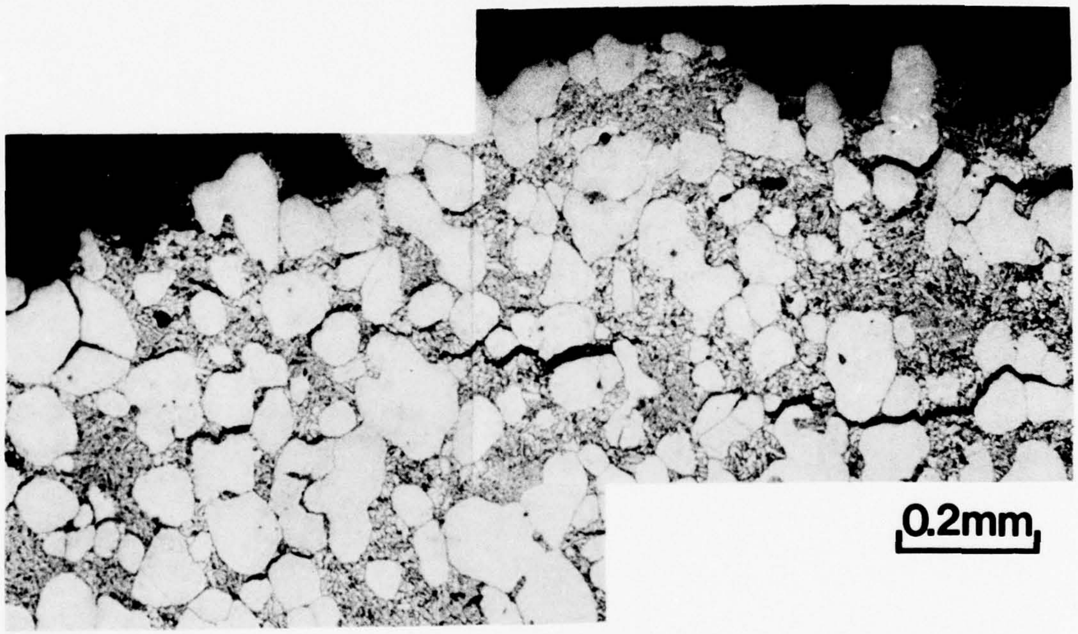

Figure 49 *Longitudinal Section Showing the Modes of Stress Rupture Cracking After HIP at 2000°F/15 ksi/4 Hr*

6. High-Cycle-Fatigue Tests

Results of the fully reversed room temperature bend tests of the thixocast and conventional Haynes 31 are presented in Table VI and as S-N curves in Figure 50. The two curves show the estimated typical and estimated design requirement data for conventional cast material[6] Relative to the conventional counterpart, the HCF capability of the thixocast material seems to be lower. However, as indicated in Table VI, all except one specimen failed from foreign inclusions which are shown to be either Si or Si and Al rich. It is probable that continued improving the cleanliness of the material would result in thixocast microstructure having HCF capability equivalent to that of the conventional cast material.

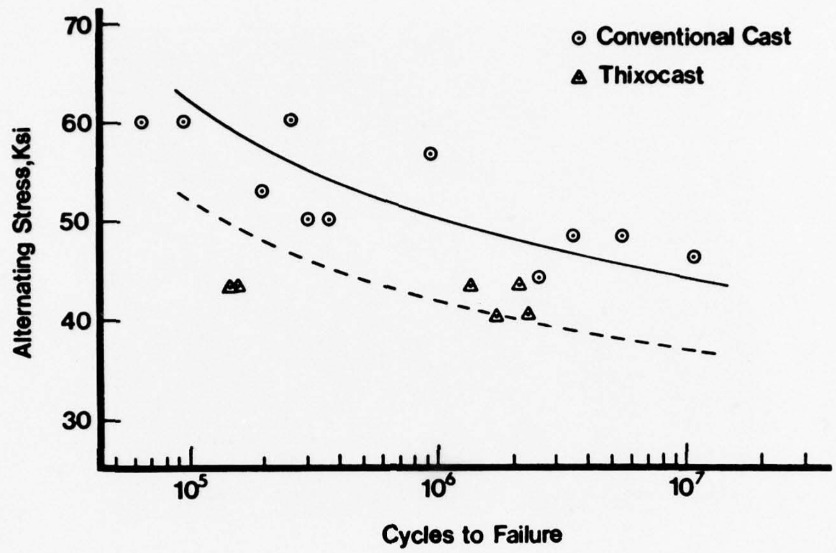

Figure 50 *S-N Curves of the Conventional Cast Haynes 31 Relative to HCF Results of the Thixocast Material After HIP at 2250°F/15 ksi/4 Hr. The solid line and the dotted line are estimated typical and design minimum data respectively for conventional cast material*

In the absence of foreign inclusions, fracture would initiate preferentially at slip bands in the primary solid. This observation is illustrated in Figures 51a and 51b. The latter shows an intergranularly nucleated crack propensity in the prior liquid toward the edge of the specimen. As Figure 52a shows, cracking propagates intergranularly across the primary solid particles rather than along the primary solid-prior liquid interface. This results in facets on the fracture surface (Figure 52b). These facets are separated by featureless areas corresponding to separation at prior liquid. These observations suggest that a simple way to improve the fatigue capability of the thixocast material would be to decrease the volume fraction of primary solid and to reduce the size of the primary solid particles. The latter can be achieved, for example, by increasing the shear rate on the semisolid slurry during the rheocasting process.

D. SUMMARY AND CONCLUSIONS

The tensile, stress-rupture, and high-cycle-fatigue properties of Haynes 31 fabricated by machine thixocasting techniques have been determined. Relative to the conventional counterpart, the thixocast material has significantly higher yield strength and marginally satisfactory tensile ductility. The higher yield strength was shown to be attributable to the fine dendrite matrix resulting from a high rate of solidification. Contributing factors to the low tensile ductility are the entrapped porosity, foreign inclusions, and early separation at the primary solid-prior liquid interface. The stress-rupture life after HIP at 2200°F exceeds the established minimum of the conventional cast material. The fine dendrite matrix also plays an important role in determining the stress rupture life. The HCF capability is slightly lower than the conventional cast material. The small fatigue debit resulted primarily from the inclusions introduced during the rheocast and machine thixocasting processes.

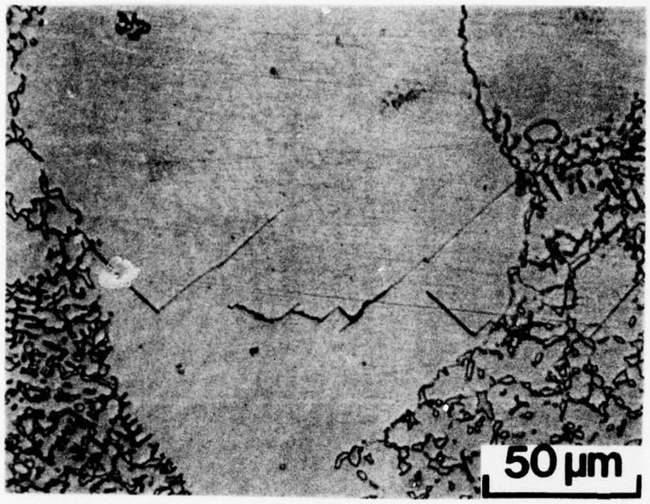

a

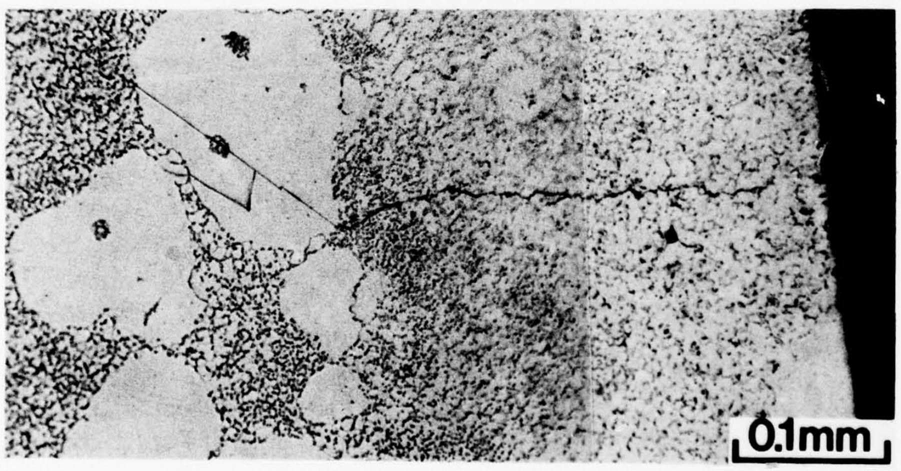

b

Figure 51 *Fatigue Cracks Observed on Surface of a Specimen Fabricated From the Thixocast Haynes 31, Showing (a) Crack Nucleation at Slip Bands in the Primary Solid Particle and (b) Propagation of an Intragranularly Nucleated Crack Through the Prior Liquid Matrix*

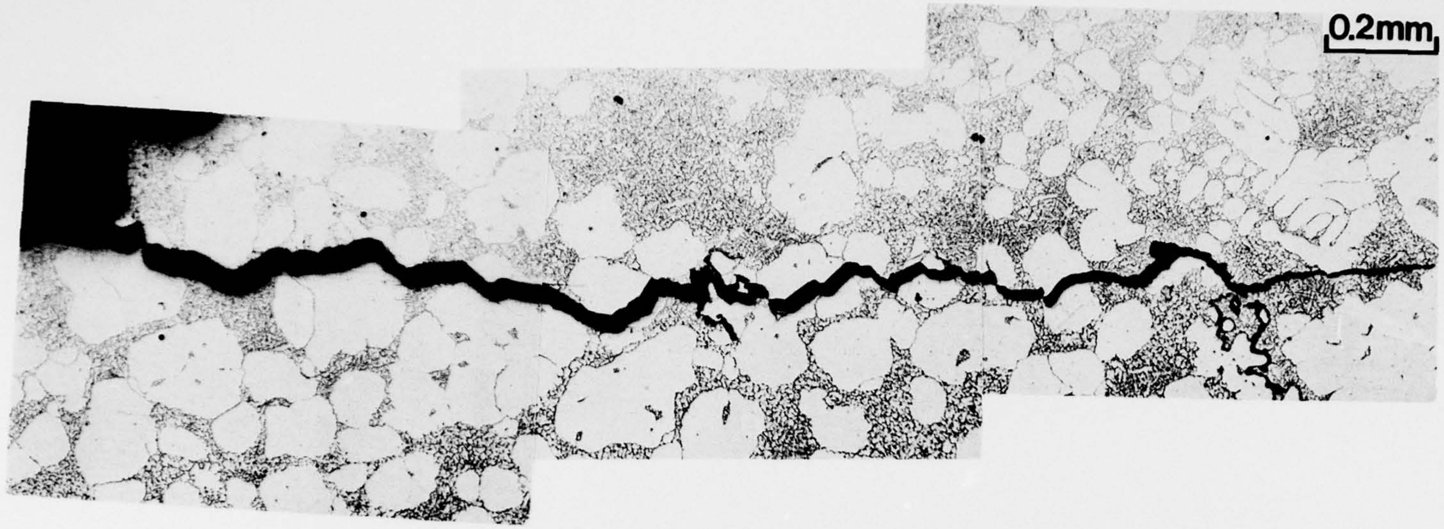

a

b

Figure 52 *(a) Fatigue Crack Propagation Path in Machine Thixocast Haynes 31 Which Results in Facets on Fracture Surface Shown in (b)*

TABLE VI – FATIGUE TEST DATA
(Mean Stress = 0)

S/N	Microstructure	Treatment	Stress (±ksi)	Cycles to Failure	Comment
39	Thixocast, 67% Solid	HIP*(a)	43	1.55×10^5	Series II, b
40	Thixocast, 74% Solid	HIP	43	1.57×10^5	Series II, b
62	Thixocast, 60% Solid	HIP	40	2.41×10^6	Series III, c
66	Thixocast, 65% Solid	HIP	43	2.15×10^6	Series III, d
69	Thixocast, 65% Solid	HIP	43	1.36×10^6	Series III, d
70	Thixocast, 60% Solid	HIP	40	1.83×10^6	Series III, ab
76A	Conventional Cast	None	60	6.4×10^4	
76B	Conventional Cast	None	60	9.6×10^4	

a Hot isostatically pressed at 2200°F under 15 ksi for 4 hours.
b Fracture initiated at multiple inclusion-nucleated crack origins.
c Fracture initiated at single natural crack origin.
d Fracture initiated at single inclusion-nucleated crack origin.

To improve the tensile ductility and stress rupture life, the following techniques are suggested from results of the present studies:

(1) Reduce the solidification rate in thixocasting to produce a coarser dendrite structure and nucleation of dendrite from the surface of the primary solid particles.

(2) Reduce the volume fraction of primary solid.

(3) Improve the cleanliness of the rheocast and thixocast processes.

To improve the HCF properties, techniques (2) and (3) can be used. Reducing the size of the primary solid particle should also be beneficial.

It can be surmised from the observations concerning volume fraction solid that the interrelation between properties and non-destructive quality are not understood, particularly in the case of Haynes 31 alloy. This effect should be more thoroughly studied on different alloys and equipment in future programs.

V. ECONOMIC CONSIDERATIONS FOR MACHINE CASTING

A. INTRODUCTION

The most recent thrust in manufacturing technology-type programs for gas turbine engine components has been to approach the "net shape" or nearly finished part concept to reduce finish machining costs. Traditionally, many gas turbine components, such as airfoils, have been fabricated by forging or investment casting techniques and have required extensive machining to reach the final dimensional shape. These machining costs make up the bulk of finished part cost and have been the target of cost reduction efforts for the past several years.

The application of machine casting, as the shaping or conversion process for airfoils, could result in parts with near-net shape dimensions. Based on prior die casting work performed by ferrous die casting firms under Pratt & Whitney Aircraft sponsorship, the near-finished shape concept was demonstrated as shown in Figure 53. Machine casting should achieve dimensional control similar to the die casting process.

B. COMPARISON OF FORGING AND MACHINE CASTING

The forging of airfoils consists of converting bar stock through several forming steps into an airfoil shaped envelope. The envelope, including the root attachment, is then finished machined. A cost breakdown of the forging process is required to make a process cost comparison between forging and machine casting of airfoils. Analysis of forged airfoil costs indicates that fully three-fourths of the final cost is consumed in finishing (machining) operations as shown in Figure 54.

Machine casting can potentially reduce these finishing costs by as much as one-half because of the ability to produce parts which require minimal finishing.

Conversion or forming costs (equipment, dies, labor, . . .) should be similar for either process and, in both cases, comprises a small part of the overall product cost. Input materials costs also comprise a small portion of the overall cost, although, in the case of machine casting, more material per part will be consumed because of gating, runners, injection biscuits, . . .

The comparison of the three cost elements (namely, material, conversion and finishing costs) for the two processes is shown in Figure 54. This data implies a potential cost savings of as much as one-third for machine casting when compared with forging. Obviously, part geometry and size will cause variations in this analysis. It should be noted that these comparisons are also based on the additional significant assumption of similar process yields.

The sensitivity of overall cost to variations in the above three cost elements is shown schematically in Figures 55, 56, and 57. A wide variation in input material cost (Figure 54) should have little effect on finished machine cast part costs. Conversion costs, or more specifically die costs, should not adversely impact finished part costs if: 1) multiple cavity dies can be employed and 2) reasonable die lives on the order of 2000 or more injections (with appropriate die repairs) can be achieved (Figure 55). Technical advances in die material performance would also reduce per-part die costs.

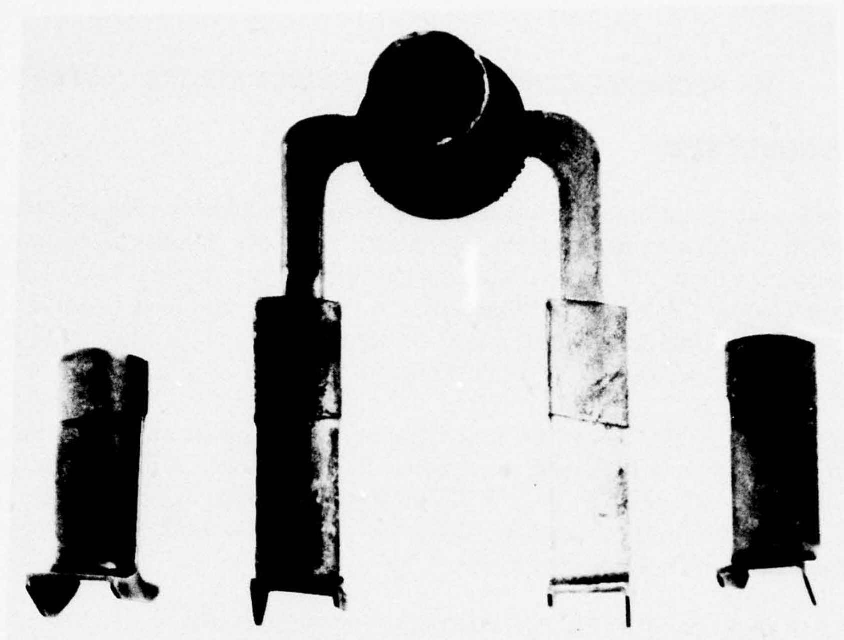

Figure 53 *Comparison of Forged and Finished Compressor Vanes (left and right) and Die Cast Vanes (center) Showing Die Casting Capability to Achieve "Not Shape"*

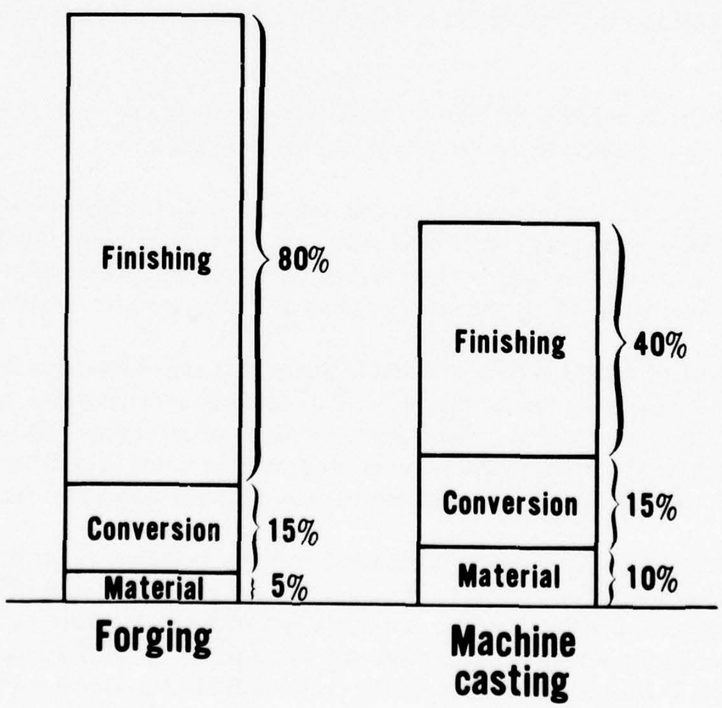

Figure 54 *Comparison of Forged Blade and Machine Cast Blade Costs*

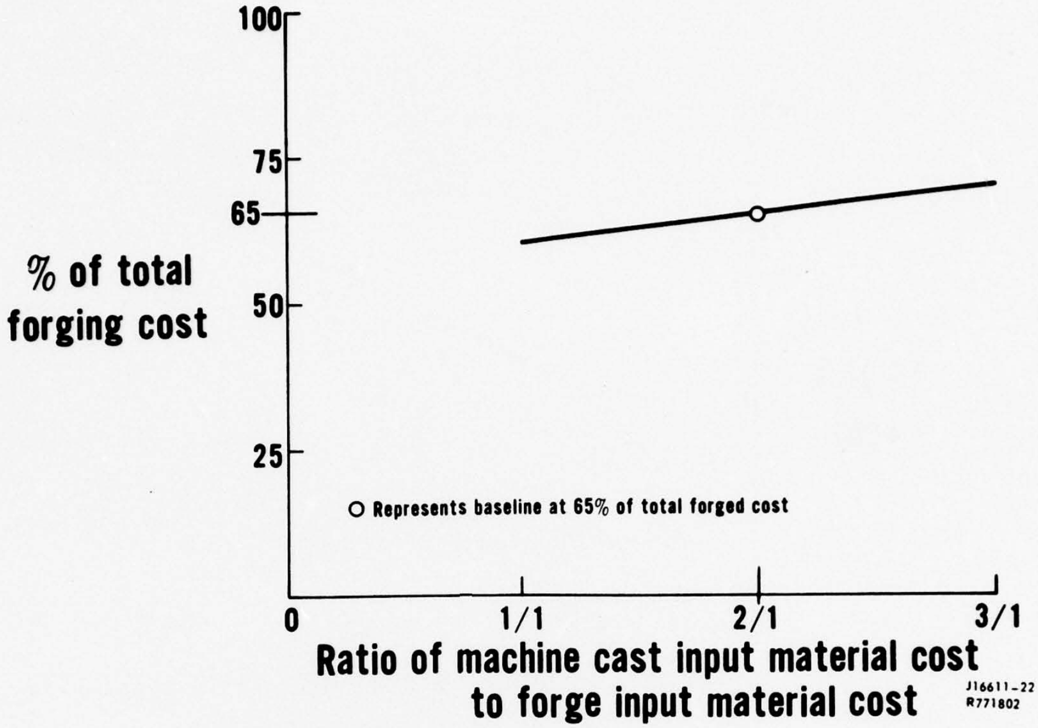

Figure 55 Impact of Material Costs on Machine Cast Part Costs

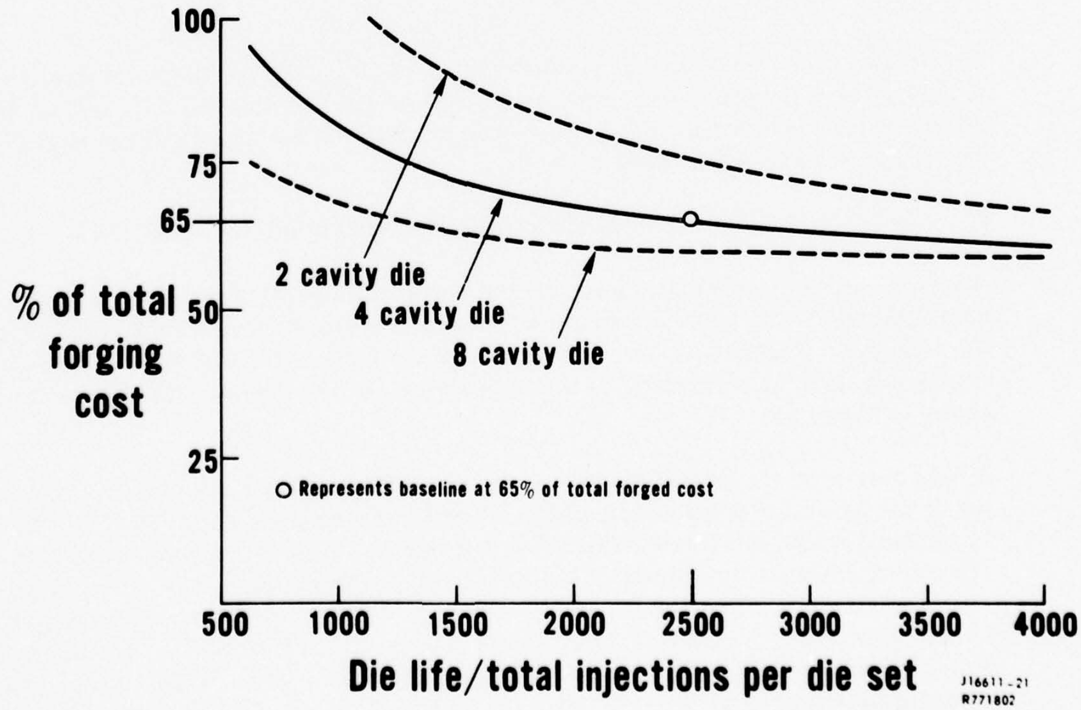

Figure 56 Impact of Tooling Costs on Machine Cast Part Costs

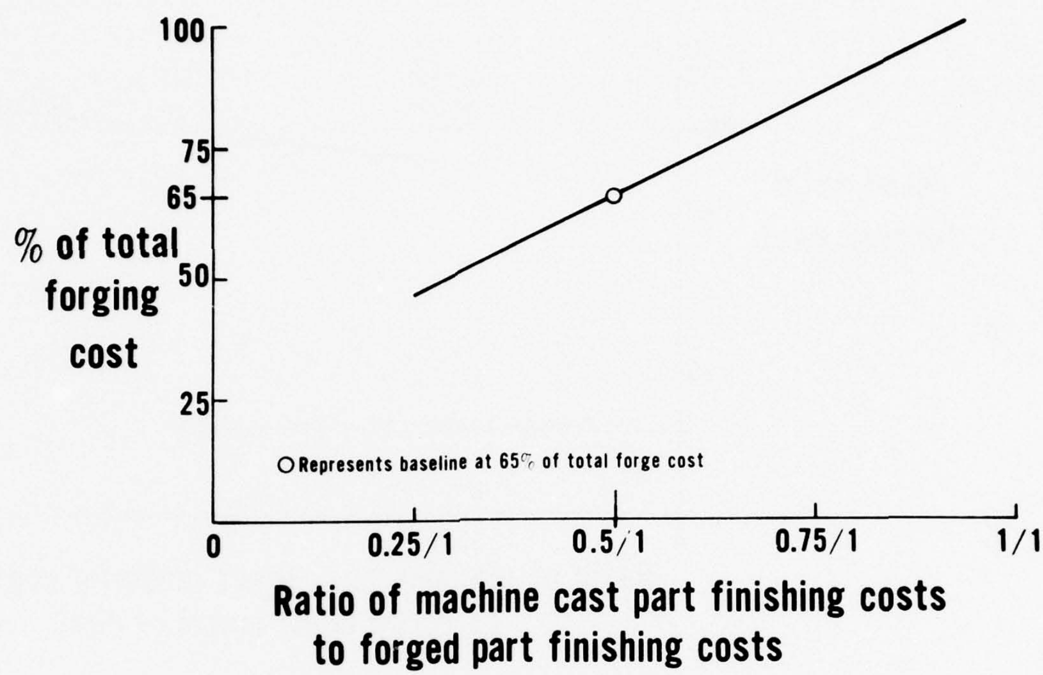

Figure 57 Impact of Finishing Costs on Machine Cast Part Costs

The primary economic impact of machine casting resides in the finishing cost area as shown in Figure 56. Any significant deviation from achieving net or near-net shape will adversely affect the cost savings that could be generated by using the machine casting process in place of forging for airfoil fabrication.

C. COMPARISON OF INVESTMENT CASTING AND MACHINE CASTING

A similar cost analysis has been made for the investment casting of airfoils. Again, the same items (material, conversion, and finishing) for a typical investment cast blade are included in the analysis. It is estimated that approximately two-thirds of the part cost for investment casting is in the area of finishing, as shown in Figure 58. The thixocasting equivalent is also shown in Figure 58.

A large portion of the finished cast part cost is associated with the complex and expensive setups for finish machining of cast airfoils. Costs for machine-cast parts would be affected by the same setup costs for detail finishing in investment forging comparison made previously. The conversion costs for investment casting, shown in Figure 58, include some post cast processing work which is done prior to machining. Conversion costs for machine cast parts are projected to be less than those for investment casting, primarily due to a reduction in the post-cast processing requirements included in the conversion area. Material costs should be similar in both processes.

The projected impact of variations in these three cost components (Figures 59, 60, and 61) on the overall cost is similar to impact obtained from the study for machine casting versus forging. Materials cost changes should have minimal effect (Figure 59), while die cost variation would have effects similar to the previous analysis (Figure 60). Again, the primary economic potential of the machine cast process is to be realized in the area of finishing costs (Figure 60). This, however, is not felt to be as great as in the case of machine cast versus forged parts.

D. SUMMARY

The concept of net shape forming is the primary ingredient in any potential cost effectiveness which the machine casting process may possess. A comparison of machine casting to forging indicates that the former process may be able to save 30-40 percent of the finished part cost because present forging techniques do not produce a net or neat-net shape airfoil. For the case of machine casting versus investment casting, savings on the order of 25 percent may be possible; but the cost motivation becomes less and less attractive as the investment cast parts are made closer to net shape. It should be noted that the assumption of both similar process yields and property level achievement are requisites for this comparison.

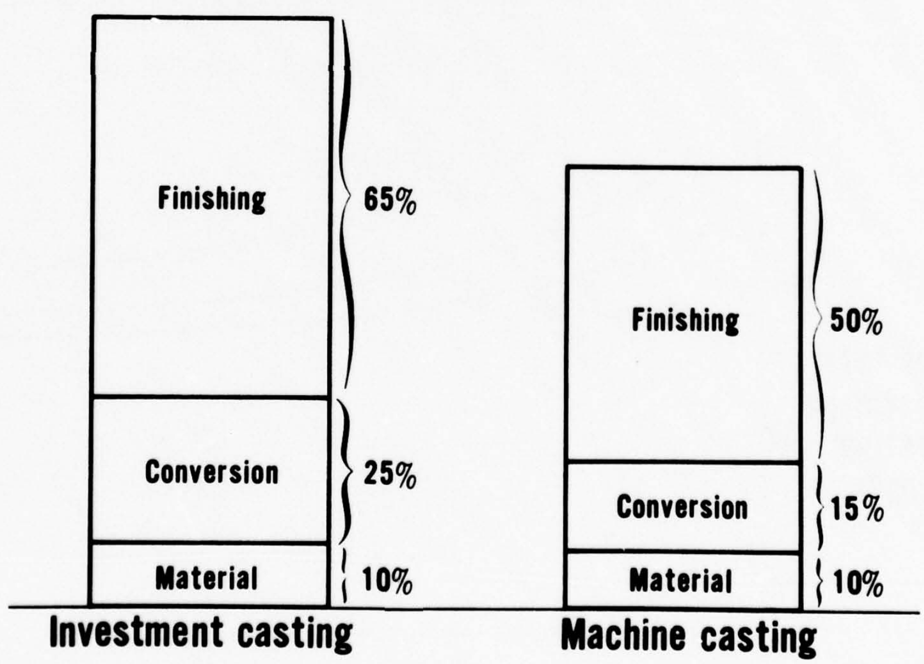

Figure 58 Comparison of Investment Cast Blade and Machine Cast Blade Costs

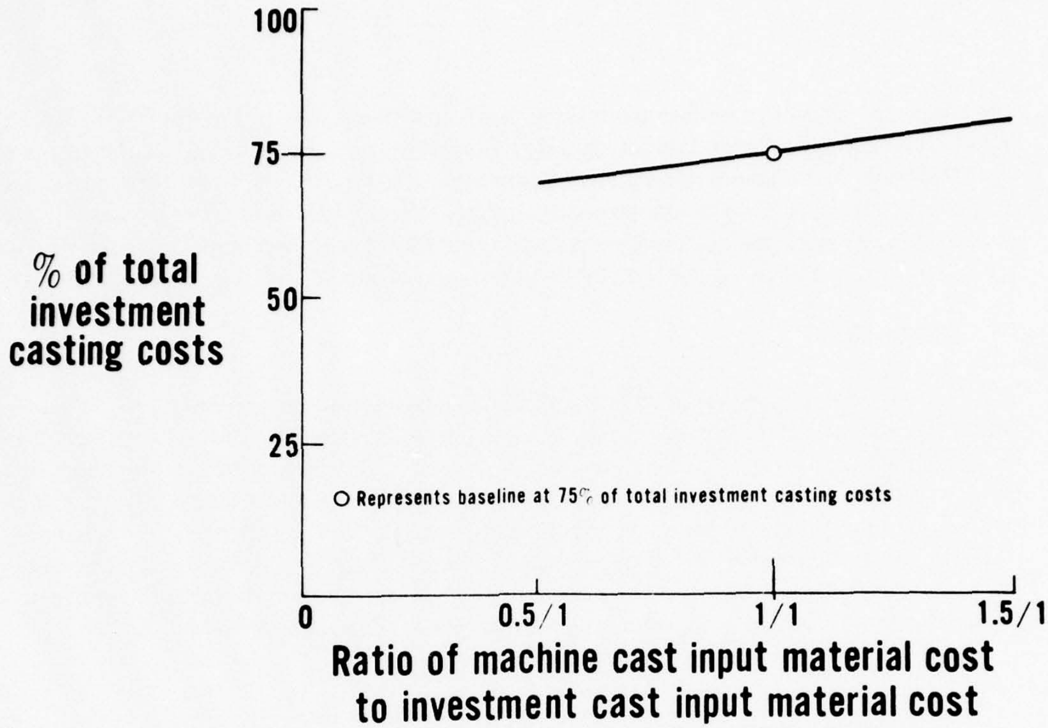

Figure 59 *Impact of Material Costs on Machine Cast Part Costs*

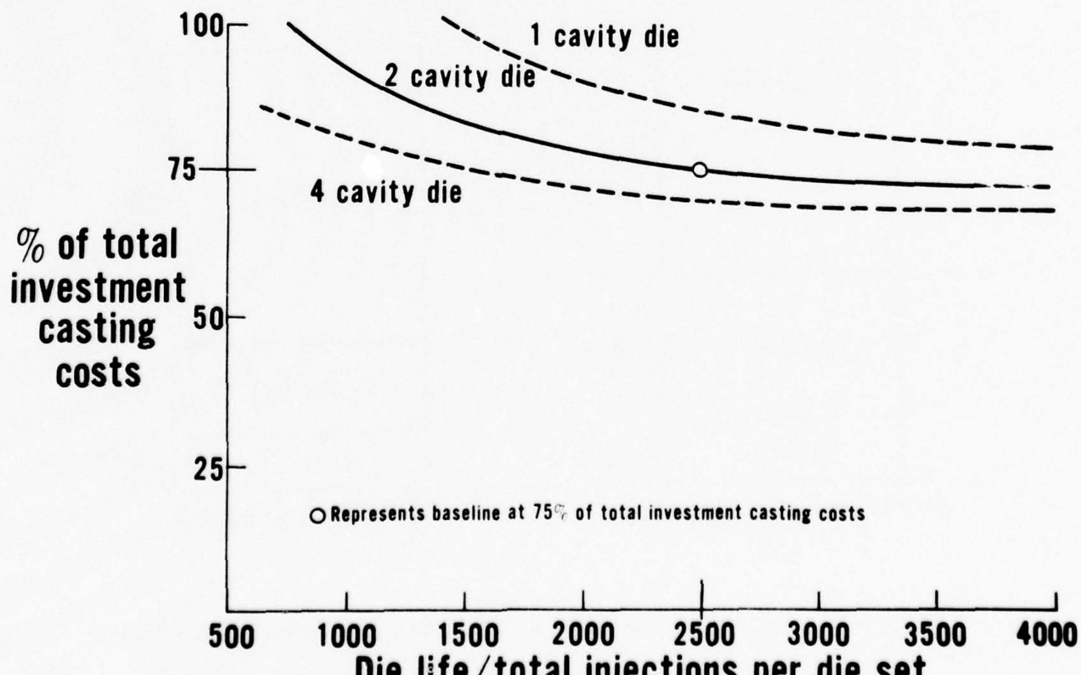

Figure 60 *Impact of Tooling Costs on Machine Cast Part Costs*

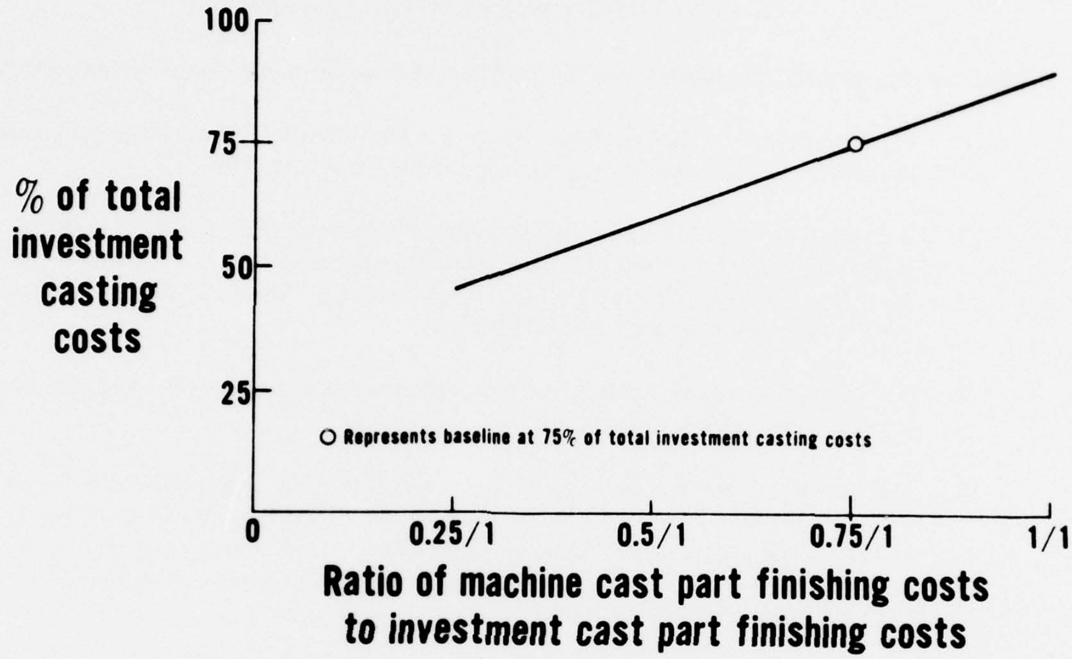

Figure 61 Impact of Finishing Costs on Machine Cast Part Costs

VI. CONCLUSION AND RECOMMENDATIONS

The following general conclusions may be reached from the work performed on this program:

1. Machine casting as a fabrication process has the potential for converting rheocast material into useful solid airfoil shapes for gas turbine engines.

2. A parametric evaluation of critical machine-casting variables indicated that for high volume fraction solid preforms, low die temperatures(100°F to 400°F) and moderate gate velocities (250 in./sec) would result in "finished" parts with acceptable nondestructive and visual qualities.

3. Mechanization of the machine casting process is both practical and desirable from a process consistency standpoint.

4. Mechanical properties (high-cycle-fatigue, stress-rupture, and tensile) are not adversely affected by the thixocast microstructure and, generally met goals for conventional Haynes 31 alloy. Hot isostatic pressing was necessary to close internal porosity probably aggravated by the particular die configurations and machine casting unit used for this program.

5. The economic evaluation indicated that the machine casting process should be capable of effectively competing with conventional forging as long as net shapped parts with minimum finish machining can be attained. It does not appear that machine casting will effectively compete with investment casting because of investment casting's growing potential for net shaped parts.

To achieve the full potential of machine casting (or other means of thixoforming) for gas turbine components, it will be necessary to further evaluate the following:

1. Vacuum rheocasting of nickel base superalloys presently used for compressor airfoils.

2. Special equipment specifically design and constructed for thixoforming application.

3. Thixoforming parametric behavior. The evaluation would require more detailed analysis and would include die materials and die design.

4. Thixocast properties, including heat treatment responses to determine property levels for comparison with bill-of-materials part property requirements. The evaluation should be comprehensive and should include studies of debits, if any, and their impact on gas turbine requirements and on the economics of thixoformed parts.

APPENDIX "A"

STATISTICAL TEST PLAN FOR MACHINE CASTING

Statistical methods are used to plan, analyze, and process results of experiments containing factors corresponding to those associated with complex development problems. By varying these factors in a planned manner, it is possible to isolate and study the effect produced by any one factor, or combination of factors upon the problem.

The use of statistical techniques widens the scope of the program by providing the maximum use of test information. By implementing these methods in the test program, cost savings are achieved through the reduction of the number of tests required and the time to obtain productive information is minimized.

For these reasons, statistical techniques will be used throughout the machine casting program where it is considered the most cost effective means of providing the desired information.

PROGRAM PLAN

Initially, the factors of gate velocity, die temperature, volume percent solid, and gate placement will be investigated for their effect upon blade quality. A statistically designed test program of the Box-Wilson type will be employed in this stage of the program. Shown both schematically and in matrix form below, testing will be conducted for each of the gate sizes to be examined.

The test plan illustrated not only quantitatively measures the impact of the four variables on blade quality, but it assesses the blade quality. Furthermore, the statistical plan permits a quantitative evaluation of the relationship between the variables and the response parameter; this is a capability which is not generally possible with the typical engineering approach.

The tests will be fully replicated for each gate geometry. The rational for repeat tests is threefold:

(1) The possibility of extraneous random effects introducing bias into the test results can be detected if such should occur.

(2) A measure of the inherent variation in the machine casting process can be obtained and used as a reference point when assessing the reproducibility of the process.

(3) It provided a means of analytically assessing the significance of the process variable effects.

DATA ANALYSIS DECISION TECHNIQUE

The Analysis of Variance (ANOVA) and regression analysis will provide the means of identifying the significant effects of the variables and evaluating their trend.

The ANOVA will be applied to the data contained in the factorial design illustrated. This analysis rests on a separation of the variance of all the observations into parts, each of which quantitatively measures the variability attributable to some specific factor or combination of factors. This method of analysis, therefore, has two important advantages over nonstatistical methods:

1. The analysis results in consistent assessments of the factor's effect on the response. If two or more independent analyses of the data are performed, they will arrive at the same measurement of the relationship between the factors and the response.

2. The analysis provides a method of interpreting the degree of certainty of the relationship between the factors and the response, i.e., whether the measured effect of the factor associated with the response is real of if it is due to random variation.

The table which follows illustrates the mechanics of the ANOVA and how the significant factors are identified.

Source of Variation	Sum of Squares	Degrees of Freedom	Mean Square	F Ratio
Main Effects				
Die Temp (T)	SS_T	DF_T	$(SS/DF)^T$	MS_T/MS_E
Vel (V)	SS_V	DF_V	$(SS/DF)_V$	MS_V/MS_E
Vol. % Solid (S)	•	•	•	•
Gate Geometry (G)	•	•	•	•
Interactions				
TXV				
TXV				
•				
•				
•				
SXG				
TXVXS				
TXVXG				
•				
•				
•				
VXSXG				
TXVXSXG				
Error	SS_E	DF_E	$(SS/DS)_E$	
Total	SS_{Total}	$N_{Total}{}^{-1}$		

The use of the F-test in the ANOVA is as follows:

1. A table of the probability that the ratio of mean squares will be equal to or exceed a given value (F - table) may be found in most statistical textbooks. The value to be used in this table is determined by: (a) stating a probability (confidence level) that one wants to associate to the statement of whether the factor caused a significant change in the response, and (b) knowing the number of degrees-of-freedom associated with the numerator (the factor mean square) and the denominator (the error mean square) of the ratio. The confidence level to be used will be 90%.

2. If the test index of any first or higher order factor is greater than or equal to the F - table value, the factor will be considered to have a significant effect on the response.

3. If the test index is less than the F - table value, it will be concluded that there is insufficient evidence to believe that the factor had a significant effect on the response.

Multiple regression analysis will be used to develop a response surface incorporating the variable main and interaction effects identified as significant process variables in the ANOVA. The mathematical model of the machine casting process will thus be based on meaningful parameters and will be considered a useful description of the physical quantities that go into making up the process. The relationship will be of the form

$$Y = a + b_1 x_1 + b_2 x_2 + \ldots\ldots$$

Where Y = quality characteristic measurement
x_i = variable main or interaction effect
a = intercept
b_i = the average change in the response associated with the change in the variable

The values of a and the b_1's are determined from the standard least squares solution whereby $\Sigma (Y_i - Y)^2$ is minimized. Y_i is the actual response obtained from the test program and Y is the response calculated from the regression equation.

The results of the statistical analysis of the machine casting parameters are tabulated in Tables A-1 and A-2.

MACHINE CASTING SCHEMATIC

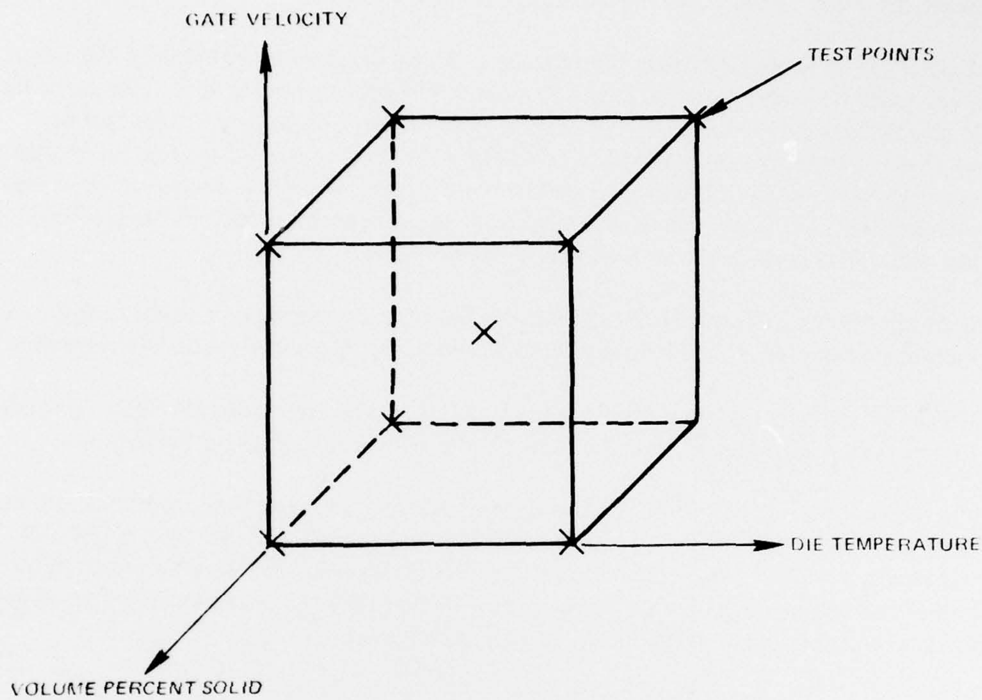

MACHINE CASTING MATRIX

DIE TEMPERATURE	T1		T2	T3	
GATE VELOCITY / VOL. % SOLID	V1	V3	V2	V1	V3
S1	X	X		X	X
S2			X		
S3	X	X		X	X

X = TEST POINT .

TABLE A-1

X-RAY QUALITY
ANALYSIS OF VARIANCE TABLE

Source of Variation	Sums of Squares	d. f.	Mean Square	Variance Ratio	Significance Priority
Volume % Solid	0.2456167	2	0.12280835	0.3069	
Die Temperature	0.0080083666	1	0.0080083666	0.0200	
Gate Velocity	0.0080083666	1	0.0080083666	0.0200	
Volume % Solid - Gate Velocity Interaction	1.114316633	2	0.551583167	1.3924	3
Volume % Solid - Die Temperature Interaction	0.7693166334	2	0.3846583167	0.9613	4
Gate Velocity - Die Temperature Interaction	1.7252083	1	1.7252083	4.3114	1
Volume % Solid - Gate Velocity - Die Temperature Interaction	1.74062417	2	0.870312085	2.1749	2
Experimental Error		23	0.40015361		
Total	5.6110917				

TABLE A-2

SURFACE QUALITY
ANALYSIS OF VARIANCE TABLE

Source of Variation	Sums of Squares	d. f.	Mean Square	Variance Ratio	Significance Priority
Volume % Solid	2.444866667	2	1.222433334	0.93033	1
Die Temperature	0.053333666	1	0.053333666	0.04059	
Gate Velocity	0.140833336	1	0.1408333336	0.10718	4
Value % Solid - Gate Velocity Interaction	0.9108666664	2	0.459333332	0.34666	
Volume % Solid - Die Temperature Interaction	1.5055866666	2	0.752933333	0.57302	3
Gate Velocity - Die Temperature Interaction	1.203333333	1	1.203333333	0.91580	2
Volume % Solid - Gate Velocity - Die Temperature Interaction	0.2198646274	2	0.109932137	0.08366	5
Experimental Error		23	1.313976072		
Total	6.47896466				

DISTRIBUTION LIST

No. of Copies	To
1	Office of the Director, Defense Research and Engineering, The Pentagon, Washington, D. C. 20301
12	Commander, Defense Documentation Center, Cameron Station, Building 5, 5010 Duke Street, Alexandria, Virginia 22314
1	Metals and Ceramics Information Center, Battelle Columbus Laboratories, 505 King Avenue, Columbus, Ohio 43201
	Chief of Research and Development, Department of the Army, Washington, D. C. 2-310
2	ATTN: Physical and Engineering Sciences Division
	Commander, Army Research Office, P. O. Box 12211, Research Triangle Park, North Carolina 27709
1	ATTN: Infomation Processing Office
	Commander, U. S. Army Materiel Development and Readiness Command, 5001 Eisenhower Avenue, Alexandria, Virginia 22333
1	ATTN: DRCDE-TC
	Commander, U. S. Army Electronics Command, Fort Monmouth, New Jersey 07703
1	ATTN: DRSEL-GG-DD
1	DRSEL-GG-DM
	Commander, U. S. Army Missile Command, Redstone Arsenal, Alabama 35809
1	ATTN: Technical Library
1	DRSMI-RSM, Mr. E. J. Wheelahan
	Commander, U. S. Army Armament Command, Rock Island, Illinois 61201
2	ATTN: Technical Library
1	DRSAR-SC, Dr. C. M. Hudson
1	DRSAR-PPW-PB, Mr. Francis X. Walter
	Commander, U. S. Army Tank-Automotive Research and Development Command, Warren, Michigan 48090
2	ATTN: DRDTA, Research Library Branch

No. of Copies	To
	Commander, White Sands Missile Range, New Mexico 88002
1	ATTN: STEWS-WS-VT
	Commander, Aberdeen Proving Ground, Maryland 21005
1	ATTN: STEAP-TL, Bldg. 305
	Commander, Frankford Arsenal, Philadelphia, Pennsylvania 19137
1	ATTN: Library, H1300, B1. 51-2
1	SARFA-L300, Mr. J. Corrie
	Commander, Picatinny Arsenal, Dover, New Jersey 07801
1	ATTN: SARPA-RT-S
	Commander, Redstone Scientific Information Center, U. S. Army Missile Command, Redstone Arsenal, Alabama 35809
4	ATTN: DRSMI-RBLD, Document Station
	Commander, Watervliet Arsenal, Watervliet, New York 12189
1	ATTN: SARWV-RDT, Technical Information Services Office
	Commander, U. S. Army Foreign Science and Technology Center, 220 7th Stree, N. E., Charlottesville, Virginia 22901
1	ATTN: DRXST-SD2
	Director, Eustis Directorate, U. S. Army Air Mobility Research and Development Laboratory, Fort Eustis, Virginia 23604
1	ATTN: Mr. J. Robinson, SAVDL-EU-SS
	Libraian, U. S. Army Aviation School Library, Fort Rucker, Alabama 36360
1	ATTN: Building 5907
	Naval Research Laboratory, Washington, D. C. 20375
1	ATTN: Dr. J. M. Krafft – Code 8430
	Chief of Naval Research, Arlington, Virginia 22217
1	ATTN: Code 471
	Air Force Materials Laboratory, Wright-Patterson Air Force Base, Ohio 45433
2	ATTN: AFML/MXE/E. Morrissey
1	AFML/LC
1	AFML/LLP/D. M. Forney, Jr.
1	AFML/MBC/Mr. Stanley Schulman

No. of Copies	To
	National Aeronautics and Space Administration, Washington, D. C. 20546
1	ATTN: Mr. G. G. Achhamer
1	Mr. G. C. Deutsch - Code RR-1
	National Aeronautics and Space Administration, Marshall Space Flight Center, Huntsville, Alabama 35812
1	ATTN: R-P&VE-M, R. J. Schwinghamer
1	S&E-ME-MM, Mr. W. A. Wilson, Building 4720
	Wyman-Gordon Company, Worcester, Massachusetts 01601
1	ATTN: Technical Library
	Defense Advanced Research Projects Agency, 1400 Wilson Boulevard, Arlington, Virginia 22209
5	ATTN: Dr. E. C. van Reuth
	National Science Foundation, 1800 G. Street, Washington, D. C. 20550
1	ATTN: Dr. Robert Reynik
	General Electric Company, Corporate Research and Development, Schenectady, New York 12301
5	ATTN: Mr. F. X. Gigliotti, Jr.
	Hitchiner Manufacturing Co., Inc., Elm Street, Milford, New Hampshire 03055
5	ATTN: Mr. G. D. Chandley
	Abex Corporation, Research Center, Mahwah, New Jersey 07430
5	ATTN: H. R. Larson
	Massachusetts Institute of Technology, Dept. of Metallurgy and Materials Science, Cambridge, Massachusetts 02139
5	ATTN: Dr. Merton C. Fleming
	TRW Equipment, TRW Inc., 23555 Euclid Avenue, Cleveland, Ohio 44117
1	ATTN: Elizabeth Barrett, T/M 3417
	Deposits & Composites Inc., 1821 Michael Faraday Drive Reston, Virginia 22090
1	ATTN: Richard E. Engdahl, President
1	Dr. Maurice Sinnott, University of Michigan, Assoc. Dir. of Engineering, Ann Arbor, Michigan 48104

No. of Copies	To
1	Fred E. Ziter, Adirondack Steel Casting Co., Shaker Road, Watervliet, New York 12189
1	Dr. Raymond J. Bratton, Westinghouse Electric Corporation Research Laboratory, Pittsburgh, Pennsylvania 15235
1	W. M. Spurgeon, Director, Mfg., Quality Control & Home Systems, Program Management Center, Bendix Research Laboratories, Bendix Center, Southfield, Michigan 48075
1	S. T. Wlodek, Director of Stellite R&D, Stellite Division, Cabot Corporation, 1020 West Park Avenue, Kokomo, Indiana 46901
1	Mr. William A. Butler, Contract Administrator, Microwave Associates, Inc., Burlington, Massachusetts 01803
1	Mr. John A. Ulrich, Sr. Vice-President, Chamberlain Manufacturing Corp., Waterloo, Iowa 50705
1	A. V. Illyn, Technical Director, Babcock & Wilcox, Old Savannah Road, Augusta, Georgia 30903
1	Mr. W. J. Welsch (Code 224), Naval Materials Industry Resources Office, N.A.E.C., Building No. 537, Philadelphia, Pennsylvania 19112
1	Mr. R. E. Cross, Federal Die Casting Co., 2222 Elston Avenue, Chicago, Illinois 60614
1	Captain Ebenezer F. Porter, 2618 S. Lynn Street, Arlington, Virginia 22202
1	Mr. Charles E. Bates, Head, Metallurgy Section, Southern Research Institute, 2000 Ninth Avenue, South, Birmingham, Alabama 35205
1	Mr. R. F. Kirby, Chief, Materials Engineering Dept., Dept. 93-39M, Airesearch Manufacturing Company of Arizona, 402 South 36th Street, P. O. Box 5217, Phoenix, Arizona 85010
1	Dr. Mervin T. Rowley, American Foundry Men's Society, Golf & Wolf Roads, Des Plaines, Illinois 60016
1	William R. Freeman, Jr., Howmet Corporation, Vice President and Technical Director, Technical Center, Gas Turbine Components Group, 699 Benston Road, Whitehall, Michigan 49461

1 Dole A Marek, General Motors Corporation, Detroit Diesel Allison, 4700 W. 10th Street, Indianapolis, Indiana 46206

General Dynamics, Convair Aerospace Division, P. O. Box 748, Ft. Worth, Texas 76101

1 ATTN: Mfg. Engineering Technical Library

1 Dr. Robert Mehrabian, Dept. of Metallurgy & Mining Engineering, University of Illinois, Urbana, Illinois 61801

1 Robert McNally, Research Library, Special Metals Corporation, Middle Settlement Road, New Hartford, New York 13413

Director, Army Materials and Mechanics Research Center, Watertown, Massachusetts 02172

2 ATTN: DRXMR-PL

1 DRXMR-PR

1 DRXMR-AP

1 DRXMR-CT

1 DRXMR-X

1 DRXMR-ER

Army Materials and Mechanics Research Center,
Watertown, Massachusetts 02172
Machine Casting of High Temperature
Alloys for Turbine Engine Components
L. F. Schulmeister et al, United Technologies
Corporation, Pratt & Whitney Aircraft Group,
Government Products Division,
West Palm Beach, Florida 33402
Technical Report - Contract DAAG 46-76-C-0029
D/A Project ARPA Order No. 2267, AMCMS
Code 6410 Final Report, 1 March 1976 to
30 May 1977

AD ________________

UNCLASSIFIED
UNLIMITED DISTRIBUTION

Key Words

Die casting
Solidification
Heat persistant alloys
Iron alloys
Compressor parts
Turbine parts
Quality assurance

The objective of this program is to evaluate the capability to machine cast parts for gas turbine engines. Machine casting in the thixatropic state is being evaluated. Partial assessment of process parameter effects, using Rheocast Haynes Alloy 31, was performed. Machine casting preforms of various volume fractions of solid were injected at different die temperatures. Results indicated internal porosity and surface condition were improved with increasing die temperature and volume fraction solid. A heat treatment response study and mechanical property evaluations were also conducted. Heat treatment studies indicated long term annealing followed by aging yielded microstructure similar to conventionally cast heat treated Haynes 31 alloy. An economic analysis was also performed.

Army Materials and Mechanics Research Center,
Watertown, Massachusetts 02172
Machine Casting of High Temperature
Alloys for Turbine Engine Components
L. F. Schulmeister et al, United Technologies
Corporation, Pratt & Whitney Aircraft Group,
Government Products Division,
West Palm Beach, Florida 33402
Technical Report - Contract DAAG 46-76-C-0029
D/A Project ARPA Order No. 2267, AMCMS
Code 6410 Final Report, 1 March 1976 to
30 May 1977

AD ________________

UNCLASSIFIED
UNLIMITED DISTRIBUTION

Key Words

Die casting
Solidification
Heat persistant alloys
Iron alloys
Compressor parts
Turbine parts
Quality assurance

The objective of this program is to evaluate the capability to machine cast parts for gas turbine engines. Machine casting in the thixatropic state is being evaluated. Partial assessment of process parameter effects, using Rheocast Haynes Alloy 31, was performed. Machine casting preforms of various volume fractions of solid were injected at different die temperatures. Results indicated internal porosity and surface condition were improved with increasing die temperature and volume fraction solid. A heat treatment response study and mechanical property evaluations were also conducted. Heat treatment studies indicated long term annealing followed by aging yielded microstructure similar to conventionally cast heat treated Haynes 31 alloy. An economic analysis was also performed.

Army Materials and Mechanics Research Center,
Watertown, Massachusetts 02172
Machine Casting of High Temperature
Alloys for Turbine Engine Components
L. F. Schulmeister et al, United Technologies
Corporation, Pratt & Whitney Aircraft Group,
Government Products Division,
West Palm Beach, Florida 33402
Technical Report - Contract DAAG 46-76-C-0029
D/A Project ARPA Order No. 2267, AMCMS
Code 6410 Final Report, 1 March 1976 to
30 May 1977

AD ________________

UNCLASSIFIED
UNLIMITED DISTRIBUTION

Key Words

Die casting
Solidification
Heat persistant alloys
Iron alloys
Compressor parts
Turbine parts
Quality assurance

The objective of this program is to evaluate the capability to machine cast parts for gas turbine engines. Machine casting in the thixatropic state is being evaluated. Partial assessment of process parameter effects, using Rheocast Haynes Alloy 31, was performed. Machine casting preforms of various volume fractions of solid were injected at different die temperatures. Results indicated internal porosity and surface condition were improved with increasing die temperature and volume fraction solid. A heat treatment response study and mechanical property evaluations were also conducted. Heat treatment studies indicated long term annealing followed by aging yielded microstructure similar to conventionally cast heat treated Haynes 31 alloy. An economic analysis was also performed.

Army Materials and Mechanics Research Center,
Watertown, Massachusetts 02172
Machine Casting of High Temperature
Alloys for Turbine Engine Components
L. F. Schulmeister et al, United Technologies
Corporation, Pratt & Whitney Aircraft Group,
Government Products Division,
West Palm Beach, Florida 33402
Technical Report - Contract DAAG 46-76-C-0029
D/A Project ARPA Order No. 2267, AMCMS
Code 6410 Final Report, 1 March 1976 to
30 May 1977

AD ________________

UNCLASSIFIED
UNLIMITED DISTRIBUTION

Key Words

Die casting
Solidification
Heat persistant alloys
Iron alloys
Compressor parts
Turbine parts
Quality assurance

The objective of this program is to evaluate the capability to machine cast parts for gas turbine engines. Machine casting in the thixatropic state is being evaluated. Partial assessment of process parameter effects, using Rheocast Haynes Alloy 31, was performed. Machine casting preforms of various volume fractions of solid were injected at different die temperatures. Results indicated internal porosity and surface condition were improved with increasing die temperature and volume fraction solid. A heat treatment response study and mechanical property evaluations were also conducted. Heat treatment studies indicated long term annealing followed by aging yielded microstructure similar to conventionally cast heat treated Haynes 31 alloy. An economic analysis was also performed.

Army Materials and Mechanics Research Center,
Watertown, Massachusetts 02172
Machine Casting of High Temperature
Alloys for Turbine Engine Components
L. F. Schulmeister et al, United Technologies
Corporation, Pratt & Whitney Aircraft Group,
Government Products Division,
West Palm Beach, Florida 33402
Technical Report - Contract DAAG 46-76-C-0029
D/A Project ARPA Order No. 2267, AMCMS
Code 6410 Final Report, 1 March 1976 to
30 May 1977

AD ____________

UNCLASSIFIED
UNLIMITED DISTRIBUTION

Key Words

Die casting
Solidification
Heat persistant alloys
Iron alloys
Compressor parts
Turbine parts
Quality assurance

The objective of this program is to evaluate the capability to machine cast parts for gas turbine engines. Machine casting in the thixatropic state is being evaluated. Partial assessment of process parameter effects, using Rheocast Haynes Alloy 31, was performed. Machine casting preforms of various volume fractions of solid were injected at different die temperatures. Results indicated internal porosity and surface condition were improved with increasing die temperature and volume fraction solid. A heat treatment response study and mechanical property evaluations were also conducted. Heat treatment studies indicated long term annealing followed by aging yielded microstructure similar to conventionally cast heat treated Haynes 31 alloy. An economic analysis was also performed.

Army Materials and Mechanics Research Center,
Watertown, Massachusetts 02172
Machine Casting of High Temperature
Alloys for Turbine Engine Components
L. F. Schulmeister et al, United Technologies
Corporation, Pratt & Whitney Aircraft Group,
Government Products Division,
West Palm Beach, Florida 33402
Technical Report - Contract DAAG 46-76-C-0029
D/A Project ARPA Order No. 2267, AMCMS
Code 6410 Final Report, 1 March 1976 to
30 May 1977

AD ____________

UNCLASSIFIED
UNLIMITED DISTRIBUTION

Key Words

Die casting
Solidification
Heat persistant alloys
Iron alloys
Compressor parts
Turbine parts
Quality assurance

The objective of this program is to evaluate the capability to machine cast parts for gas turbine engines. Machine casting in the thixatropic state is being evaluated. Partial assessment of process parameter effects, using Rheocast Haynes Alloy 31, was performed. Machine casting preforms of various volume fractions of solid were injected at different die temperatures. Results indicated internal porosity and surface condition were improved with increasing die temperature and volume fraction solid. A heat treatment response study and mechanical property evaluations were also conducted. Heat treatment studies indicated long term annealing followed by aging yielded microstructure similar to conventionally cast heat treated Haynes 31 alloy. An economic analysis was also performed.

Army Materials and Mechanics Research Center,
Watertown, Massachusetts 02172
Machine Casting of High Temperature
Alloys for Turbine Engine Components
L. F. Schulmeister et al, United Technologies
Corporation, Pratt & Whitney Aircraft Group,
Government Products Division,
West Palm Beach, Florida 33402
Technical Report - Contract DAAG 46-76-C-0029
D/A Project ARPA Order No. 2267, AMCMS
Code 6410 Final Report, 1 March 1976 to
30 May 1977

AD ____________

UNCLASSIFIED
UNLIMITED DISTRIBUTION

Key Words

Die casting
Solidification
Heat persistant alloys
Iron alloys
Compressor parts
Turbine parts
Quality assurance

The objective of this program is to evaluate the capability to machine cast parts for gas turbine engines. Machine casting in the thixatropic state is being evaluated. Partial assessment of process parameter effects, using Rheocast Haynes Alloy 31, was performed. Machine casting preforms of various volume fractions of solid were injected at different die temperatures. Results indicated internal porosity and surface condition were improved with increasing die temperature and volume fraction solid. A heat treatment response study and mechanical property evaluations were also conducted. Heat treatment studies indicated long term annealing followed by aging yielded microstructure similar to conventionally cast heat treated Haynes 31 alloy. An economic analysis was also performed.

Army Materials and Mechanics Research Center,
Watertown, Massachusetts 02172
Machine Casting of High Temperature
Alloys for Turbine Engine Components
L. F. Schulmeister et al, United Technologies
Corporation, Pratt & Whitney Aircraft Group,
Government Products Division,
West Palm Beach, Florida 33402
Technical Report - Contract DAAG 46-76-C-0029
D/A Project ARPA Order No. 2267, AMCMS
Code 6410 Final Report, 1 March 1976 to
30 May 1977

AD ____________

UNCLASSIFIED
UNLIMITED DISTRIBUTION

Key Words

Die casting
Solidification
Heat persistant alloys
Iron alloys
Compressor parts
Turbine parts
Quality assurance

The objective of this program is to evaluate the capability to machine cast parts for gas turbine engines. Machine casting in the thixatropic state is being evaluated. Partial assessment of process parameter effects, using Rheocast Haynes Alloy 31, was performed. Machine casting preforms of various volume fractions of solid were injected at different die temperatures. Results indicated internal porosity and surface condition were improved with increasing die temperature and volume fraction solid. A heat treatment response study and mechanical property evaluations were also conducted. Heat treatment studies indicated long term annealing followed by aging yielded microstructure similar to conventionally cast heat treated Haynes 31 alloy. An economic analysis was also performed.